UNIVERSITY OF CALIFORNIA, SAN DIEGO

Mitochondrial Quality Control is Essential for Cardiac Progenitor Cell and Cardiac Function

A dissertation submitted in partial satisfaction of the requirements
for the degree Doctor of Philosophy

in

Biomedical Sciences

by

Amabel Marie Cristobal Orogo

Committee in Charge:

Professor Åsa Gustafsson, Chair
Professor Joan Heller Brown
Professor Ju Chen
Professor Anne Murphy
Professor David Roth

2016

The Dissertation of Amabel Marie Cristobal Orogo is approved, and it is acceptable in quality and form for publication on microfilm and electronically:

_____

_____

_____

_____

_____

Chair

University of California, San Diego

2016

DEDICATION

I dedicate this work to my family and thank them for their love and support.

TABLE OF CONTENTS

LIST OF ABBREVIATIONS

AMPK	AMP-activated Protein Kinase
ANP	Atrial Natriuretic Peptide
ATG	Autophagy-Related Protein
ATP	Adenosine Triphosphate
α-MHC	Alpha Myosin Heavy Chain
BNIP3	BCL2/Adenovirus E1B 19 kDa Interacting Protein 3
BNIP3L	BCL2/Adenovirus E1B 19 kDa Interacting Protein 3-like
BPM	Beats Per Minute
BW	Body Weight
β-gal	β-galactosidase
β-MHC	Beta Myosin Heavy Chain
CPC	Cardiac Progenitor Cell
COX I	Mitochondrial Complex I
COX II	Mitochondrial Complex II
COX III	Mitochondrial Complex III
COX IV	Mitochondrial Complex IV
DM	Differentiation Medium
DRP1/DNM1L	Dynamin-related Protein 1/Dynamin-1-like Protein
EF	Ejection Fraction
ETC	Electron Transport Chain
FCCP	Carbonyl Cyanide-4-(trifluoromethoxy)phenylhydrazone

FS	Fractional Shortening
FUNDC1	FUN14 Domain Containing 1
GAPDH	Glyceraldehyde 3-phosphate Dehydrogenase
GFP	Green Fluorescent Protein
H&E	Hematoxylin & Eosin
H_2O_2	Hydrogen Peroxide
HR	Heart Rate
HW	Heart Weight
IMM	Inner Mitochondrial Membrane
IVS; d	Interventricular septal thickness at diastole
IVS; s	Interventricular septal thickness at systole
KO	Knockout
LAMP2	Lysosome-associated Membrane Protein 2
LC3	Microtubule-associated Protein 1 Light Chain 3
LV	Left Ventricle
LVID; d	Left ventricular internal dimension at diastole
LVID; s	Left ventricular internal dimension at systole
LVPW; d	Left ventricular posterior wall thickness at diastole
LVPW; s	Left ventricular posterior wall thickness at systole
LW	Lung Weight
MI	Myocardial Infarction
mtDNA	Mitochondrial DNA

MFN1/2	Mitofusin 1/2
MV E/A	Mitral Valve Early Peak Velocity/Atrial Peak Velocity
NIX	Nip3-like Protein X
NRF2	Nuclear Factor, Erythroid 2-like 2
OCR	Oxygen Consumption Rate
OMM	Outer Mitochondrial Membrane
OXPHOS	Oxidative Phosphorylation
PGC-1α	Peroxisome Proliferator-activated Receptor (PPAR) Gamma Coactivator 1-Alpha
PINK1	PTEN-induced Putative Kinase 1
POLG	Mitochondrial DNA Polymerase Gamma
qPCR	Quantitative Real-Time Polymerase Chain Reaction
ROS	Reactive Oxygen Species
siRNA	Small Interfering RNA
TEM	Transmission Electron Microscopy
TG	Transgenic
TIM23	Translocase of Inner Mitochondrial Membrane 23
TOM20	Translocase of Outer Mitochondrial Membrane 20
TMRM	Tetramethylrhodamine Methyl Ester
UBL	Ubiquitin-Like
WT	Wild-type

LIST OF FIGURES

LIST OF TABLES

ACKNOWLEDGEMENTS

First, I would like to acknowledge my advisor Dr. Åsa Gustafsson for guiding me throughout my graduate training. I would like to thank her for her support and patience. She has been a great mentor who has helped me become a better scientist.

I would also like to thank members of the Gustafsson lab, past and present, who I consider my second family. Thank you for the food and the laughs, and for everyone's help and advice. I am grateful to everyone who has been a part of Team CPC and has helped me in any way with my project.

I would like to thank our collaborator Dr. Anne Murphy for all her help with the Seahorse experiments. I also want to acknowledge Dr. Nicole Purcell who was my mentor during my first BMS rotation, and has continued to provide me with support and career advice.

I would like to acknowledge the UC San Diego Biomedical Sciences Graduate Program and the Department of Pharmacology for providing us with training opportunities, as well as organizing coursework and events for the graduate students.

Parts of Chapters 2, 3, 4, and 5 were originally published in the *Journal of Biological Chemistry*. Orogo AM, Gonzalez ER, Kubli DA, Baptista IL, Ong SB, Prolla TA, Sussman MA, Murphy AN, Gustafsson ÅB. Accumulation of Mitochondrial DNA Mutations Disrupts Cardiac Progenitor Cell Function and Reduces Survival. *The Journal of Biological Chemistry*. 290(36):22061-75,

 The dissertation author was the primary investigator and author of this paper.

The $POLG^{D257A}$ mice were provided by Dr. Tomas Prolla (University of Wisconsin-Madison). This work was supported by the UCSD Graduate Training Program in Cellular and Molecular Pharmacology (NIH/NIGMS Institutional Training Grant T32GM007752) and predoctoral fellowships from the American Heart Association Western States Affiliate (14PRE18210008) and Ruth L. Kirschstein National Research Service Award (NIH/NHLBI F31HL123309).

VITA

EDUCATION

2009	Bachelor of Science, Molecular Toxicology, University of California, Berkeley
2016	Doctor of Philosophy, Biomedical Sciences, University of California, San Diego

PUBLICATIONS

Orogo AM, Gonzalez ER, Kubli DA, Baptista IL, Ong SB, Prolla TA, Sussman MA, Murphy AN, Gustafsson ÅB. Accumulation of Mitochondrial DNA Mutations Disrupts Cardiac Progenitor Cell Function and Reduces Survival. J Biol Chem. 290(36):22061-75, 2015.

Samse K, Emathinger J, Hariharan N, Quijada P, Ilves K, Völkers M, Ormachea L, De La Torre A, Orogo AM, Alvarez R, Din S, Mohsin S, Monsanto M, Fischer KM, Dembitsky WP, Gustafsson ÅB, Sussman MA. Functional Effect of Pim1 Depends upon Intracellular Localization in Human Cardiac Progenitor Cells. J Biol Chem. 290(22):13935-47, 2015.

Orogo AM, Gustafsson ÅB. Therapeutic targeting of autophagy: potential and concerns in treating cardiovascular disease. Circ Res. 116(3):489-503, 2015.

Orogo AM, Gustafsson ÅB. Cell Death in the Myocardium: My Heart Won't Go On. IUBMB Life. 65(8):651-656, 2013.

Orogo AM, Choi SS, Minnier BL, Kruhlak NL. Construction and Consensus Performance of (Q)SAR Models for Predicting Phospholipidosis using a Dataset of 743 Compounds. Mol. Inform. 31(10):725-739, 2012.

Hanna RA, Quinsay MN, Orogo AM, Giang K, Rikka S, Gustafsson ÅB. Microtubule-associated Protein 1 Light Chain 3 (LC3) Interacts with Bnip3 Protein to Selectively Remove Endoplasmic Reticulum and Mitochondria via Autophagy. J Biol Chem. 287(23):19094-104, 2012.

ABSTRACTS

Orogo AM, Gonzalez ER, Kubli DA, Murphy AN, Gustafsson ÅB. Acquisition of Mitochondrial DNA Mutations Impairs Mitochondrial Function in Cardiac Progenitor Cells. Selected for poster presentation at American Heart Association Basic Cardiovascular Sciences 2015 Scientific Sessions, July 2015, New Orleans, Louisiana.

Orogo AM, Kubli DA, Murphy AN, Gustafsson ÅB. Accumulation of Mitochondrial DNA Mutations Impairs Survival, Proliferation, and Differentiation of Cardiac Progenitor Cells. Selected for poster presentation at American Heart Association Basic Cardiovascular Sciences 2014 Scientific Sessions, July 2014, Las Vegas, Nevada. Abstract was scored among top 10% of accepted abstracts and was invited to re-present abstract as a poster presentation in "Best of AHA Specialty Conferences: BCVS 2014" at American Heart Association Scientific Sessions, November 2014, Chicago, Illinois.

Orogo AM, Ong S-B, Zhang X, Murphy AN, Sussman MA, Gustafsson ÅB. AMP-Dependent Protein Kinase Regulates Mitochondrial Reprogramming and Differentiation Potential of Cardiac Progenitor Cells. Selected for poster presentation at American Heart Association Scientific Sessions, November 2012, Los Angeles, California. Circulation. 126:A17301, 2012.

Kruhlak NL, Cross KP, Orogo AM. Characterization of a QSAR Model for Phospholipidosis Using a Hierarchical Scaffold Tree of Significant Molecular Features. Selected for poster presentation at 50th Annual Meeting of the Society of Toxicology, Washington, DC.

Orogo AM, Choi SS, Minnier BL, Kruhlak NL. Expansion of a Phospholipidosis Database for QSAR Modeling with Multiple Software Platforms. Selected for poster presentation at 49th Annual Meeting of the Society of Toxicology, Salt Lake City, Utah. Poster also presented at the 46th Annual Meeting of the Drug Information Association, June 2010, Washington, DC.

AWARDS

National Research Service Award, NIH/NHLBI F31 Diversity Predoctoral Fellowship (2014-2016)
American Heart Association Predoctoral Fellowship (2014)
Cardiovascular Outreach Award for Basic Cardiovascular Sciences 2014 Scientific Sessions, American Heart Association (2014)
BCVS Minority Travel Grant for Scientific Sessions 2012, Council on Basic Cardiovascular Sciences, American Heart Association (2012)

ABSTRACT OF THE DISSERTATION

Mitochondrial Quality Control is Essential for Cardiac Progenitor Cell and Cardiac Function

by

Amabel Marie Cristobal Orogo

Doctor of Philosophy in Biomedical Sciences

University of California, San Diego, 2016

Professor Åsa Gustafsson, Chair

Cardiac progenitor cells (CPCs) have the potential to repair the myocardium after pathological injury. Mitochondria regulate stem cell function and adapt to the metabolic needs of the differentiating cell. I investigated the importance of mitochondria in CPC function and found that mitochondrial biogenesis and network expansion occur during lineage commitment, and blocking mitochondrial expansion along the tubulin network leads to impaired differentiation.

Aging is associated with accumulation of mitochondrial DNA (mtDNA) mutations. I investigated the consequences of mtDNA mutations on CPC function using mice with a proofreading-defective mitochondrial polymerase gamma (POLG) enzyme. I demonstrated that acquisition of mtDNA mutations impairs CPC survival, proliferation, and differentiation.

Autophagy is a process by which long-lived proteins and organelles are engulfed by autophagosomes for delivery to lysosomes for degradation. Mitophagy is the selective removal of dysfunctional mitochondria and is involved in mitochondrial quality control. As cells age, mitophagy is necessary to clear defective mitochondria to prevent their accumulation. Not much is known about mitophagy in CPCs. Parkin is an E3 ubiquitin ligase that ubiquitinates proteins on the outer mitochondrial membrane to facilitate mitophagy. Mitophagy receptors such as BNIP3, NIX, and FUNDC1 can also mediate mitophagy independently of Parkin and ubiquitination.

POLG CPCs have increased mitophagy, but this is not enough to rescue their impaired function. POLG CPCs have intact mitophagy in response to acute stress, but have impaired mitophagy in response to differentiation. I found that gene expression of NIX and FUNDC1 increased during differentiation and likely mediate mitophagy in CPCs.

Parkin promotes removal of damaged mitochondria in the myocardium in response to acute stress. I investigated whether Parkin-mediated mitophagy plays a role in clearing damaged mitochondria in the hearts of aging POLG

mice. Modifying Parkin levels by cardiac-specific overexpression or genetic ablation did not alter autophagy and cardiac function. These results suggest that Parkin-mediated mitophagy does not play a role in clearing mitochondria with mtDNA mutations.

My findings demonstrate that mitochondrial quality control is essential for cell homeostasis and survival. It is critical to understand mechanisms regulating mitophagy in order to improve regenerative potential of CPCs and identify potential targets for heart disease.

CHAPTER 1: INTRODUCTION

Current Therapies for Heart Disease

Cardiovascular disease is the leading cause of mortality in the United States and in the world, accounting for more than 17 million deaths per year globally (Writing Group et al., 2016b). The American Heart Association (AHA) has identified 7 risk factors that increase the risk for heart disease, which include smoking, physical inactivity, poor diet/nutrition, obesity, high cholesterol, high blood pressure, and diabetes (Writing Group et al., 2016a). Although many risk factors can be addressed by modifying behaviors, certain health factors such as family history and genetics cannot simply be altered by a change in lifestyle. Aging is another major risk factor for developing cardiovascular disease, with the prevalence and incidence of heart disease correlating with advancing age in both men and women (Writing Group et al., 2016b).

Every year in the United States, about 610,00 people die of heart disease and 735,000 people suffer from a heart attack (CDC, 2015). During a heart attack or myocardial infarction (MI), loss of blood flow to the heart leads to oxygen and nutrient deprivation, resulting in loss of cardiomyocytes and damage to heart muscle (Whelan et al., 2010). Interventions to reintroduce oxygenated blood limit infarct size, but can also induce reperfusion injury and further cell death (Freude et al., 2000). Thus, both permanent coronary occlusion and ischemia/reperfusion after MI stimulate massive myocardial cell

death that can lead to cardiac dysfunction, pathological remodeling, and heart failure (Whelan et al., 2010; Wencker et al., 2003). The simplest treatment options for heart failure include oral medications such as angiotensin-converting enzyme inhibitors, aldosterone antagonists, angiotensin receptor blockers, and β-blockers (NHLBI, 2015). As heart failure worsens, medical procedures may be necessary, and these include surgery (coronary artery bypass), implantable devices (pacemakers, implantable cardioverter defibrillators, cardiac resynchronization device, left ventricular assist devices), and heart transplants, which are a last resort for end stage heart failure (NHLBI, 2015).

In the past decade, there has been great interest in utilizing regenerative medicine for ischemic and dilated cardiomyopathies. Numerous clinical trials have tested various allogeneic and autologous stem cell populations derived from the bone marrow or the heart for safety and efficacy (Yousef et al., 2009; Hare et al., 2012; Bartunek et al., 2013; Mushtaq et al., 2014; Heldman et al., 2014; Bartunek et al., 2016; Chakravarty et al., 2016). Stem cells are an attractive therapeutic strategy because of their potential to replace cardiomyocytes lost after an MI or ability to stimulate resident progenitor cells to generate new cardiomyocytes. Regenerating damaged myocardium using stem cells continues to be an active and challenging area of research. Therefore, it is important to identify the ideal cell populations and thoroughly investigate their function in order to effectively utilize stem cells in patients with heart failure.

Cardiac Progenitor Cells

The heart contains a pool of c-kit-positive cardiac progenitor cells (CPCs) which have the potential to repair the myocardium after injury by secreting paracrine factors and producing new cardiomyocytes and vasculature (Leri et al., 2011). However, the functional role of endogenous CPCs in the myocardium and how they contribute to repair are still unclear and controversial. Initial studies reported that injection of CPCs into the infarct region leads to generation of new cardiac myocytes and blood vessels by the CPCs (Beltrami et al., 2003). Another report has shown that endogenous CPCs are required for both cardiac homeostasis and regeneration after injury (Ellison et al., 2013). However, a recent study has found that differentiation of endogenous CPCs into cardiomyocytes occurs at a very low rate even after injury (van Berlo et al., 2014). Another study reported that new cardiomyocytes are generated from pre-existing myocytes and that endogenous CPCs do not play a critical role in myocardial homeostasis and repair (Senyo et al., 2013). Finally, two recent publications using *in vivo* lineage tracing studies show that c-kit positive CPCs are endothelial in nature and contribute minimally to cardiomyocytes (Liu et al., 2016; Sultana et al., 2015).

Nevertheless, although the functional role of endogenous CPCs is controversial, it is clear that infusion of CPCs into the injured myocardium leads to repair and improved function. For example, in animal models of myocardial

infarction or doxorubicin-induced cardiomyopathy, injection of CPCs reduces injury and improves left ventricular function (Li et al., 2011; Fischer et al., 2009; De Angelis et al., 2010). The use of autologous CPCs in patients with ischemic cardiomyopathy is showing promising results in the SCIPIO clinical trial (Bolli et al., 2011; Chugh et al., 2012). Thus, it is important to study the biology of CPCs to further understand the mechanisms that underlie its positive effect on the ischemic myocardium.

Mitochondria and Stem Cells

Mitochondria are the powerhouse of the cell and generate ATP through oxidative phosphorylation. Various studies have demonstrated that mitochondria are critical regulators of stem cell function. Embryonic, neuronal, and mesenchymal stem cells have been reported to contain few immature mitochondria that are clustered in the perinuclear region and rely on glycolysis for energy production (Wang et al., 2010; Chung et al., 2007; Chen et al., 2008). However, differentiation of stem cells requires metabolic reprogramming to meet the increased energy demand that occurs concomitantly with a shift from cytosolic anaerobic glycolysis to mitochondrial respiration (Chung et al., 2007; Spitkovsky et al., 2004; Chung et al., 2010). Very little attention has been given to the role of mitochondria in CPCs. Therefore, studying alterations that occur in mitochondria during CPC differentiation will provide more insight on the role of mitochondria in CPC survival and function.

Aging and Mitochondrial DNA Mutations

Studies have found that CPC function is reduced with age, which reduces their regenerative capacity (Mohsin et al., 2013; Hariharan et al., 2015; Goichberg et al., 2013). Stem cell therapies for cardiovascular disease primarily target geriatric patients who also suffer from co-morbidities such as obesity, diabetes, and smoking. All these factors may have a detrimental effect on the function of the stem cell populations. Thus, autologous CPCs might have reduced regenerative capacity once they are transplanted back into the patient's heart if the patient is unhealthy. The mechanisms underlying age-related changes in CPC function are still unclear, and a deeper understanding of biological processes that regulate CPC function and survival is needed so that more effective strategies to repair the heart can be developed.

Mitochondria regulate several key processes in the cell including metabolism, heme synthesis, and cell death. Mitochondria also produce energy through oxidative phosphorylation (OXPHOS) which is critical for cellular development, differentiation, and growth (Atamna, 2004; Nunnari & Suomalainen, 2012; Xu et al., 2013). Mitochondria contain their own DNA that is replicated independently of the nuclear DNA. The mitochondrial DNA (mtDNA) encodes 37 genes and 13 of those are subunits of the respiratory complexes or ATP synthase. The mtDNA is more susceptible to genetic mutations than nuclear DNA because of constant exposure to reactive oxygen

species generated by the respiratory chain, less efficient DNA repair, and absence of histones (Richter et al., 1988). Studies have reported that mtDNA mutations and deletions accumulate with age in various tissues in humans and rodents, which can lead to impaired mitochondrial function (Dai et al., 2009; Corral-Debrinski, Shoffner, et al., 1992; Wanagat et al., 2002; Bratic & Larsson, 2013). Mutations in mtDNA in the heart have also been demonstrated after treatment with cardiotoxic therapies such as doxorubicin (Lebrecht & Walker, 2007) or nucleoside reverse transcriptase inhibitors (Frerichs et al., 2002). In addition, mtDNA mutations and damage have appeared in patients with coronary atherosclerotic disease (Corral-Debrinski, Shoffner, et al., 1992) or after myocardial infarction (Ide et al., 2001).

The contribution of mtDNA mutations to aging has been confirmed by studies in mice expressing a proofreading-deficient mitochondrial DNA polymerase γ (POLG). POLG is the only polymerase in the mitochondria and has multiple functions to replicate, repair, and proofread the mtDNA. Therefore, a mutation that leads to a defect in POLG function will have detrimental effects on the mtDNA integrity. These mice accumulate mtDNA mutations in cells at a faster rate than wild-type mice, which leads to an accelerated aging phenotype and reduced lifespan (Trifunovic et al., 2004; Kujoth et al., 2005). Moreover, accumulation of mtDNA mutations in the heart is associated with increased oxidative damage and apoptosis, which results in the development of cardiomyopathy at 13-14 months of age (Dai et al., 2010). Very little is known

about the effect of mtDNA mutations on CPC function, and studying the consequences of accumulating mtDNA mutations will provide greater insight on the critical role of mitochondria in CPCs.

Autophagy

Macroautophagy, commonly referred to as autophagy, is an evolutionarily conserved process by which long-lived proteins and damaged organelles are engulfed by autophagosomes and subsequently delivered to lysosomes (Yang & Klionsky, 2010). During nucleation, BECLIN1 forms a complex with VPS34 and VPS15 to initiate phagophore formation (Kihara et al., 2001). ATG proteins facilitate assembly and elongation of the phagophore to form the autophagosome membrane that surrounds cargo. During this step, cytosolic LC3 I is conjugated to phosphatidylethanolamine to form LC3 II, which is bound to the autophagosome (Ichimura et al., 2000). The mature double membrane autophagosome then fuses with a lysosome, allowing contents to be degraded by lysosomal enzymes (Figure 1.1). Autophagy is a cellular quality control mechanism that maintains cellular homeostasis. Under normal conditions, autophagy occurs at low levels to facilitate turnover of cytoplasmic components, and is rapidly increased in response to stress or nutrient deprivation (Mizushima, 2007). Alterations in autophagy are associated with cardiovascular disease and aging (Nishino et al., 2000; Nakai et al., 2007;

Taneike et al., 2010; Gatica et al., 2015; Shirakabe et al., 2016). Therefore, autophagy is now being considered a potential therapeutic target in the heart.

Mechanisms of Mitophagy

Autophagy was previously believed to be a nonselective bulk degradation process, but more studies have emerged demonstrating that autophagosomes can recognize and engulf specific organelles, including peroxisomes (Iwata et al., 2006), endoplasmic reticulum (Hanna et al., 2012), and mitochondria (Quinsay et al., 2010) in mammalian cells. Mitophagy is the selective removal of damaged mitochondria by autophagy, and is involved in mitochondrial turnover and quality control in the heart (Kubli & Gustafsson, 2012). However, very little is known about mechanisms of mitophagy in CPCs.

The PINK1/Parkin mitochondrial quality control pathway has been mainly studied in the brain in the context of Parkinson's disease, but has also been shown to play a role in clearing defective mitochondria in the heart in response to stress (Kubli et al., 2013; Chen & Dorn, 2013; Dorn, 2016). PINK1 is a serine-threonine kinase that is present on the outer mitochondrial membrane (OMM). Under baseline conditions, intact mitochondrial membrane potential in healthy mitochondria drives PINK1 import to the inner mitochondrial membrane (IMM), where PINK1 is cleaved at the N-terminus and is recognized by the ubiquitin proteasomal system for constitutive degradation (Greene et al., 2012; Yamano & Youle, 2013). However, damaged mitochondria which have accumulated

unfolded proteins or cannot maintain intact membrane potential are unable to import PINK1. This leads to accumulation of PINK1 on the OMM and recruitment of Parkin, an E3 ubiquitin ligase (Narendra, Jin, et al., 2010; Jin & Youle, 2013). Ubiquitin is linked to proteins on the OMM, and when PINK1 accumulates on the OMM, it phosphorylates ubiquitin at the Ser65 residue (Koyano et al., 2014). Parkin has high affinity for Ser65-phosphorylated ubiquitin, which drives its recruitment to the OMM (Kazlauskaite et al., 2014). PINK1 phosphorylates Parkin's ubiquitin-like (UBL) domain at Ser65, stabilizing Parkin in its "open" conformation and allowing Parkin to ubiquitinate its substrates on the OMM (Kondapalli et al., 2012).

Parkin is present in the cytosol under baseline conditions but rapidly translocates to depolarized mitochondria (Narendra et al., 2008). Parkin ubiquitinates proteins on the OMM to facilitate mitophagy (Figure 1.2 A). Several Parkin targets on the outer mitochondrial membrane have been identified, including MFN1/2, MIRO1/2, VDAC, mitochondrial Hexokinase 1/2, FIS1, TOM20, and TOM70, as well as autophagy adaptor SQSTM1/p62 (Sarraf et al., 2013). MFN2 is a Parkin receptor and is necessary for Parkin recruitment to uncoupled mitochondria, and its phosphorylation by PINK1 promotes Parkin translocation to mitochondria (Chen & Dorn, 2013).

Ubiquitinated proteins on the OMM recruit adaptor proteins which can bind to both the cargo and to LC3 II present on the autophagosome membrane (Figure 1.2 A). SQSTM1/p62 is an adaptor protein that contains a ubiquitin-

associated domain and an LC3-interacting region that binds to LC3 (Lamark et al., 2009). Interestingly, SQSTM1/p62 is not required for Parkin-mediated mitochondrial clearance (Narendra, Kane, et al., 2010). Other adaptor proteins such as NBR1 (Lamark et al., 2009), Optineurin (Wild et al., 2011), and NBP52 have been identified in other cells and serve similar functions as SQSTM1/p62. Recent data has shown that NBR1 is also dispensable for Parkin-mediated mitophagy (Shi et al., 2015). Optineurin recruitment to damaged mitochondria is Parkin-dependent, but SQSTM/p62 is not required (Wong & Holzbaur, 2014). Other adaptor proteins that have not yet been identified may compensate for SQSTM1/p62 deficiency and require further investigation.

There are also autophagy receptors present on the mitochondrial membrane that function independently of ubiquitin and adaptor proteins. The mitophagy receptors BNIP3, NIX, and FUNDC1 are present on the OMM and can directly bind to LC3 II on the autophagosome membrane to mediate selective removal of mitochondria in cells in response to hypoxia (Hanna et al., 2012; Novak et al., 2010; Quinsay et al., 2010; Liu et al., 2012) (Figure 1.2 B).

Rationale and Specific Aims of the Thesis

Mitochondria are critical for generating ATP and regulating cell survival, and must undergo alterations to meet the energy demands required for differentiation and maintenance of proper cell function (Figure 1.3). Mitochondria contain their own genome, and mtDNA mutations that accumulate

with age can lead to generation of dysfunctional mitochondria that could have detrimental consequences to cell function (Figure 1.4). Studying the effect of mtDNA mutations on CPC function will provide greater insight on the role of mitochondria in stem cells, and how to improve the therapeutic potential of CPCs in the context of aging and heart disease. As cells age, they need to utilize cellular processes such as mitophagy to clear accumulating defective mitochondria. However, not much is known about the mechanisms of mitophagy in CPCs. Parkin is expressed in the heart and plays a role in stress adaptation by mediating clearance of depolarized mitochondria. However, the role of Parkin-mediated mitophagy in aging hearts with accumulating mtDNA mutations has not been examined. I hypothesize that mitochondrial quality control is critical for maintaining optimal cardiac progenitor cell and cardiac function. I also hypothesize that Parkin-mediated mitophagy plays a role in clearing damaged mitochondria in CPCs and cardiomyocytes that have accumulated mtDNA mutations. To investigate this hypothesis, I propose the following specific aims:

Aim 1: Investigate the functional importance of mitochondria in CPC function and the consequence of mtDNA mutations

Hypothesis: Accumulating mtDNA mutations will produce dysfunctional mitochondria that leads to impaired CPC function (survival, proliferation, differentiation).

Aim 2: Investigate functional role of Parkin-mediated mitophagy in the aging myocardium

Hypothesis: Parkin-mediated mitophagy is impaired aging hearts due to mtDNA mutations. Parkin deficiency will accelerate cardiac dysfunction, and overexpressing Parkin in the heart will rescue the accelerated cardiac aging phenotype.

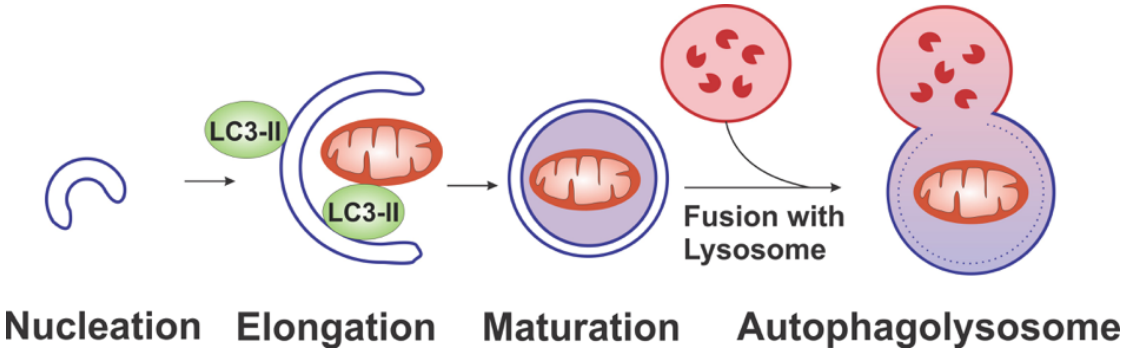

Figure 1.1: Overview of autophagy. In autophagy, the autophagosome engulfs damaged proteins and organelles by forming a double-membrane vesicle around the cargo. The autophagosome fuses with a lysosome and the contents are degraded by lysosomal enzymes. Mitophagy is the selective degradation of defective mitochondria by autophagy.

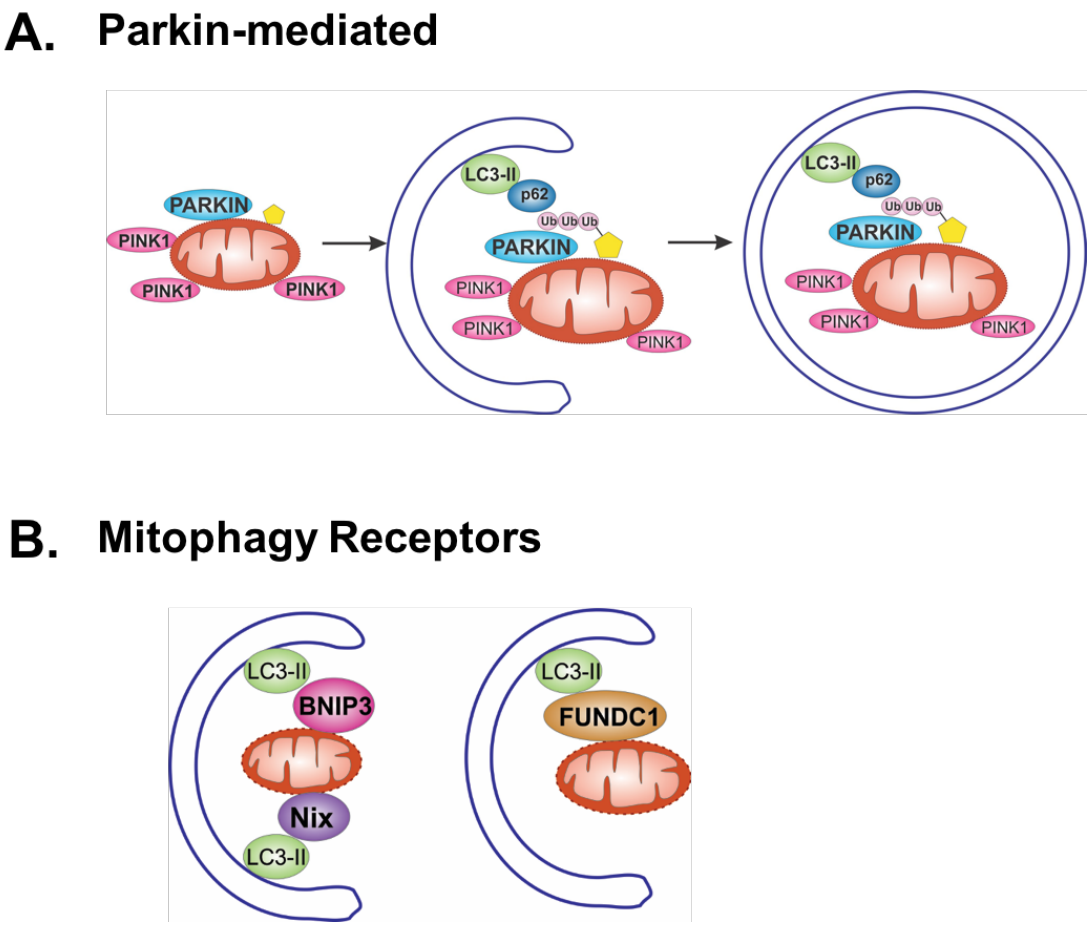

Figure 1.2: Mechanisms of mitophagy. A. Parkin is recruited to depolarized mitochondria and ubiquitinates outer mitochondrial membrane proteins. The mitochondria are sequestered in the autophagosome and eventually degraded in the lysosome. **B.** Mitophagy receptors such as BNIP3, BNIP3L/NIX and FUNDC1 are present on the outer mitochondrial membrane and recruit the autophagosome by directly interacting with LC3 II on the autophagosome membrane.

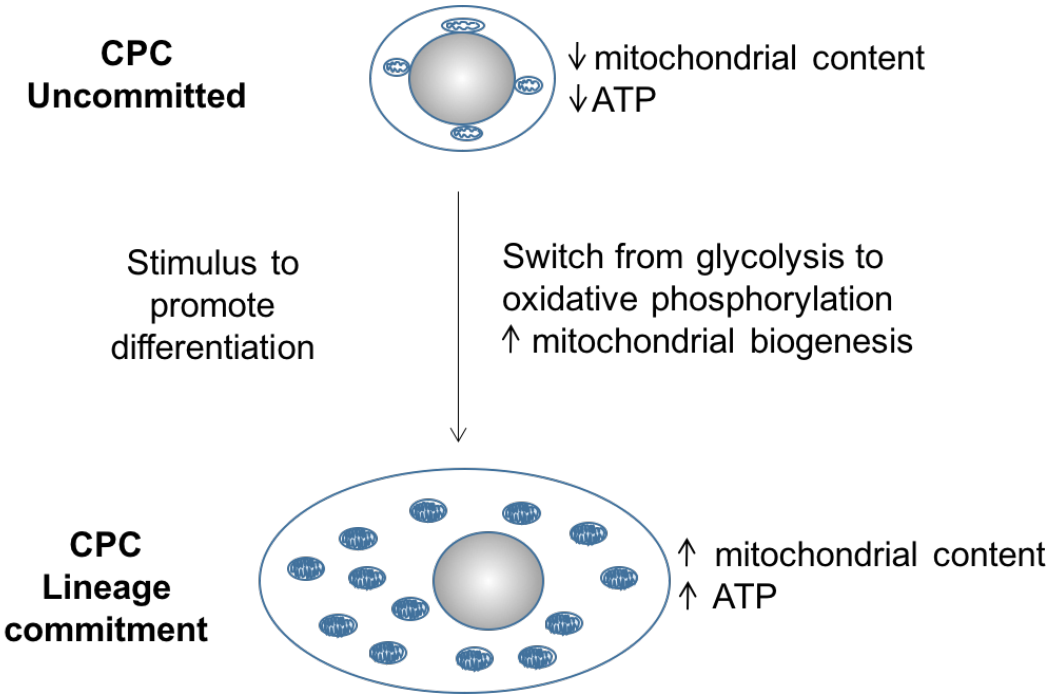

Figure 1.3: CPCs undergo mitochondrial reprogramming during lineage commitment. Undifferentiated CPCs contain few mitochondria and must upregulate mitochondrial biogenesis and oxidative phosphorylation upon differentiation.

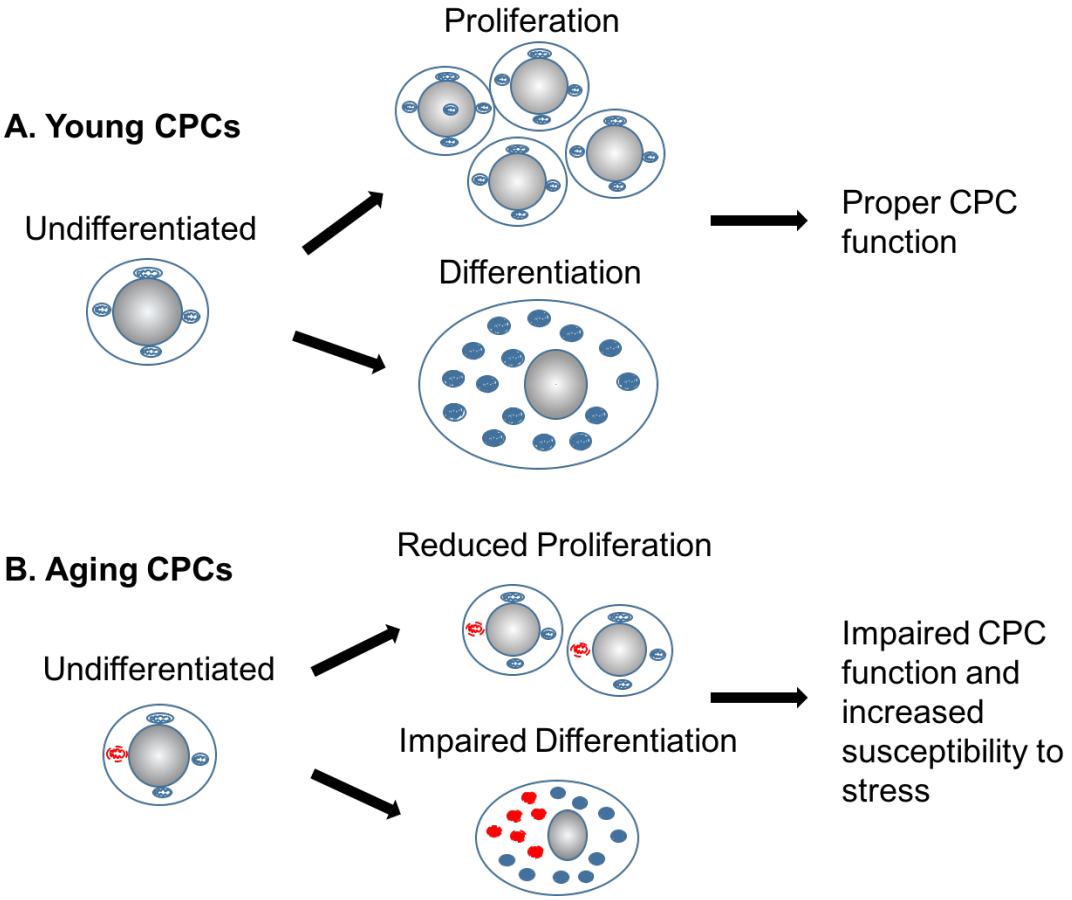

Figure 1.4: Aging leads to impaired CPC function. A. Young CPCs have functional mitochondrial quality control processes and expand healthy mitochondria during differentiation. **B.** Aging is associated with increased mtDNA mutations and reduced mitochondrial clearance by autophagy, leading to accumulation of defective mitochondria and reduced function.

CHAPTER 2: EXPERIMENTAL METHODS AND MATERIALS

Animals

All experimental procedures were performed in accordance with institutional guidelines and approved by the Institutional Animal Care and Use Committee of the University of California San Diego. $POLG^{D257A}$ mice were obtained from Dr. Tomas Prolla, University of Wisconsin-Madison (Kujoth et al., 2005). $Parkin^{-/-}$ mice were obtained from Jackson Laboratories and their cardiac phenotype has been previously characterized (Kubli et al., 2013).

Generation of Mouse Lines

Mice heterozygous for the $POLG^{D257A}$ mutation were crossed to generate mice with WT and mutant $POLG^{D257A/D257A}$ genotypes (Kujoth et al., 2005). Two additional mouse lines were also generated. Heterozygous $POLG^{D257A}$ mice were crossed with Parkin TG mice for several generations to obtain mice with WT, $POLG^{D257A/D257A}$, Parkin TG, and $POLG^{D257A/D257A}$/Parkin TG genotypes. The Parkin TG mice overexpress Parkin under the transcriptional control of the cardiomyocyte-specific α-myosin heavy chain (α-MHC) promoter. Heterozygous $POLG^{D257A}$ mice were also crossed with $Parkin^{-/-}$ mice to obtain mice with WT, $POLG^{D257A/D257A}$, $Parkin^{-/-}$, and $POLG^{D257A/D257A}$/$Parkin^{-/-}$ genotypes. These mice are referred to as WT, POLG, Parkin TG, POLG/Parkin TG, Parkin KO, and POLG/Parkin KO throughout the text.

Cardiac Progenitor Cell Isolation and Culture

C-kit positive CPCs were isolated from 2-month-old male wild-type FVB mice. CPCs were also isolated from male mice homozygous for the $POLG^{D257A}$ mutation on a C57Bl/6 background (Kujoth et al., 2005), and control CPCs isolated from wild-type, sex-matched litter mates. All c-kit positive adult CPCs were isolated and cultured as previously described (Beltrami et al., 2003; Fransioli et al., 2008), with slight modifications.

Mice were injected with heparin and anesthetized with ketamine-xylazine. The heart was carefully removed from the chest and tied to a cannula attached to a Langendorff Myocyte Isolation System (Radnoti). The heart was then perfused with basic buffer for 10 minutes, followed by perfusion with Collagenase II digestion solution (Worthington Biochemical) for 9-10 minutes. The heart was removed from the cannula and placed in a conical tube with incubation buffer containing fatty acid-free BSA to stop further digestion. The heart was minced into small pieces and resuspended using a sterile pipette to dissociate cells, and the mixture was centrifuged at 100 x g for 1 minute at 4°C. The supernatant was passed through a 30 μm filter (Miltenyi) and subsequently centrifuged at 600 x g for 10 minutes at 4°C. The supernatant was discarded and the remaining cell pellet was resuspended in a solution containing 100 μl of washing buffer and 20 μl of CD117/c-kit-conjugated magnetic microbeads. This mixture was incubated on a rocker for 20 minutes at 4°C. The cells were passed through a MiniMACS sorting column and c-kit-positive cells were selected using

magnetic-activated cell sorting (Miltenyi). Finally, the cells eluted from the magnetic column were resuspended in CPC growth media containing Dulbecco's Modified Eagle Medium and Ham's F-12 medium (1:1 ratio), 10% embryonic stem cell FBS, leukemia inhibitory factor (10 ng/ml), insulin transferrin selenium, epidermal growth factor (20 ng/ml), basic fibroblast growth factor (10 ng/ml), and antibiotic/antimycotic. Cells were allowed to grow undisturbed for at least 5 days before replacing the growth media. CPCs were expanded in culture for several passages until a sufficient number of cells were obtained for experiments. To activate differentiation, CPCs were incubated in α-Minimum Essential Medium containing antibiotic/antimycotic and 10 nM dexamethasone for up to seven days.

Quantitative Polymerase Chain Reaction

Genomic DNA was extracted using GenElute Mammalian Genomic DNA Miniprep Kit (Sigma-Aldrich) and PCR amplified with TaqMan Universal Master Mix II. 18s rRNA was used as a control for nuclear DNA and d-loop for mtDNA quantitation, using primer sequences previously described (Rikka et al., 2011). For gene expression assays, RNA was extracted from CPCs using the RNeasy Mini Kit (Qiagen) and from heart tissue using the RNeasy Fibrous Tissue Mini Kit (Qiagen). cDNA was synthesized from 500 ng RNA using the QuantiTect Reverse Transcription Kit (Qiagen) following manufacturer's protocols. Taqman primers for *Ppargc1a*, *Ppargc1b*, *Gata-4*, *Gata-6*, *Pecam1*, *Cox4i1*, *Cox1*,

Park2, *PARK2* (human), *Bnip3*, *Bnip3l/Nix*, *Fundc1*, *Myh7*, *Nppa*, *Sqstm1*, *Atg5*, *Atg7*, *Becn1*, *Rab7*, *Pink1*, *Mfn2*, *Rn18s*, and the TaqMan Universal Master Mix II were purchased from Applied Biosystems/Life Technologies/Thermo Fisher Scientific. qPCR was carried out on a CFX96 Real-Time PCR Detection System (Bio-Rad). Relative amounts of mRNA were normalized to *Rn18s* and fold change in gene expression was calculated using the $2(^{-\Delta\Delta Ct})$ method.

Subcellular Fractionation for Western Blot

Mice at were anesthetized with 100 mg/kg sodium pentobarbital and hearts were snap-frozen in liquid nitrogen. Hearts were minced in homogenization buffer containing 250 mM sucrose, 5 mM KH2PO4, 2 mM $MgCl_2$, 10 mM MOPS pH 7.4, 1 mM EGTA, 0.1% fatty acid-free BSA, and protease inhibitor cocktail (Roche). Hearts were homogenized by Polytron at 11,000 rpm, followed by 3-4 strokes using the Teflon tissue grinder to further homogenize the tissue. Homogenates were incubated with 20% Triton X-100 buffer (1% final concentration) for 45 minutes to induce further cell lysis, followed by centrifugation at 15,000 rpm for 20 minutes to obtain cleared whole heart lysates. Protein concentration was determined by Bradford assay.

To obtain the mitochondrial fraction, whole heart homogenates were centrifuged at 600 x g for 5 minutes at 4°C to remove nuclear contamination and debris. The supernatant was transferred to a new tube and the centrifugation step was repeated. The supernatant was collected and transferred to another

tube and centrifuged at 3000 x g for 10 minutes at 4°C. The resulting supernatant contained the cytosolic fraction and the pellet contained the mitochondrial fraction. The mitochondrial pellet was washed in homogenization buffer and centrifuged at 3000 x g for 10 minutes at 4°C, and this wash step was performed three times. The resulting mitochondria pellet was resuspended and lysed in Triton X-100 lysis buffer containing 50 mM Tris-HCl, 150 mM NaCl, 1 mM EGTA, 1 mM EDTA, 1% Triton X-100, and protease inhibitor cocktail (Roche).

Separation of Soluble and Insoluble Fractions

Hearts were minced in detergent-free lysis buffer containing 50 mM Tris-HCl, 150 mM NaCl, 1 mM EGTA, 1 mM EDTA, and protease inhibitor cocktail (Roche). Samples were homogenized using a Polytron at 22,000 rpm for 3 seconds and centrifuged at 6000 x g for 5 minutes at 4° C. Triton X-100 was added to achieve a final concentration of 0.1%, and samples were incubated on a rocker for 45 minutes at 4° C. Supernatant (soluble fraction) was transferred to a fresh tube and protein concentration was determined by Bradford assay. Soluble fractions were normalized in NuPAGE sample buffer and DTT. The remaining pellets containing insoluble proteins were rinsed with detergent-free lysis buffer and resuspended in 1X NuPAGE sample buffer with DTT. Both soluble and insoluble samples were heated at 70° C for 10 minutes, followed by centrifugation at 10,000 x g for 5 minutes.

Western Blot

CPCs were prepared in Triton X-100 lysis buffer with protease inhibitor and protein concentrations were determined using the Bradford assay.

Samples were loaded and run on Invitrogen NuPAGE Bis-Tris gels. The membranes were probed with the following antibodies: MitoProfile Total OXPHOS Rodent WB Antibody cocktail (MitoSciences), COX IV Subunit 4 (Invitrogen/Life Technologies), AMPK, p-AMPK, Hexokinase I, Hexokinase II, PKM1/2, LC3, Parkin, GAPDH (Cell Signaling Technology), DLP1, Tim23 (BD Biosciences), MFN1, TOM20, Ubiquitin (Santa Cruz Biotechnology), p62 (Abcam), PINK1 (Cayman), BNIP3, MFN2, Tubulin (Sigma-Aldrich), and Actin (GeneTex). Membranes were imaged using a ChemiDoc XRS+ System (Bio-Rad).

Mitochondrial Respiration Measurements of Isolated Mitochondria

Intact mitochondria were isolated from 2 month-old mice. Hearts were minced in isolation buffer containing 100 mM KCl, 50 mM MOPS pH 7.4, 1 mM EGTA, 5 mM $MgSO_4$, 1 mM ATP, and 0.2% fatty acid-free BSA. The tissue was further homogenized with a Polytron tissue grinder at 11,000 rpm for 2.5 seconds, followed by 3-4 strokes with a Teflon tissue grinder. The heart homogenate was centrifuged at 600 x g for 5 minutes at 4°C and the supernatant was collected and centrifuged again. The supernatant was then centrifuged at 3,000 x g for 10 minutes at 4°C to obtain a mitochondrial pellet.

Two washes were performed with isolation buffer and the final wash was performed with BSA-free isolation buffer. Finally, the mitochondrial pellet was resuspended in 100 μl buffer containing 70 mM sucrose, 200 mM mannitol, 2 mM Tris base, and 20 mM HEPES pH 7.4. Mitochondrial protein concentrations were determined using Bradford assay.

Oxygen consumption measurements were taken at 30°C using an Oxygraph apparatus (Hansatech Instruments) as previously described (Kubli et al., 2013). 125 μg of mitochondria were added to a final volume of 1 ml respiration buffer containing 10 mM $MgCl_2$, 100 mM KCl, 50 mM MOPS pH 7.0, 1 mM EGTA, 5 mM KH_2PO_4, and 0.2% fatty acid-free BSA. Complex I-dependent oxygen consumption was measured using 2 mM pyruvate and 2 mM malate as substrates. Complex II-dependent oxygen consumption was measured using 5 μM rotenone to inhibit Complex I and 5 mM succinate as substrate. Complex IV-dependent respiration was measured by addition of 1 μM Antimycin A and 0.4 mM TMPD + 1 mM ascorbate. Oligomycin (5 μg/ml) was added to inhibit ATP synthase followed by carbonyl cyanide-4-(trifluoromethoxy)phenylhydrazone (FCCP) (1 μM) to obtain maximal respiration rate.

Intact mitochondria were also isolated from 6 month-old mouse hearts and mitochondrial respiration was measured using the Seahorse XF96 Analyzer (Seahorse Bioscience – Agilent Technologies) following a modified protocol originally optimized in the Seahorse XF24 Analyzer (Rogers et al., 2011). Hearts

were homogenized using a Polytron followed by a Teflon tissue grinder, in buffer containing 70 mM sucrose, 210 mM mannitol, 5 mM HEPES, 1 mM EGTA, and 0.5% fatty acid-free BSA. The homogenate was centrifuged at low speed (500 x g for 10 minutes at 4°C). The supernatant was collected and centrifuged at 12,000 x g for 10 minutes at 4°C to obtain a mitochondrial pellet. The pellet was washed in buffer and centrifuged at 12,000 x g for 10 minutes at 4°C, and this wash step was performed twice. Finally, the pellet was resuspended in a small volume (~20 μl) of buffer and the protein concentration was determined by Bradford assay. Mitochondria were plated on a 96-well microplate at densities of either 0.5 μg or 1 μg per well. Assay media (70 mM sucrose, 220 mM mannitol, 10 mM KH_2PO_4, 5 mM $MgCl_2$, 2 mM HEPES, 1 mM EGTA, 0.2% BSA, and 4 mM ADP) containing different substrates were used to assess glucose metabolism (10 mM pyruvate and 1 mM malate), fatty acid oxidation (40 μM palmitoylcarnitine and 1 mM malate), and Complex II-dependent oxygen consumption (10 mM succinate and 2 μM rotenone). Oligomycin (2 μM) was added to inhibit ATP synthase followed by three successive additions of 1.5 μM FCCP to obtain maximal respiration rate. Data were analyzed using Wave for Desktop (Seahorse Bioscience – Agilent Technologies).

Mitochondrial Respiration Measurements of CPCs

Mitochondrial oxygen consumption of monolayers of CPCs was measured using the Seahorse XF96 analyzer (Seahorse Bioscience – Agilent

Technologies), adapted from a previously described protocol (Rikka et al., 2011). CPCs were plated at 2 x 10^4 or 1 x 10^4 cells per well 24 hours before measurement of O_2 consumption rates. Assays were run in unbuffered, serum-free DMEM containing 10 mM glucose, 3 mM glutamine, and 1 mM pyruvate. CPCs were allowed to equilibrate on the plate before addition of 2 μM oligomycin to measure ATP-linked respiration. Three successive additions of 500 nM FCCP were added to measure maximal respiration. Data were analyzed using Wave for Desktop software (Seahorse Bioscience).

Immunofluorescence Microscopy

CPCs were treated with Compound C to inhibit AMPK pharmacologically and treated with Nocodazole to inhibit microtubule polymerization. Immunofluorescence was used to assess the effects of the pharmacological treatments on mitochondrial morphology and differentiation. Cells were fixed in 4% paraformaldehyde (Ted Pella) in 1X PBS, permeabilized in 0.2% Triton X-100 in 1X PBS, and blocked in 5% normal goat serum. CPCs and heart tissue sections were stained with antibodies against CD117/c-kit (R&D Systems), TOM20 (Santa Cruz Biotechnology), Tubulin (Sigma-Aldrich), COX IV (Invitrogen), GATA-4 (Santa Cruz Biotechnology), p-AMPK (Cell Signaling Technologies) and LAMP2 (Sigma-Aldrich). The CD117/c-kit fluorescent signal was amplified using the TSA Plus Fluorescence System (Perkin Elmer). Cells were incubated in Alexa Fluor 488 or 594 secondary antibodies (Life

Technologies), followed by Hoechst 33342 (10 μg/ml, Life Technologies) to stain nuclei. Cells were imaged using a Carl Zeiss Axio Observer Z1, and Z-stacks were acquired using a high-resolution AxioCam MRm digital camera, a 63X oil immersion objective, and Zeiss AxioVision 4.8 software (Carl Zeiss). A minimum of 100 cells per group were counted for each condition.

Transmission Electron Microscopy

Adult mouse hearts and CPCs were fixed in modified Karnovsky's fixative containing 2.5% glutaraldehyde and 2% paraformaldehyde in 0.15 M sodium cacodylate buffer pH 7.4 for at least 4 hours, post-fixed in 1% osmium tetroxide in 0.15 M cacodylate buffer for 1 hour, and stained with 2% uranyl acetate for 1 hour. Samples were embedded in Durcupan epoxy resin, sectioned on a Leica UCT ultramicrotome, and mounted on carbon-coated copper slot grids. Sections were stained with 2% uranyl acetate and Sato's lead stain. Sections were examined on a TECNAI G2 Spirit BioTWIN Transmission Electron Microscope equipped with an Eagle 4k HS digital camera (FEI).

Proliferation Assay

CPCs were seeded in a 12-well tissue culture plate and cell number was determined after 24 and 72 hours by counting using a hemocytometer. CPCs were also seeded in a 96-well black wall clear bottom plate (Corning) and cell number was measured with the CyQUANT NF Cell Proliferation Assay Kit (Life

Technologies). Fluorescence measurements were made using a SpectraMax M3 microplate reader and SoftMax Pro 5.4 software (Molecular Devices).

Cell Death Assay

CPCs were treated with H_2O_2 (Sigma-Aldrich), Doxorubicin Hydrochloride (Sigma-Aldrich), Sunitinib Malate (BioVision), or 2-deoxyglucose (Sigma-Aldrich). Cells were stained with Hoechst 33342 (10 μg/ml, Life Technologies) and YO-PRO-1 Iodide (100 nM, Life Technologies) for 15 minutes and immediately imaged using a Carl Zeiss Axio Observer Z1 at 10X magnification, AxioCam MRm digital camera, and Zeiss AxioVision 4.8 software (Carl Zeiss).

Senescence Assay

CPCs were seeded in a 12-well tissue culture plate and the Senescence Detection Kit (Abcam) was used to measure senescence-associated-β-galactosidase activity according to manufacturer's protocol. Cells were observed under a brightfield microscope and at least 100 cells were counted per well.

Glycolysis Assay

CPCs were seeded in a 12-well tissue culture plate and incubated in growth medium for 4 days. L-lactate concentration in the growth medium was

measured using a Glycolysis Cell-Based Assay Kit (Cayman Chemical) according to manufacturer's protocol. Colorimetric measurements were made using a SpectraMax M3 microplate reader and SoftMax Pro 5.4 software (Molecular Devices).

ATP Assay

ATP levels were measured using the CellTiter-Glo Luminescent Cell Viability Assay (Promega, Madison, WI) according to the manufacturer's protocol. CPCs (40,000 cells/100 µl) were added to a 96 well black wall clear bottom plate (Corning). Luminescent measurements were made using a SpectraMax M3 microplate reader and SoftMax Pro 5.4 software (Molecular Devices).

Assessment of mitochondrial membrane potential

CPCs were incubated with tetramethylrhodamine methyl ester (TMRM) (25 nM, Invitrogen) and Hoechst 33342 (10 µg/ml, Life Technologies) for 15 minutes at 37°C. Live cells were examined using a Carl Zeiss Axio Observer Z1 at 40X magnification. Fluorescence intensity was quantified using ImageJ software.

Assessment of Autophagy and Mitophagy

To assess baseline autophagic flux, CPCs were treated with DMSO or 50 nM Bafilomycin A1 (EMD Millipore) for 2 hours prior to homogenization and Western blot analysis. To visualize lysosomes, CPCs were fixed and stained with LAMP2 (Sigma-Aldrich). To assess mitochondrial autophagy, CPCs were infected with an adenovirus encoding GFP-LC3 as previously described (Hanna et al., 2012). Cells were treated with DMSO or 50 nM Bafilomycin A1 for 3 hours, fixed, and stained with anti-TOM20.

To assess Parkin-mediated mitophagy, CPCs were infected with β-gal or mCherry-Parkin adenovirus and treated with 25 μM FCCP for 24 hours to induce mitochondrial damage. Western blotting for TIM23 was used to assess mitochondrial clearance in CPCs.

Cells were imaged at 63X magnification and Z-stacks acquired using a Carl Zeiss Axio Observer Z1. LAMP2 staining was quantified using ImageJ software. Mitophagy was assessed by analyzing colocalization between GFP-LC3 positive autophagosomes and TOM20 labeled mitochondria.

Echocardiography

Echocardiography was performed as previously described (Kubli et al., 2013) using a Vevo770 In Vivo Micro-Imaging System with an RMV707B 15-45 MHz imaging transducer (VisualSonics Inc.). Mice were maintained under light anesthesia through a nose cone (0.5-1% isoflurane, 98-99.5% O_2). Mice were

placed in a supine position on a recirculating water warming pad while acquiring measurements. Cardiac parameters were quantified using the VisualSonics software.

Histology

Prior to tissue collection, mice were anesthetized with 100 mg/kg sodium pentobarbital. Hearts were perfused with 200 mM KCl to induce arrest at diastole before harvesting. Hearts were fixed in 10% neutral buffered formalin for 24 hours and transferred to 70% dehydrant alcohol for another 24 hours. Hearts were processed, embedded in paraffin, and cut into sections using a microtome (Leica Biosystems).

To visualize general size and wall thickness, hearts were cut at the coronal plane to obtain a 4-chamber view. Sections were cut at 10 μm thickness and stained with hematoxylin and eosin (H&E). Sections were imaged using a Carl Zeiss Axio Observer Z1 camera attached to a dissection microscope (Zeiss Stemi 2000-C). Images were taken at 1.0 X magnification.

Statistical Analyses

All values are expressed as means $\pm$ standard error. Student's t-test was used to compare two sets of data. For data comparing more than 2 groups, statistical analyses were performed using one-way or two-way ANOVA,

followed by Tukey's multiple comparison test (GraphPad Prism 7, GraphPad Software, Inc.). P values < 0.05 were considered statistically significant.

Chapter 2, in part, was originally published in the *Journal of Biological Chemistry*. Orogo AM, Gonzalez ER, Kubli DA, Baptista IL, Ong SB, Prolla TA, Sussman MA, Murphy AN, Gustafsson ÅB. Accumulation of Mitochondrial DNA Mutations Disrupts Cardiac Progenitor Cell Function and Reduces Survival. *The Journal of Biological Chemistry*. 290(36):22061-75, 2015. © 2015 The American Society for Biochemistry and Molecular Biology. The dissertation author was the primary investigator and author of this paper.

CHAPTER 3: CARDIAC PROGENITOR CELLS UNDERGO MITOCHONDRIAL REPROGRAMMING DURING DIFFERENTIATION

Introduction

Mitochondria are the major source of ATP in the cell and play a central role in cellular bioenergetic function. Uncommitted CPCs contain few mitochondria and must undergo metabolic changes during differentiation in order to meet the increasing energy demand of the cell. Currently, little is known about mitochondrial function and alterations that occur in CPCs during lineage commitment. Various types of stem cells have to undergo a transition from glycolysis to oxidative phosphorylation (OXPHOS) during differentiation by upregulating mitochondrial biogenesis (Cho et al., 2006; Chung et al., 2007; Wang et al., 2010). Increased mitochondrial mass and mitochondrial DNA (mtDNA) are accompanied by increased synthesis of OXPHOS and antioxidant proteins that permit efficient generation of ATP and removal of reactive oxygen species (ROS) generated by the electron transport chain (ETC). Likewise, CPCs contain few mitochondria that should expand during differentiation to facilitate an energetic transition. Here, I have investigated the mitochondrial reprogramming that occurs during CPC differentiation and demonstrate the important role of mitochondria in differentiating CPCs.

Results

CPC Differentiation is Accompanied by Mitochondrial Expansion

First, I isolated c-kit+ CPCs from the hearts of 10-12 week old WT mice by magnetic-activated cell sorting. C-kit is a transmembrane receptor with tyrosine kinase activity that is highly expressed on the surface of stem and progenitor cells. C-kit binds to stem cell factor (SCF), which activates a signaling cascade that leads to differentiation, growth, and proliferation (Matsui et al., 2004). I incubated CPCs in differentiation medium (DM) containing 10 nM dexamethasone, which has been shown to stimulate differentiation in mouse and human CPCs after 7 days (Fransioli et al., 2008; D'Amario et al., 2011). I examined the effects of differentiation on mitochondrial content and distribution by fluorescence microscopy. At Day 0, undifferentiated CPCs had a large nuclear-cytoplasmic ratio and contained few mitochondria, which were primarily localized to the perinuclear region (Figure 3.1 A). After 7 days of differentiation, CPCs grew larger in size and mitochondrial content increased (Figure 3.1 A). The increase in mitochondrial content and cell size correlated with reduced c-kit expression (Figure 3.1 A). Furthermore, I visualized mitochondrial ultrastructure by transmission electron microscopy and found that the undifferentiated CPC contained immature mitochondria with little cristae structure. In contrast, after 7 days in DM, the mitochondria were longer and more electron dense (Figure 3.1 B). In eukaryotic cells, the cytoskeleton plays a role in organelle transport and cell morphology (Anesti & Scorrano, 2006).

Since the CPCs increased in size and expanded their mitochondrial network during differentiation, I investigated whether mitochondria moved along the microtubules as they are transported to the cell periphery. I found that after CPCs were incubated in DM for 7 days, mitochondria co-localized with tubulin as they expanded their network (Figure 3.2).

When CPCs commit to a lineage, they downregulate c-kit expression and upregulate transcription factors and proteins specific to that lineage (D'Amario et al., 2011). I investigated whether CPCs commit to the cardiac myocyte lineage by staining for GATA-4, an early cardiomyocyte marker. The GATA family of zinc finger transcription factors regulate myocardial differentiation, growth, and survival. GATA-4 is one of the earliest transcription factors expressed in developing murine cardiac cells and is continually expressed in cardiac myocytes throughout the life of the animal (Pikkarainen et al., 2004). I found that at Day 0, very few CPCs stained positive for GATA-4 (Figure 3.3 A and B). After 7 days of differentiation, approximately 55% of CPCs stained positive for GATA-4 (Figure 3.3 B). Cells positive for GATA-4 have also expanded their mitochondria (Figure 3.3 A). Real-time quantitative PCR (qPCR) confirmed increased transcripts of *Gata-4*, a cardiac lineage marker, in CPCs in DM at Day 7. In addition, CPCs also increased gene expression of *Gata-6*, a smooth muscle marker, and *Pecam1*, an endothelial cell marker (Figure 3.3 C). These results indicate that CPC lineage commitment occurs concurrently with expansion of mitochondria.

Mitochondrial Biogenesis is Activated Upon CPC Differentiation

Mitochondrial biogenesis is defined as the growth and division of pre-existing mitochondria, and this process is regulated by PGC-1α, a member of the PPARγ co-activator (PGC) family of transcriptional co-activators (Rowe et al., 2010). To examine activation of mitochondrial biogenesis, I measured PGC-1α (*Ppargc1a*) mRNA levels by qPCR, and found significantly increased levels after 7 days of differentiation (Figure 3.4 A). During mitochondrial biogenesis, existing mitochondria must replicate their own genome (mtDNA) as they divide to ensure that the new mitochondria also contain their own mtDNA. PGC-1α has been shown to stimulate mitochondrial proliferation which correlated with an increase in cellular mitochondrial DNA (mtDNA) content (Wu et al., 1999). I measured mtDNA content by qPCR and confirmed that CPCs had increased mtDNA content after 7 days in DM (Figure 3.4 B). CPCs also exhibited significantly increased expression of mitochondrial OXPHOS protein subunits (Figure 3.4 C). These proteins are part of the respiratory chain located in the inner mitochondrial membrane and are important for generating ATP by oxidative phosphorylation.

AMP-activated Protein Kinase (AMPK) is an intracellular energy sensor activated in response to increased energy demand and has been reported to act as an upstream regulator of PGC-1α (Rowe et al., 2010). Differentiation is an energy-requiring process that increases demand for ATP. Therefore, I investigated whether AMPK may be involved in the CPC differentiation process.

I found increased phosphorylation of AMPK in cultured CPCs upon incubation in differentiation medium, suggesting activation of AMPK (Figure 3.5 A). CPCs have been reported to migrate to the border zone after a myocardial infarction, where they differentiate into cells of various lineages (Fransioli et al., 2008; Huang et al., 2010). I detected CPCs in the border zone of the mouse heart 7 days after myocardial infarction, and the CPCs stained positive for phosphorylated AMPK (Figure 3.5 B). These results suggest that both PGC-1α and AMPK are activated during CPC differentiation.

Inhibition of Mitochondrial Expansion Disrupts CPC Differentiation

To determine the importance of AMPK during CPC differentiation, I inhibited AMPK activity and assessed its effect on CPC differentiation. Treatment of CPCs with 10 μM of Compound C, an AMPK inhibitor, negatively impacted mitochondrial expansion and differentiation. CPCs treated with Compound C displayed mitochondrial clustering in the perinuclear region and reduced GATA-4 nuclear staining after 7 days in DM (Figure 3.6 A). Surprisingly, Compound C treatment led to a compensatory increase in PGC-1α expression (Figure 3.6 B) and increased levels of mitochondrial OXPHOS proteins (Figure 3.6 C) after 7 days of differentiation. However, Compound C treatment led to a decrease in tubulin levels (Figure 3.6 C) and impaired microtubule expansion (Figure 3.7) suggesting that mitochondrial biogenesis is increased but their movement and proper cellular localization is impaired.

My data suggest that mitochondrial transport and network expansion occurs via the microtubule network (Figure 3.2). To confirm the importance of the tubulin network, I treated CPCs with 50 ng/ml of Nocodazole to disrupt tubulin polymerization during 7 days of differentiation. CPCs treated with Nocodazole exhibited mitochondrial and microtubule clustering around the perinuclear region (Figure 3.7), which coincided with reduced GATA-4 staining in the nucleus (Figure 3.8). Similar to the effects of Compound C, Nocodazole treatment resulted in impaired mitochondrial expansion and differentiation in CPCs. These results indicate that the microtubule network is essential for mitochondrial network expansion in differentiating CPCs.

Discussion

I have demonstrated that differentiation of CPCs leads to activation of mitochondrial biogenesis, which correlates with lineage commitment. The new mitochondria are moved along the microtubule network to their new location. Differentiating CPCs activated AMPK and PGC-1α, which are known regulators of mitochondrial biogenesis. AMPK is also important for proper tubulin formation (Nakano et al., 2010). Treatment with Compound C to inhibit AMPK or treatment with Nocodazole to inhibit tubulin polymerization resulted in defective mitochondrial expansion and impaired differentiation of CPCs. Thus, maintaining an intact tubulin network is essential for mitochondrial network expansion, and blocking mitochondrial expansion leads to defective

differentiation. These results show that mitochondria play a critical role in CPC differentiation. Interestingly, my data also show that activation of mitochondrial biogenesis is not affected during differentiation despite inhibition of AMPK, suggesting that there are other upstream regulators of PGC-1α that may compensate for AMPK inactivation. Upstream regulators of PGC-1α include β-adrenergic/cyclic AMP pathway, calcium/calmodulin-dependent protein kinase, p38 MAPK, and nitric oxide (Finck & Kelly, 2006).

Adult stem and progenitor cells carefully regulate self-renewal and differentiation to maintain tissue homeostasis. Adult stem cells such as hematopoietic stem cells reside in hypoxic niches which promotes glycolytic metabolism (Folmes et al., 2012). Although adult stem and progenitor cells do not contain abundant mitochondria, they must be capable of undergoing a metabolic transition and activating oxidative phosphorylation to support the energy demands of differentiation. Since mitochondria are important for regulating cellular metabolism, and metabolic plasticity is important for regulating stemness and differentiation (Gaspar et al., 2014), then mitochondria must play an important role in regulating stemness and differentiation in CPCs.

In addition to mitochondrial status, nutrient sensing pathways such as AMPK allow cells to adapt to energy needs and activate the metabolic switch (Ochocki & Simon, 2013). Mitochondrial biogenesis and metabolic shifts occur early during differentiation of human embryonic stem cells into cardiomyocytes (St John et al., 2005). However, it is still unclear whether activation of

mitochondrial biogenesis precedes loss of pluripotency, or if loss of pluripotency stimulates mitochondrial biogenesis and a metabolic shift (Wanet et al., 2015). Increasing our understanding of the signals that activate mitochondrial biogenesis in CPCs and the mechanisms of how mitochondria regulate CPC self-renewal and differentiation will allow us to develop strategies to improve the therapeutic potential of stem cells for cardiac regenerative medicine.

Chapter 3, in part, was originally published in the *Journal of Biological Chemistry*. Orogo AM, Gonzalez ER, Kubli DA, Baptista IL, Ong SB, Prolla TA, Sussman MA, Murphy AN, Gustafsson ÅB. Accumulation of Mitochondrial DNA Mutations Disrupts Cardiac Progenitor Cell Function and Reduces Survival. *The Journal of Biological Chemistry*. 290(36):22061-75, 2015. The dissertation author was the primary investigator and author of this paper.

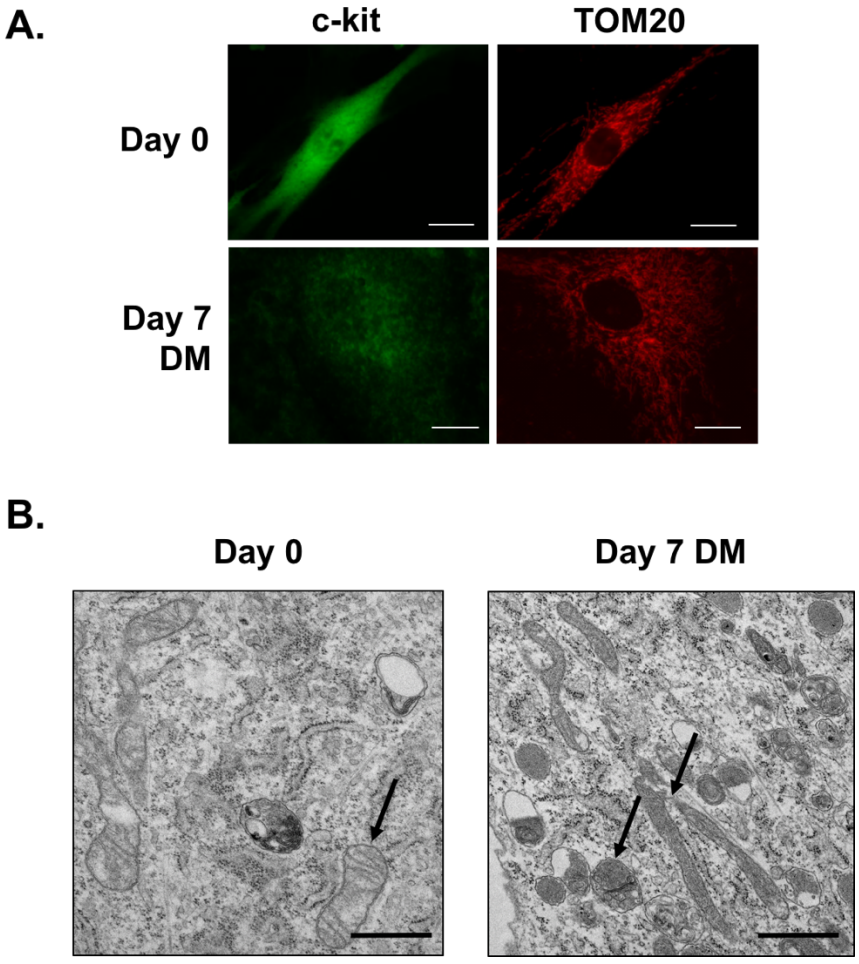

Figure 3.1: CPCs expand their mitochondria during differentiation. A. Mitochondrial content increased and c-kit expression decreased in CPCs after 7 days of incubation in DM. Cells were fixed and stained with antibodies against c-kit and Tom20. Scale bar = 20 μm. **B.** Transmission electron micrographs of CPCs show that mitochondria (arrows) are immature at Day 0. At Day 7, mitochondria appear elongated and have increased electron density. Scale bar = 1 μm.

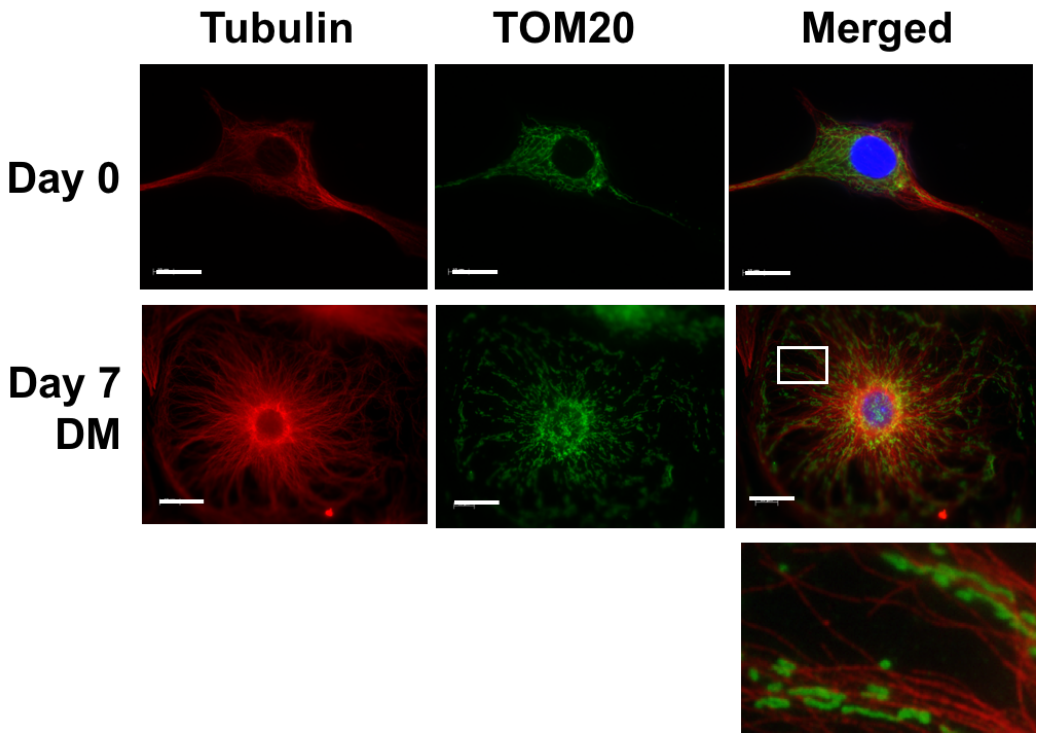

Figure 3.2: Mitochondria co-localize with tubulin in differentiating CPCs. Cells were fixed and stained with antibodies against Tubulin and TOM20. Scale bar = 20 μm.

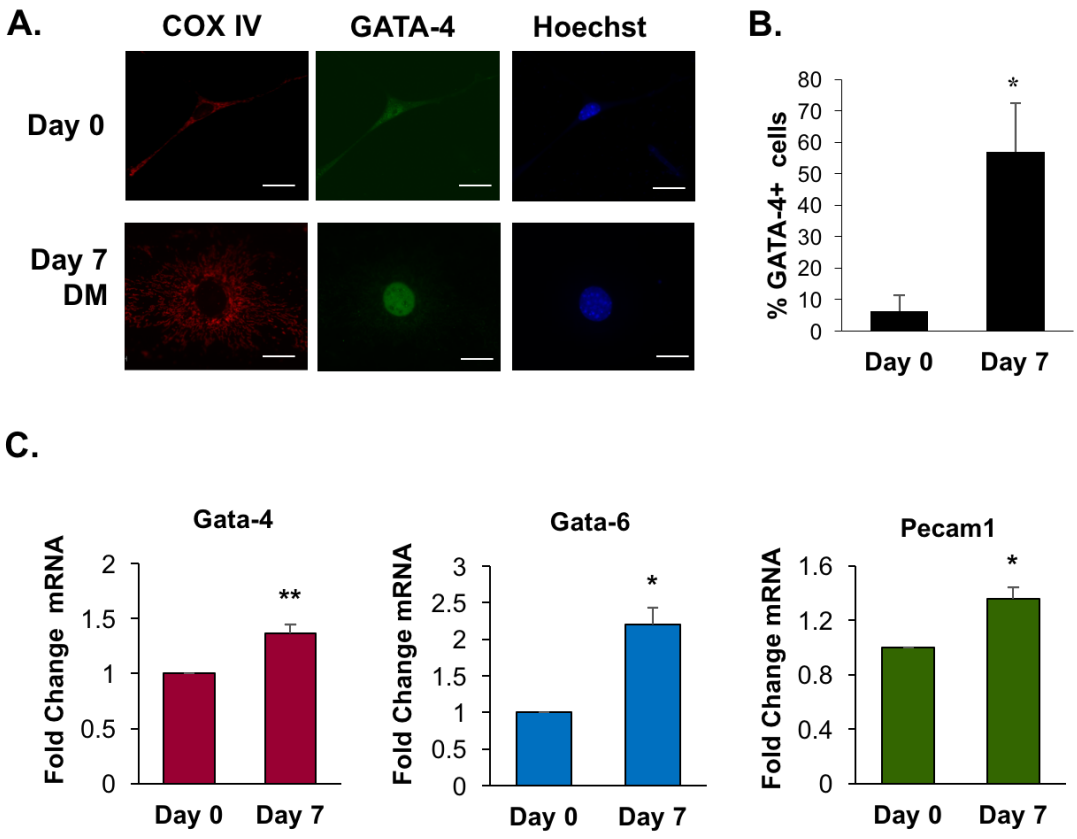

Figure 3.3: Mitochondrial expansion correlates with lineage commitment. **A.** CPCs were positive for the cardiac lineage marker GATA-4 after 7 days of differentiation. CPCs were fixed at Day 0 and Day 7 and stained with antibodies against COXIV and GATA-4. Scale bar = 20 μm. **B.** Percentage of GATA-4 positive cells were quantified (n=3). **C.** Analysis of real-time qPCR of *Gata-4* (n=6), *Gata-6* (n=3), and *Pecam1* (n=4) gene expression at day 0 and day 7. (*p<0.05; **p<0.01)

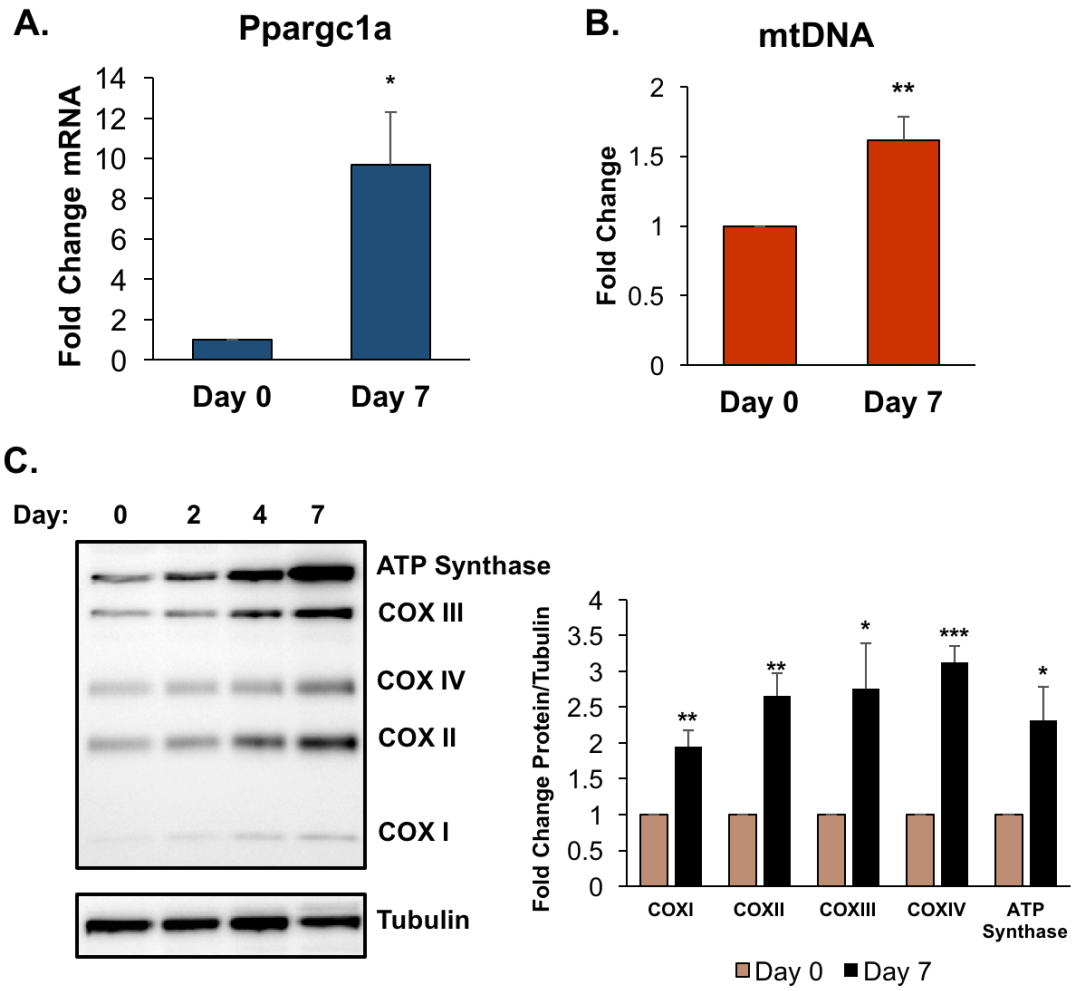

Figure 3.4: Mitochondrial biogenesis is activated upon CPC differentiation. A. Real time qPCR of mitochondrial biogenesis regulator PGC-1α (*Ppargc1a*) gene expression at day 0 and day 7 (n=4). **B.** Real-time qPCR of mtDNA content at day 0 and day 7 (n=8). **C.** Representative Western blot and quantification of mitochondrial OXPHOS proteins before and after 7 days of differentiation (n=3). (*p<0.05; **p<0.01, ***p<0.001)

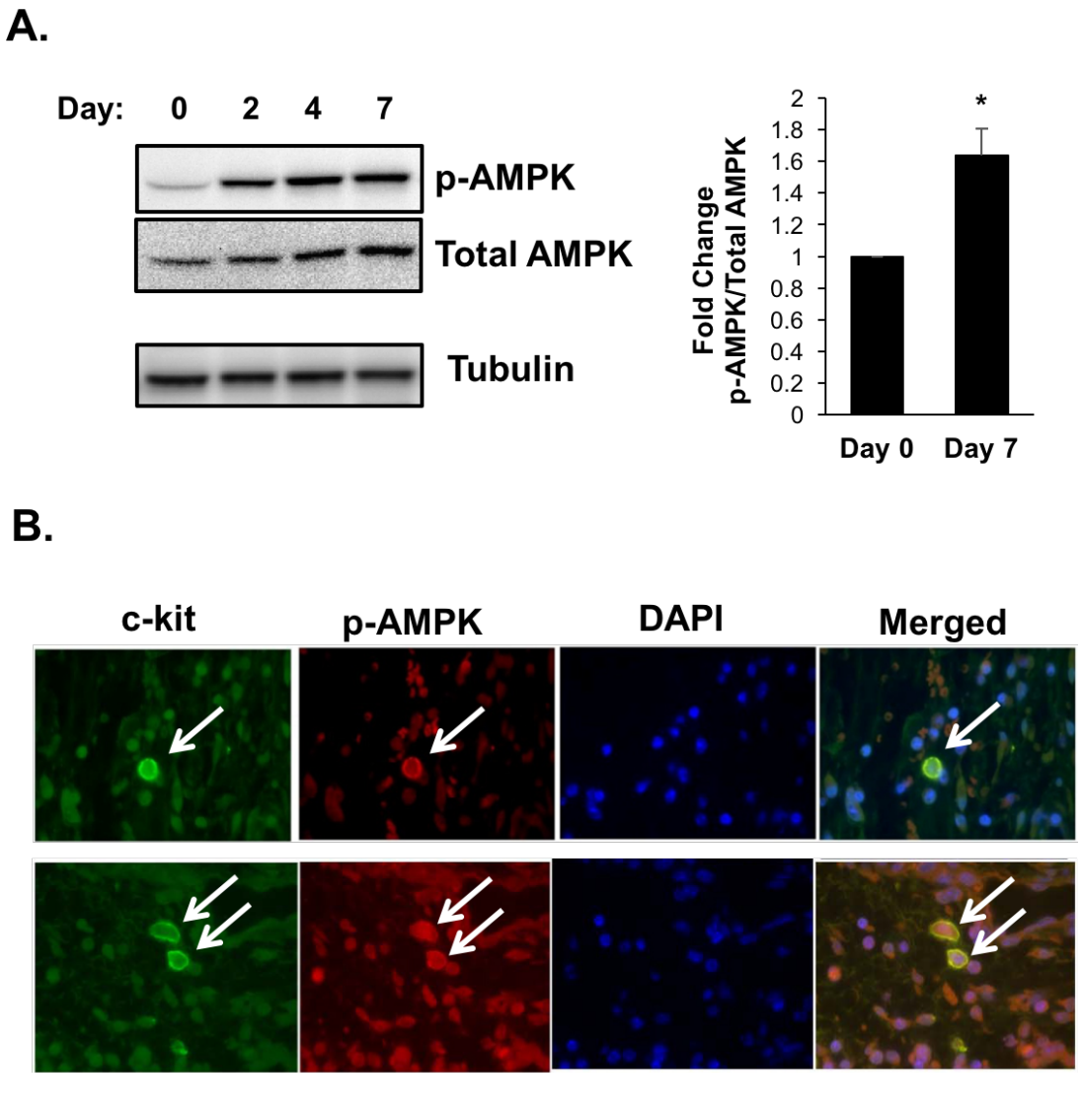

Figure 3.5: AMPK is activated during CPC differentiation. A. Phosphorylation of AMPK was increased upon differentiation of cultured CPCs. The presence of phosphorylated AMPK was assessed by Western blot and bands were quantified (n=3). **B.** Mouse heart tissue sections were fixed and stained with antibodies against c-kit and p-AMPK seven days post-myocardial infarction. C-kit+ CPCs in the border zone stained positive for p-AMPK (arrows). (*$p<0.05$)

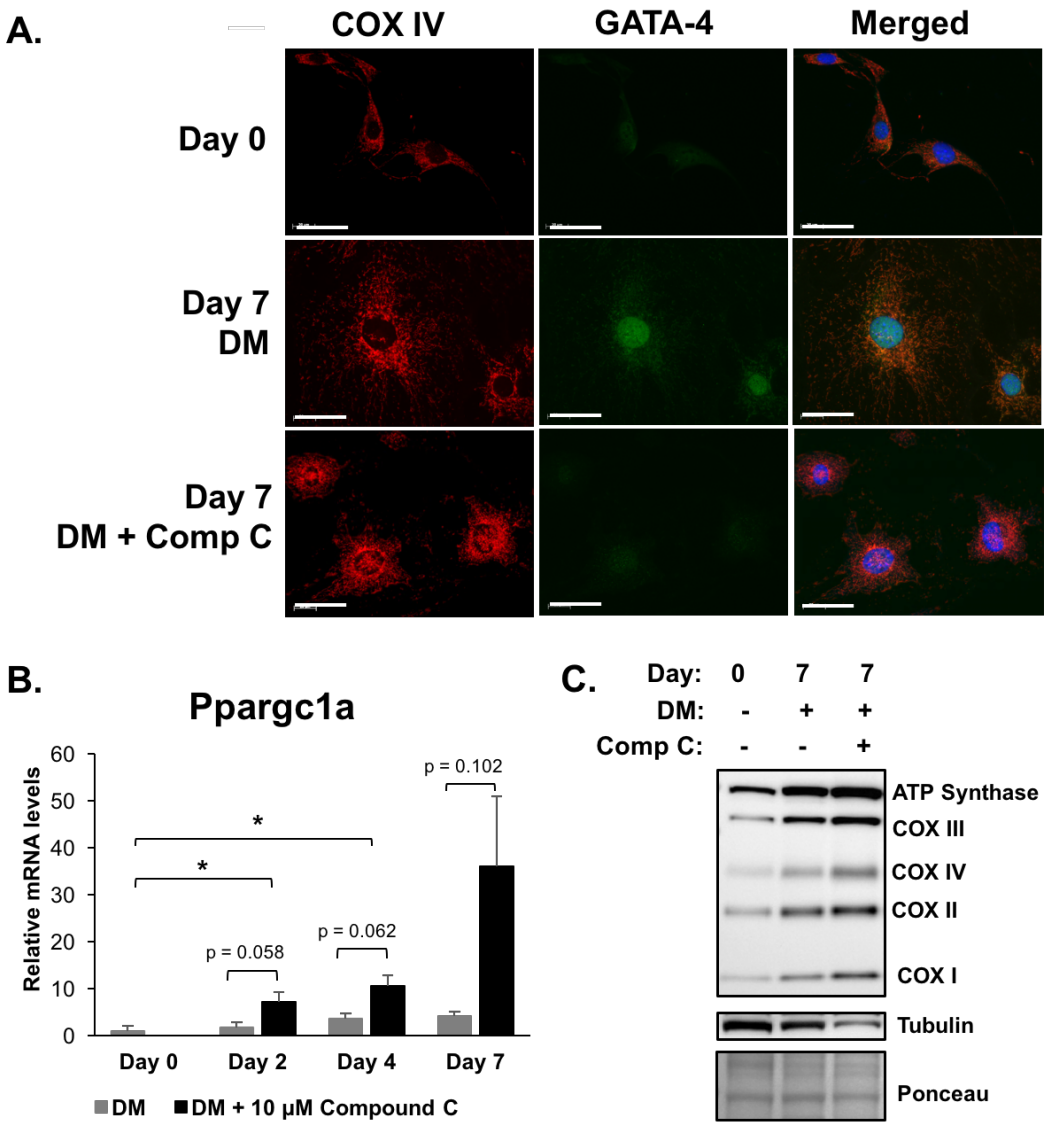

Figure 3.6: Inhibition of AMPK impairs CPC differentiation but not mitochondrial biogenesis. A. CPCs treated with 10 μM Compound C exhibited mitochondrial clustering in the perinuclear region and reduced staining for GATA-4. Cells were stained with antibodies against COXIV and GATA-4. Scale bar = 40 μm. **B.** CPCs treated with Compound C exhibited a compensatory increase in PGC-1α (*Ppargc1a*) expression at 7 days of differentiation (n=3). **C.** Representative Western blot of OXPHOS proteins and Tubulin levels after Compound C treatment. (*p<0.05)

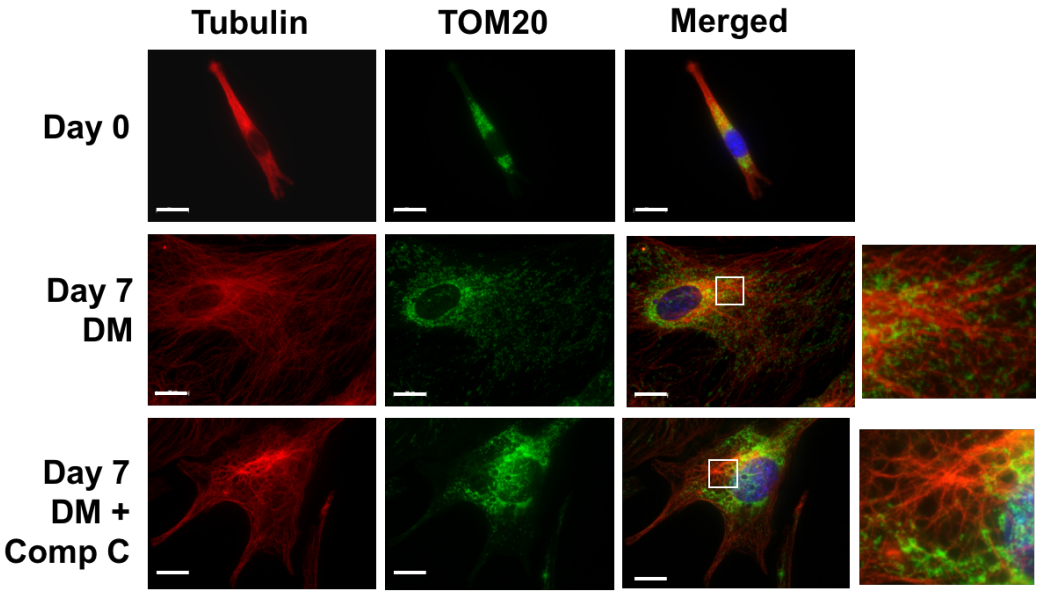

Figure 3.7: Inhibition of the microtubule network impairs mitochondrial expansion in CPCs. Differentiating CPCs had impaired mitochondrial expansion along the microtubule network in the presence of Compound C. Cells were stained for Tubulin and TOM20. Scale bar = 20 μm.

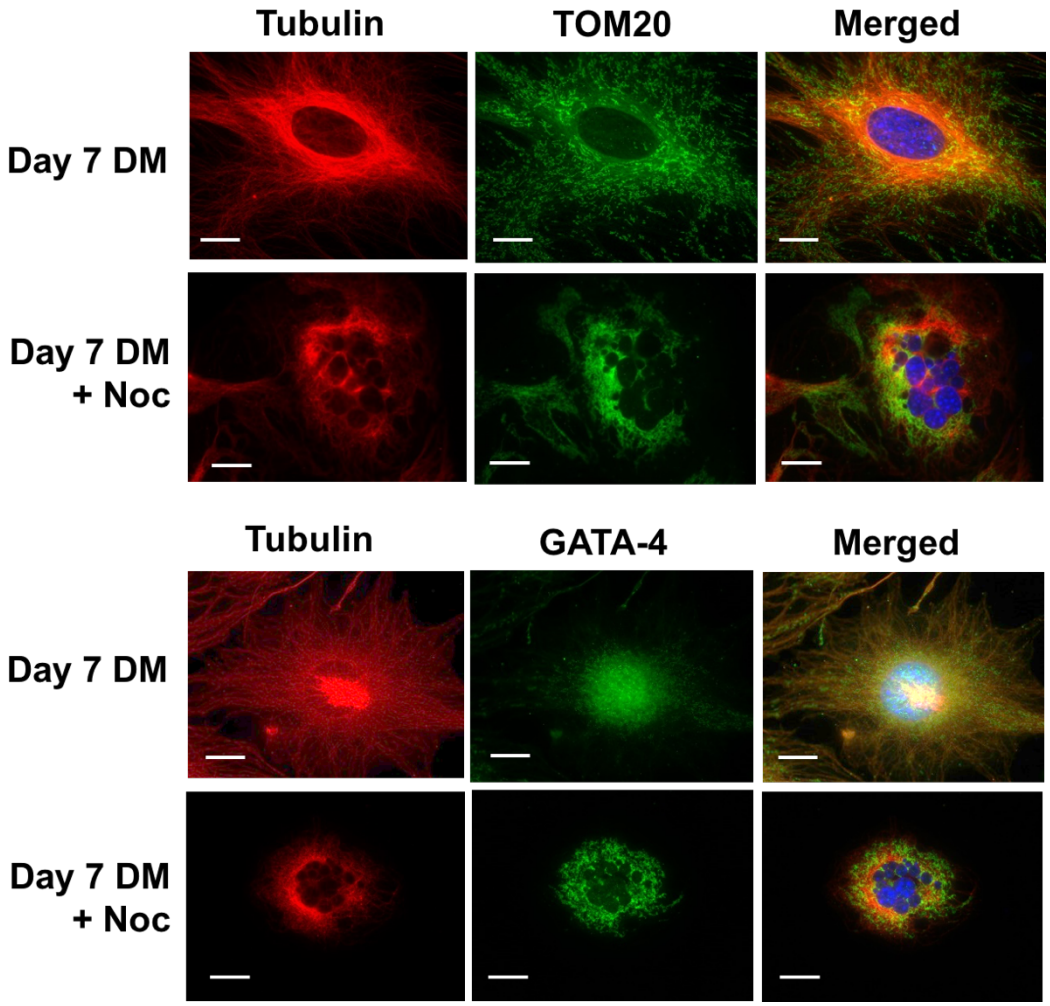

Figure 3.8: Inhibition of the microtubule network impairs CPC differentiation. CPCs had impaired mitochondrial network expansion and differentiation after 7 days in the presence of 50 ng/ml Nocodazole. Cells were stained for Tubulin, TOM20, and GATA-4. Scale bar = 20 μm.

CHAPTER 4: ACCUMULATION OF MITOCHONDRIAL DNA MUTATIONS IMPAIRS CARDIAC PROGENITOR CELL SURVIVAL AND FUNCTION

Introduction

Mitochondria contain their own genome which encodes for several subunits of the respiratory complexes and ATP Synthase. Mitochondrial DNA (mtDNA) mutations accumulate with age in various tissues, and this can lead to dysfunctional mitochondria (Dai et al., 2009; Corral-Debrinski, Horton, et al., 1992; Wanagat et al., 2002; Khaidakov et al., 2003). Mitochondrial DNA polymerase γ (POLG) is the only DNA polymerase found in the mitochondria and is responsible for both replication and repair of mtDNA (Kaguni, 2004). Mice expressing a proofreading-deficient POLG enzyme accumulate mtDNA mutations in cells faster than WT mice, which leads to accelerated aging and reduced lifespan (Trifunovic et al., 2004; Kujoth et al., 2005). Thus, these mice are useful tools to investigate the relationship between mtDNA mutations and aging.

Mitochondria play an important role in regulating self-renewal and differentiation of stem and progenitor cells. I have shown in Chapter 3 that mitochondrial biogenesis is activated upon differentiation in cardiac progenitor cells (CPCs), and mitochondrial expansion along the microtubule network correlates with lineage commitment. However, very little is known about how aging and accumulation of mtDNA mutations affect CPC function. The incidence

of heart disease increases with age, and most candidates for autologous stem cell therapy are older. CPCs from older patients have reduced regenerative potential and may not be the optimal choice for restoring myocardial function (Mohsin et al., 2013; Hariharan et al., 2015). Here, I investigated the effect of accumulating mtDNA mutations on CPC survival, proliferation, and differentiation to better understand the relationship between aging and CPC function.

Results

Accumulation of mtDNA mutations impairs CPC proliferation and increases susceptibility to cell death

To explore the role of mitochondria in CPC function and survival, I isolated CPCs from 2 month-old mice expressing a proofreading-defective POLG enzyme and their wild-type (WT) litter mates. The POLG mice undergo premature aging and develop cardiomyopathy with a reduced lifespan due to accumulation of mtDNA mutations (Kujoth et al., 2005). However, at 2 months of age, I observed no significant differences in body weight, heart weight/body weight, or lung weight/body weight ratios (Figure 4.1 A) and cardiac function measured by echocardiography (Figure 4.1 B) in POLG mice compared with age-matched WT litter mates. To examine the effect of the POLG mutation on mitochondrial respiration, mitochondria were isolated from the hearts of 2 month-old WT and POLG mice and mitochondrial oxygen consumption was

assessed. I found no differences in Complex I, Complex II, and Complex IV activity (Figure 4.2 A), respiratory control ratio (Figure 4.2 B), and mitochondrial OXPHOS protein content (Figure 4.2 C). Furthermore, I examined mitochondrial ultrastructure in the heart by transmission electron microscopy and observed similar mitochondrial morphology and organization in WT and POLG hearts at this age (Figure 4.2 D). Overall, these data indicate that the POLG mutation does not affect cardiac and mitochondrial function at this early age.

Next, I investigated whether CPCs isolated from the hearts of these 2 month-old mice were affected by the mutated POLG. Proliferation is important for self-renewal and maintenance of the CPC population in the heart, and I found that the POLG CPCs had significantly reduced proliferation compared with WT CPCs (Figure 4.3 A). Stem cells with declining replicative capacity undergo senescence, which contributes to the aging process. I assessed the activity of senescence-activated β-galactosidase, which accumulates in senescent cells. I found that the POLG CPCs exhibited increased accumulation of this enzyme compared to WT CPCs (Figure 4. 3 B). In addition, the POLG CPCs were more sensitive to cell death after treatment with H_2O_2 (Figure 4.4 A). Treatment with doxorubicin, an anthracycline topoisomerase inhibitor, or sunitinib, a tyrosine kinase inhibitor, also resulted in increased cell death in POLG CPCs (Figure 4.4 B and C). These data suggest that accumulation of mtDNA mutations in the POLG CPCs reduces their proliferative capacity, induces senescence, and increases their susceptibility to stress.

mtDNA mutations contribute to abnormal mitochondrial morphology and reduced differentiation potential

Cells undergo alterations in mitochondrial morphology to adapt to changes in cellular environment (Kasahara & Scorrano, 2014). When examining the effect of accumulating mtDNA mutations on mitochondrial morphology, I discovered that the mutant POLG CPCs contained fragmented mitochondria under baseline conditions (Figure 4.5 A and B). Although WT CPCs increased in cell size and expanded their mitochondrial network after incubation in DM, POLG CPCs maintained their fragmented mitochondria. Instead, the mitochondria clustered in the perinuclear region and failed to move in response to the differentiation stimulus (Figure 4.5 A). The abnormal mitochondrial morphology was also associated with reduced activation of the differentiation program in the POLG CPCs. I observed significantly fewer GATA-4-positive POLG CPCs compared with WT after incubation in DM (Figure 4.5 C). The POLG CPCs also had significantly reduced levels of *Gata-4* transcripts compared with WT CPCs after incubation in DM (Figure 4.5 D). These data demonstrate that accumulation of mtDNA mutations leads to abnormal mitochondrial morphology and impaired activation of the differentiation program in CPCs.

The fragmented mitochondrial morphology suggested that proteins involved in mitochondrial dynamics may be altered in POLG CPCs. Surprisingly, I observed a reduction in the mitochondrial fission protein DRP1 in POLG CPCs

after 7 days in DM (Figure 4.6). Interestingly, mitochondrial fusion proteins MFN1 and MFN2 were increased in WT CPCs, but not in POLG CPCs, upon activation of differentiation (Figure 4.6). Thus, there is a shift in the balance between fission and fusion proteins toward fusion in WT CPCs, but not in POLG CPCs, upon activation of differentiation. Furthermore, I analyzed mitochondrial ultrastructure in CPCs by transmission electron microscopy and saw drastic differences between WT and POLG CPCs. Mitochondria in undifferentiated WT CPCs had underdeveloped cristae that became more electron-dense upon activation of the differentiation program (Figure 4.7). The mitochondria also became more elongated. In contrast, mitochondria in POLG CPCs were swollen with abnormal cristae structure under baseline conditions and failed to increase cristae density after differentiation (Figure 4.7). These data suggest that accumulation of mtDNA mutations leads to impaired mitochondrial dynamics and differentiation program in the CPCs.

POLG CPCs have impaired mitochondrial biogenesis and energetics

The abnormal mitochondrial morphology and distribution in POLG CPCs are indicators of defective mitochondrial function. Because the primary function of mitochondria is to supply the cell with energy via oxidative phosphorylation (OXPHOS), I compared mitochondrial OXPHOS protein levels between WT and POLG CPCs. Incubation of WT CPCs in DM resulted in increased expression of OXPHOS proteins. In contrast, POLG CPCs had reduced levels of select

OXPHOS proteins, most notably in Complex III and Complex IV subunits (Figure 4.8 A). I observed no increase in nuclear- and mitochondrial-encoded subunits of Complex IV in the POLG CPCs after incubation in DM for 7 days (Figure 4.8 B). The baseline protein levels were already significantly lowered in POLG CPCs compared with WT at day 0. Interestingly, I found that Complex IV Subunit 1 (*Cox1*) and Subunit 4 (*Cox4i1*) transcripts were similar in WT and POLG CPCs at day 0 (Figure 4.8 C), suggesting that the differences in protein levels between WT and POLG CPCs may be attributed to reduced protein stability in the POLG CPCs.

I previously found that PGC-1α is upregulated in response to DM in WT CPCs (Figure 3.4 A). Interestingly, I found that in contrast to WT CPCs, the POLG CPCs failed to induce mitochondrial biogenesis transcriptional co-activators PGC-1α or PGC-1β to the same extent as WT CPCs during differentiation (Figure 4.9). Because the POLG mouse model accumulates mtDNA mutations at an accelerated rate, and aging also leads to accumulation of mtDNA mutations, I also compared mitochondrial content in CPCs from 3 month-old and 24 month-old mice. I found that CPCs from the aging mice had reduced baseline levels of certain OXPHOS subunits at day 0 (Figure 4.10 A and B), similar to the POLG CPCs. The CPCs from the 24 month-old mice also failed to increase OXPHOS proteins during 7 days of incubation in DM (Figure 4.10 A and B). Overall, these data suggest that accumulation of mtDNA

mutations and aging impair the activation of mitochondrial biogenesis in response to differentiation.

The data indicated that POLG CPCs have abnormal mitochondrial structure and contain reduced levels of critical proteins involved in OXPHOS. Therefore, I assessed the level of mitochondrial respiration in WT and POLG CPCs by measuring oxygen consumption using the Seahorse XF Analyzer. In WT CPCs, increased oxygen consumption rate corresponded with increased cell number in response to the mitochondrial uncoupler FCCP (Figure 4.11 A). Surprisingly, POLG CPCs had no detectable oxygen consumption regardless of cell number (Figure 4.11 B), indicating that these cells have shut down mitochondrial respiration. The OXPHOS complexes are also responsible for generating the mitochondrial membrane potential, which is used by the F_0F_1-ATPase for ATP synthesis (Hatefi, 1985). I confirmed that the POLG CPCs had significantly reduced mitochondrial membrane potential as assessed by reduced TMRM staining (Figure 4.12). TMRM uptake by mitochondria is dependent on the membrane potential. However, cellular ATP levels were similar in WT and POLG CPCs (Figure 4.13 A). Therefore, I examined whether the POLG CPCs relied on glycolysis to support their energy demands by assessing extracellular lactate, a glycolytic byproduct. I found that the POLG CPCs had significantly increased extracellular L-lactate compared with WT CPCs (Figure 4.13 B). The addition of 2-deoxyglucose to the growth medium to inhibit glycolysis resulted in rapid death of the POLG CPCs (Figure 4.13 C).

Overall, these data suggest that POLG CPCs depend on glycolysis to meet their energy demands.

Studies have found that differentiation is associated with a metabolic transition from glycolysis to OXPHOS (Chung et al., 2007; Chung et al., 2010). Because the data indicate that POLG CPCs do not utilize OXPHOS for ATP production and differentiation is associated with an increase in energy demand, I examined the effect of differentiation on cell survival in these cells. I observed that a significant number of POLG CPCs underwent cell death in DM (Figure 4.14 A). To gain further insight into the metabolic switch that occurs during differentiation, I analyzed levels of glycolytic enzymes in WT and POLG CPCs. I found that mitochondria-associated Hexokinase I increased in WT during differentiation but remained low in POLG CPCs. Hexokinase II, PKM1/2, and GAPDH decreased with time upon incubation in DM in both WT and POLG CPCs (Figure 4.14 B and C). These results suggest that both WT and POLG CPCs down-regulated cytosolic glycolysis during differentiation. However, because POLG CPCs are unable to concurrently activate OXPHOS, the resulting energy deficiency combined with increased energy demand leads to activation of cell death.

Discussion

In this chapter, I demonstrated that acquiring mtDNA mutations disrupted mitochondrial function, which led to a decline in the replicative and regenerative

capacities of CPCs. The POLG CPCs relied on glycolysis for energy production and were unable to transition from glycolysis to mitochondrial respiration. Activation of the differentiation program led to deactivation of glycolysis in both WT and POLG CPCs, but the POLG CPCs were unable to meet the increased energy demand and underwent cell death instead. These findings demonstrate the importance of mtDNA integrity in CPC homeostasis and regenerative potential, and the consequences of accumulating mtDNA mutations.

This study suggests that susceptibility to mtDNA mutations differs between cells within the same tissue. At 2 months of age, the POLG mice had normal cardiac structure and function, suggesting that post-mitotic tissues such as the heart are less susceptible to mtDNA mutations than tissues with more rapid cellular turnover such as CPCs. Although quiescent CPCs reside in niches in the heart, they still proliferate to maintain their pool as well as migrate to the border zone after a myocardial infarction where they can proliferate and differentiate (Huang et al., 2010; Fransioli et al., 2008). In addition, isolating and expanding CPCs in culture increases the frequency of mtDNA mutations and accelerates the aging phenotype. Thus, accumulation of mtDNA in CPCs result in dysfunctional mitochondria that could impair their ability to participate in the repair process.

Chapter 4, in part, was originally published in the *Journal of Biological Chemistry*. Orogo AM, Gonzalez ER, Kubli DA, Baptista IL, Ong SB, Prolla TA,

Sussman MA, Murphy AN, Gustafsson ÅB. Accumulation of Mitochondrial DNA Mutations Disrupts Cardiac Progenitor Cell Function and Reduces Survival. *The Journal of Biological Chemistry*. 290(36):22061-75, 2015. The dissertation author was the primary investigator and author of this paper.

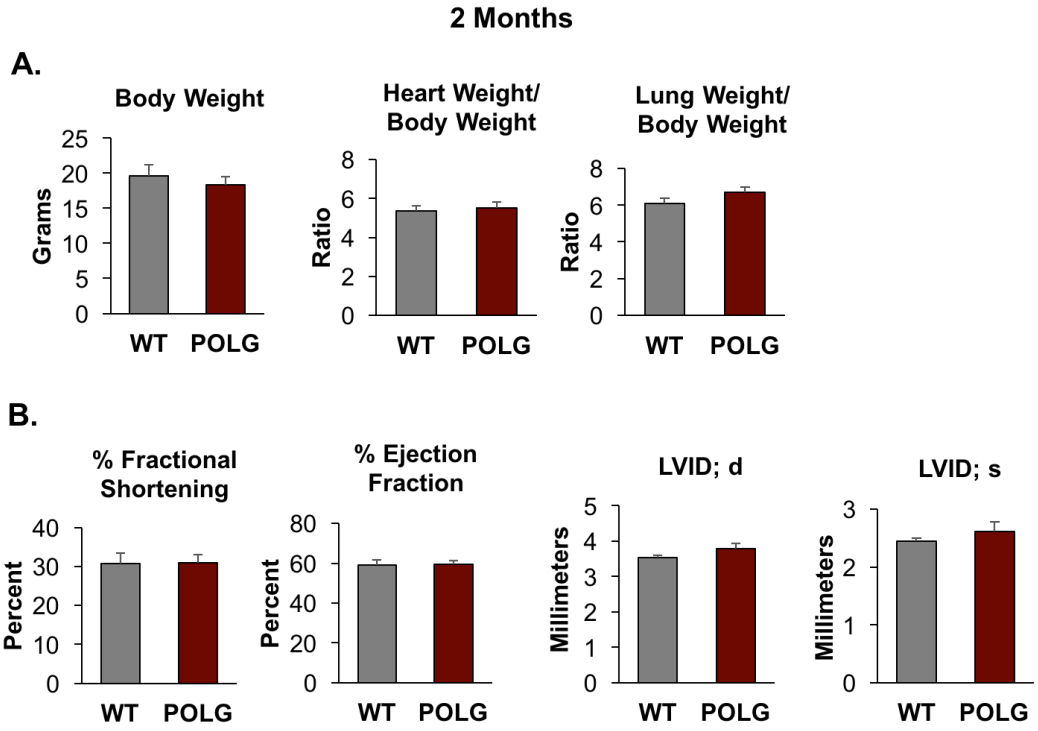

Figure 4.1: Baseline parameters and echocardiography of WT and POLG mice at 2 months. A. Average body weight, heart weight/body weight, and lung weight/body weight ratios of WT and POLG mice at 2 months of age (n=5). **B.** Echocardiographic analysis of % fractional shortening, % ejection fraction, left ventricular internal dimension at diastole (LVID; d), and left ventricular internal dimension at systole (LVID; s) (n=4).

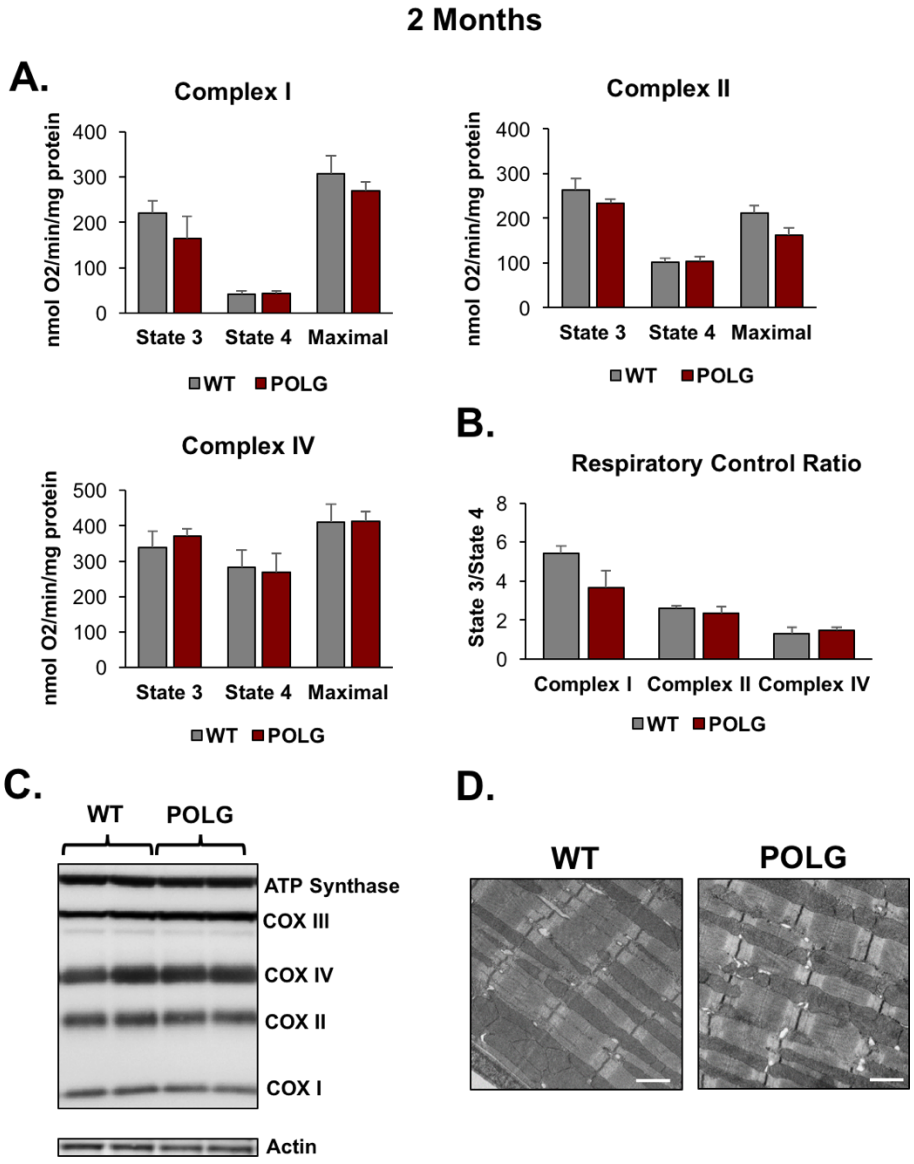

Figure 4.2: Mitochondrial function is not impaired in POLG mouse hearts at 2 months. A. Respiration measurements of isolated mitochondria from the hearts of 2 month-old WT and POLG mice. Oxygen consumption was measured after addition of substrates and inhibitors specific for Complex I, Complex II, and Complex IV activity using an oxygen electrode (n=3). **B.** Respiratory control ratio was calculated by dividing state 3/state 4 oxygen consumption (n=3). **C.** Representative Western blot of mitochondrial OXPHOS proteins in WT and POLG mouse hearts at 2 months of age (n=2). **D.** Transmission electron micrographs show normal mitochondrial ultrastructure in the hearts of 2 month-old WT and POLG mice. Scale bar = 1 μm.

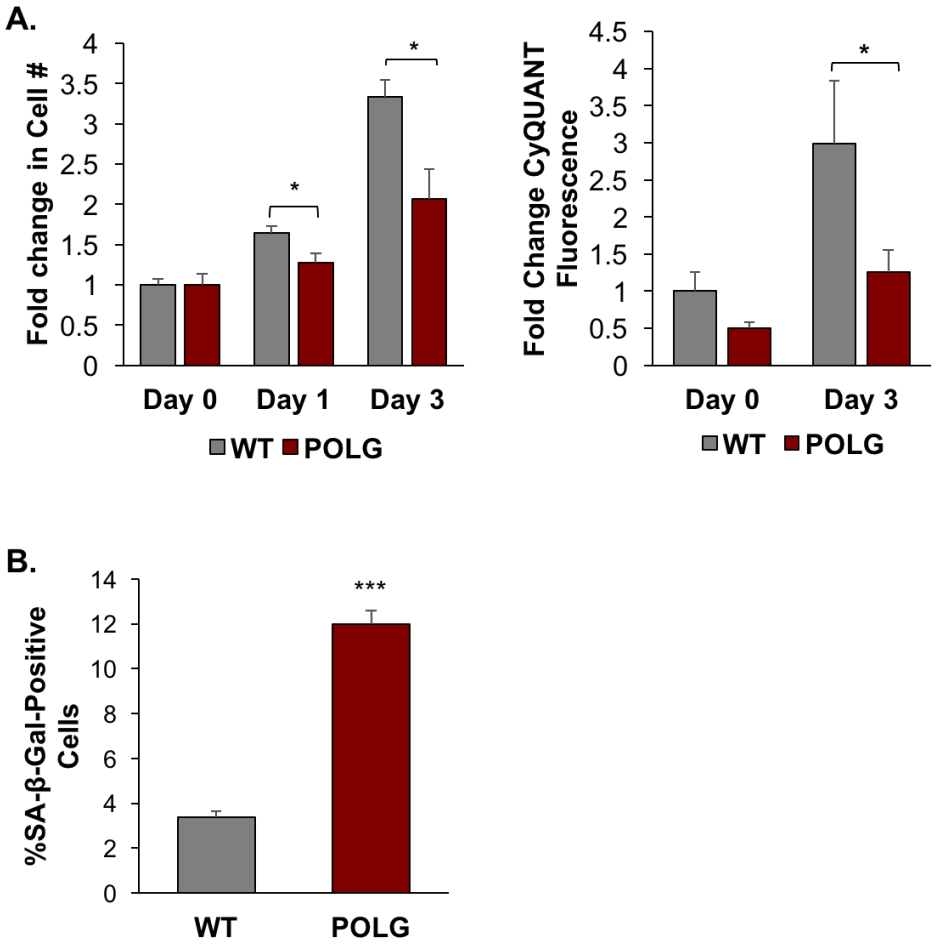

Figure 4.3: POLG CPCs exhibit reduced proliferation and increased senescence. A. WT and POLG CPCs were incubated in growth medium for up to 3 days and proliferation was determined by assessing changes in cell number (n=4) or by CyQUANT fluorescence (n=9). **B.** Senescence-activated β-galactosidase activity was detected in WT and POLG CPCs (n=3). (*$p<0.05$; ***$p<0.001$)

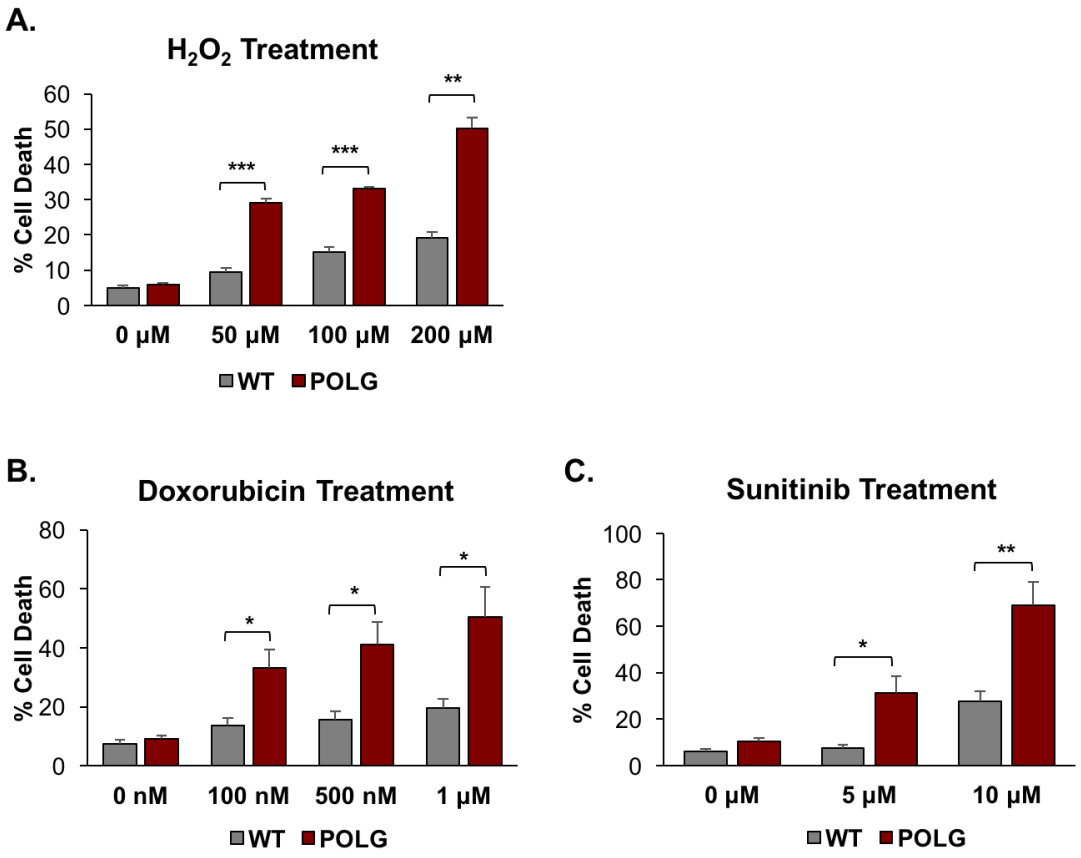

Figure 4.4: POLG CPCs are more sensitive to stress. WT and POLG CPCs were treated with **A.** H_2O_2 (n=3), **B.** Doxorubicin (n=3), and **C.** Sunitinib (n=3). CPCs were treated for 24 hours and cell death was assessed using YO-PRO-1 staining. (*p<0.05; **p<0.01; ***p<0.001)

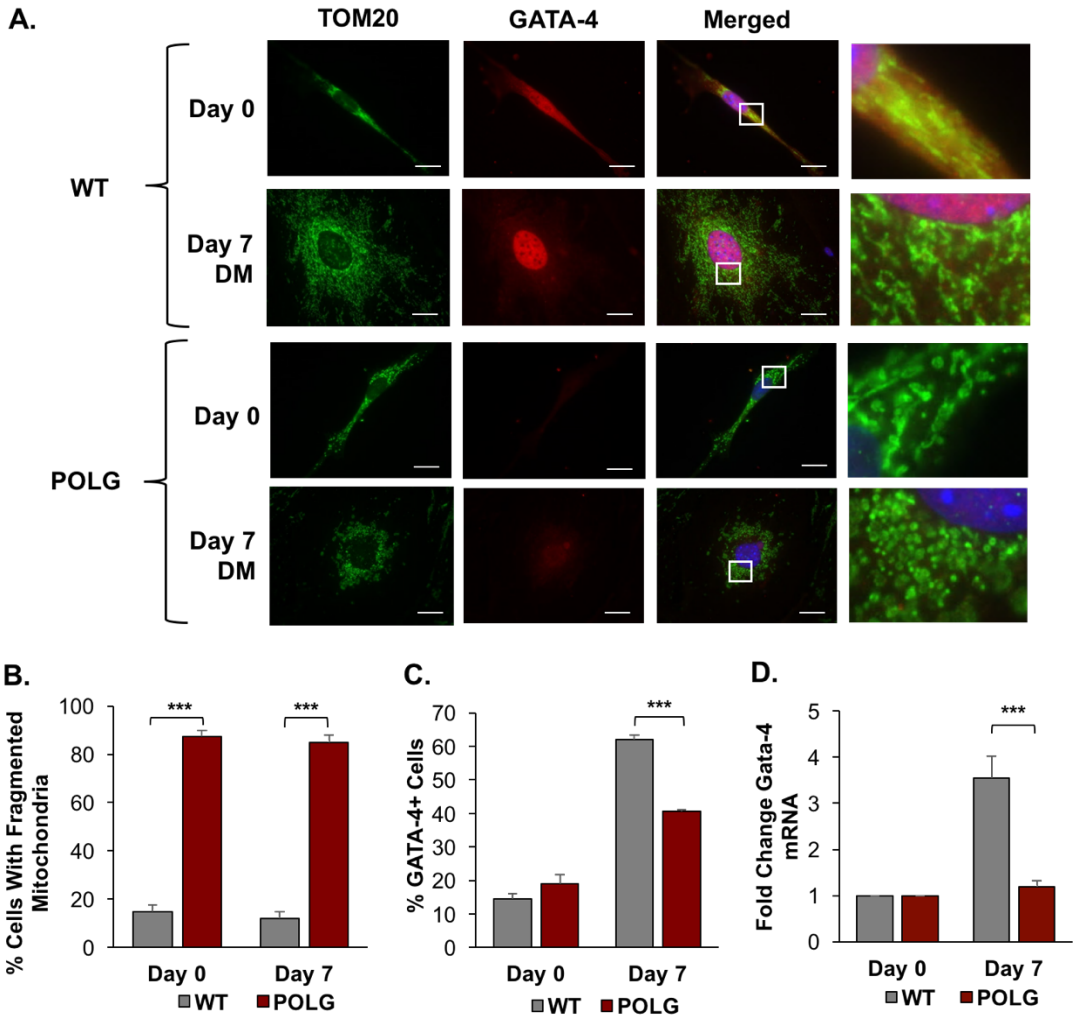

Figure 4.5: POLG CPCs have abnormal mitochondrial morphology and impaired differentiation. A. The mitochondrial network in POLG CPCs had a fragmented appearance at both day 0 and day 7 of differentiation. Cells were fixed and stained for TOM20 and GATA-4. Scale bar = 20 μm. **B.** Quantitation of percentage of cells containing fragmented mitochondria (n=3). **C.** Quantitation of percentage of cells positive for GATA-4 (n=3). **D.** Real-time qPCR analysis of *Gata-4* transcript levels in WT and POLG CPCs at day 0 and day 7 (n=4). (***p<0.001)

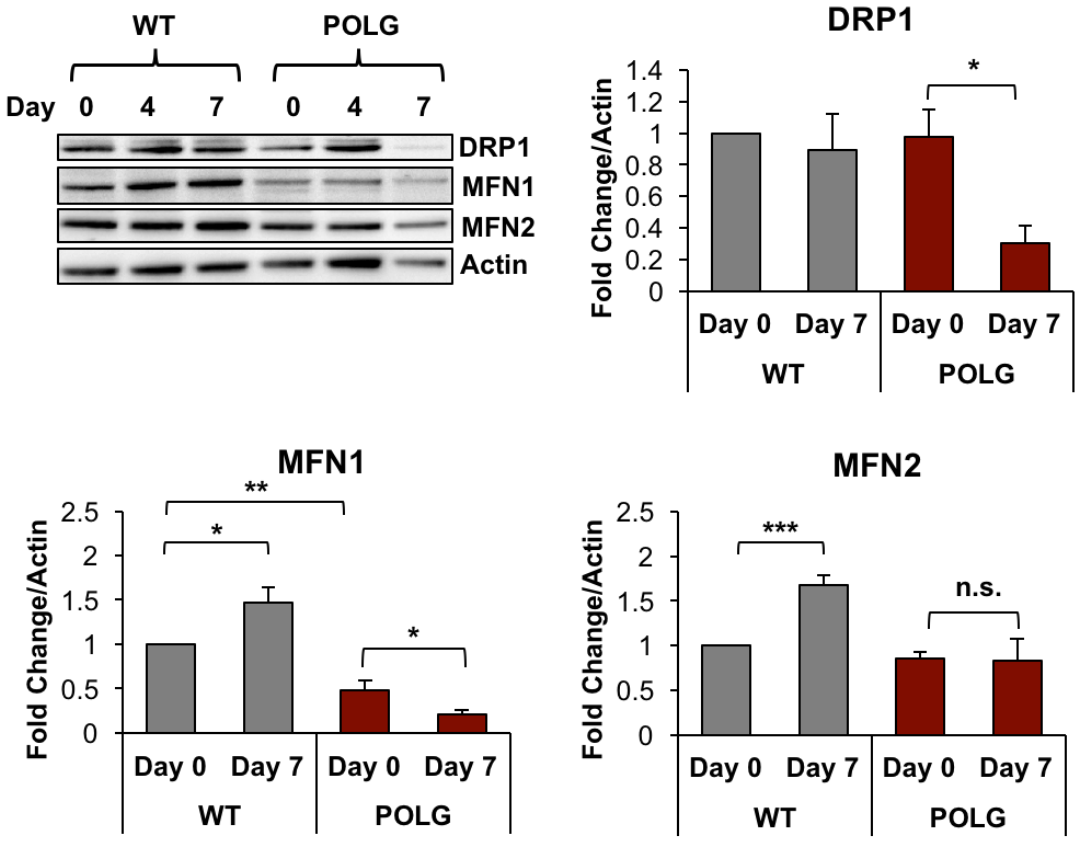

Figure 4.6: Western blots of mitochondrial fusion and fission proteins in WT and POLG CPCs. Representative Western blots and band quantitation of mitochondrial fission protein DRP1 (n=4) and mitochondrial fusion proteins MFN1 (n=5) and MFN2 (n=4) in WT and POLG CPCs at day 0 and day 7 in DM. (*p<0.05; **p<0.01; ***p<0.001)

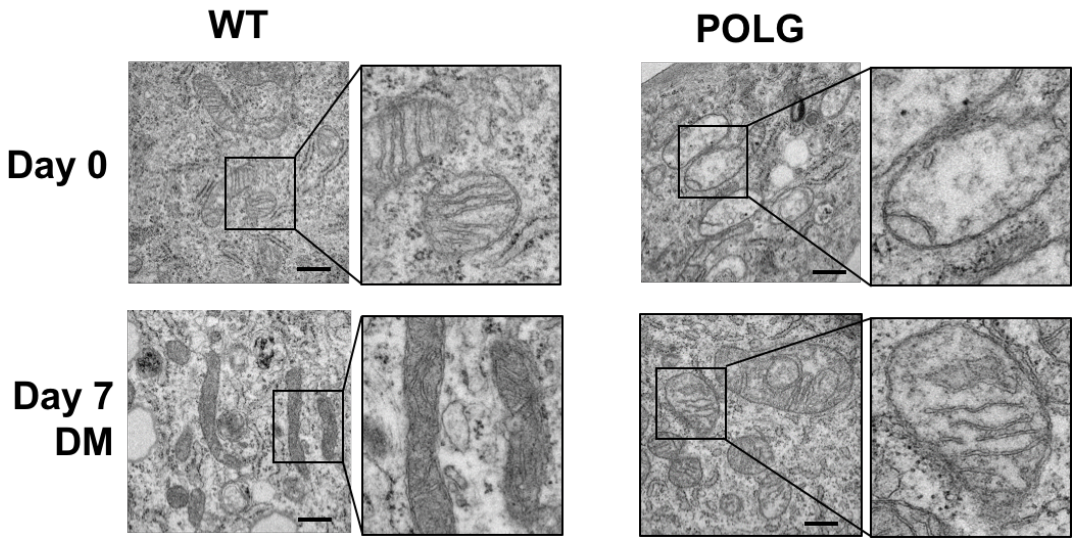

Figure 4.7: Transmission electron micrographs show abnormal mitochondrial ultrastructure in POLG CPCs. Transmission electron micrographs of WT and POLG CPCs under baseline conditions and after incubation in DM. CPCs contain morphologically immature mitochondria. Mitochondrial electron density increased in WT CPCs after 7 days of differentiation. POLG CPCs had abnormal mitochondrial structure with very little cristae structure. Scale bar = 500 nm.

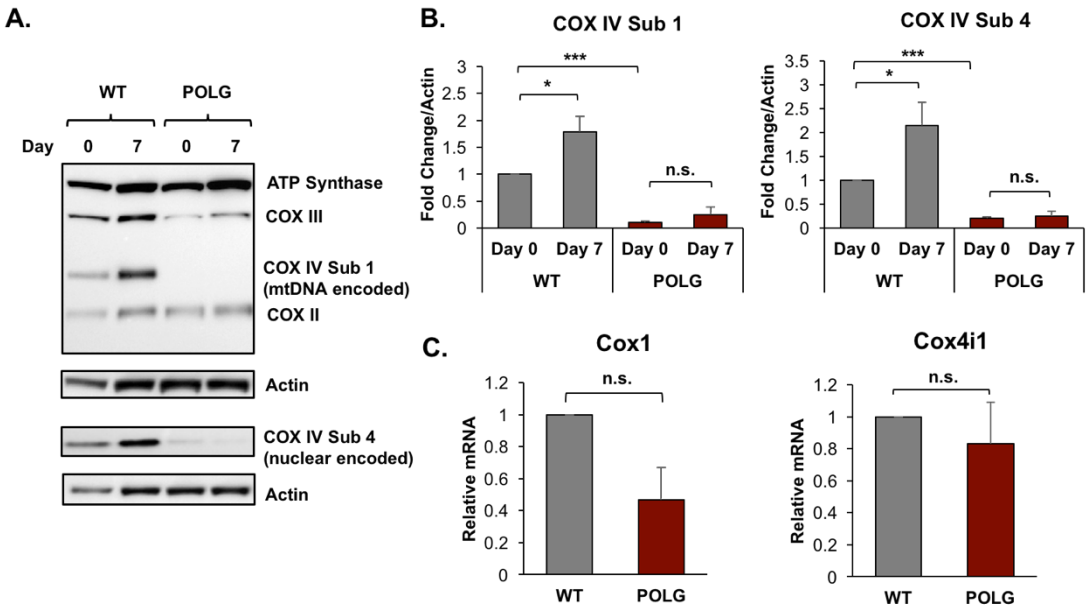

Figure 4.8: Western blots and qPCR analysis of OXPHOS proteins in WT and POLG CPCs. A. Representative Western blots revealed reduced levels of selective OXPHOS subunits in POLG CPCs. **B.** Quantitation of mtDNA-encoded Complex IV subunit 1 (n=5) and nuclear-encoded subunit 4 (n=5) protein expression. **C.** Real-time qPCR analysis of Complex IV subunit 1 (*Cox1*) and Complex IV subunit 4 (*Cox4i1*) gene expression at baseline (n=3). (*p<0.05; ***p<0.001)

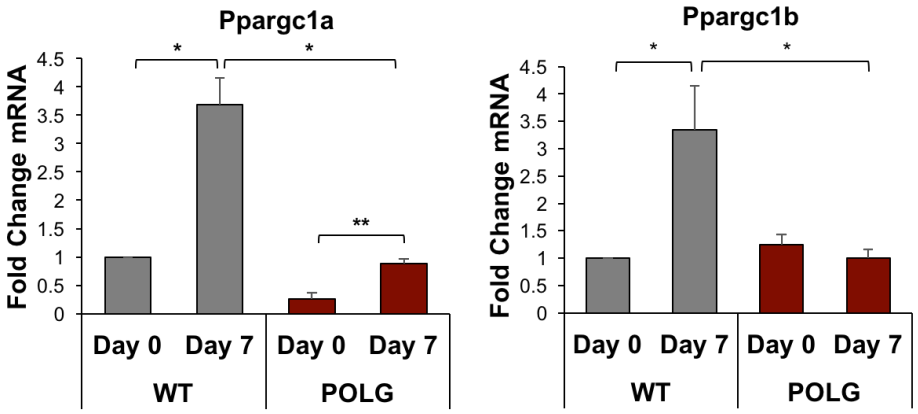

Figure 4.9: POLG CPCs have impaired activation of mitochondrial biogenesis upon differentiation. Real-time qPCR analysis of PGC-1α (*Ppargc1a*) and PGC-1β (*Ppargc1b*) gene expression at day 0 and day 7 in WT and POLG CPCs (n=3). (*p<0.05; **p<0.01)

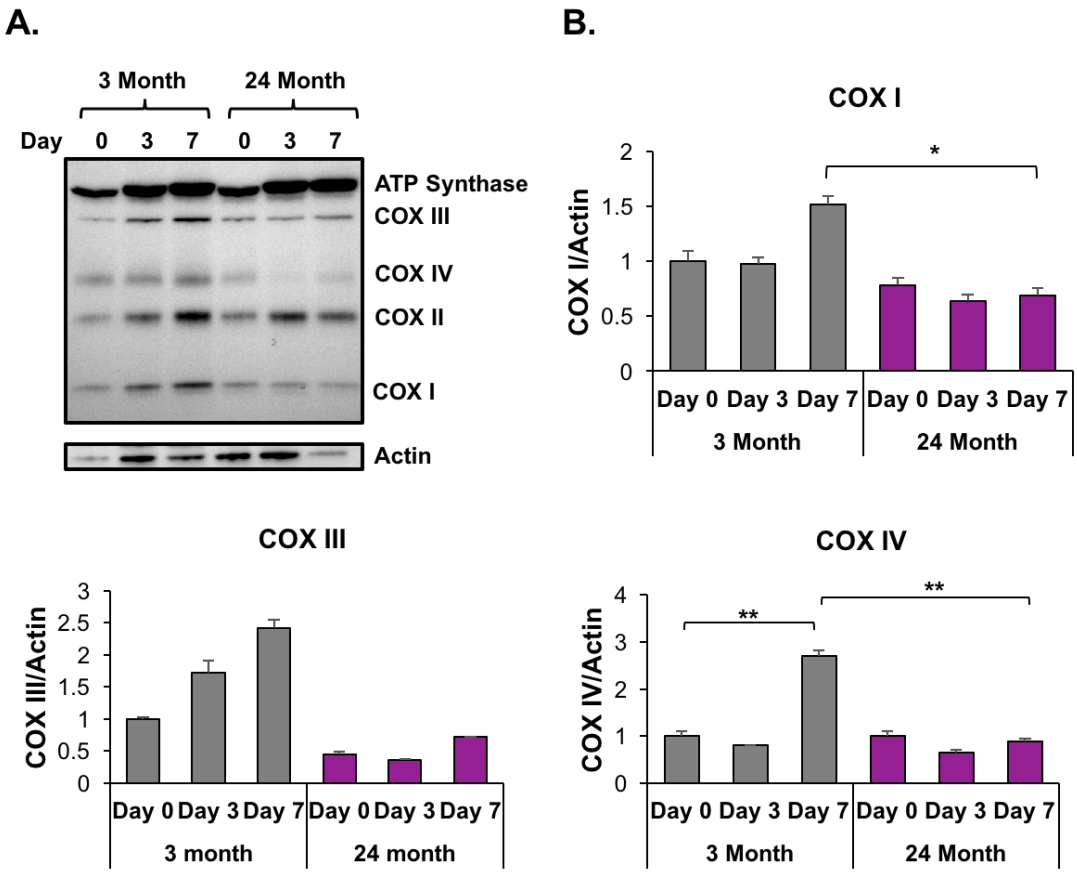

Figure 4.10: Western blot of OXPHOS proteins in CPCs from 3 month and 24 month-old mice. A. Representative Western blots of CPCs show reduced levels of select OXPHOS subunits in CPCs isolated from aging (24 month-old) mice. **B.** Quantitation of complex I, III, and IV protein levels normalized to 3 Month day 0 (n=3). (*p<0.05; **p<0.01)

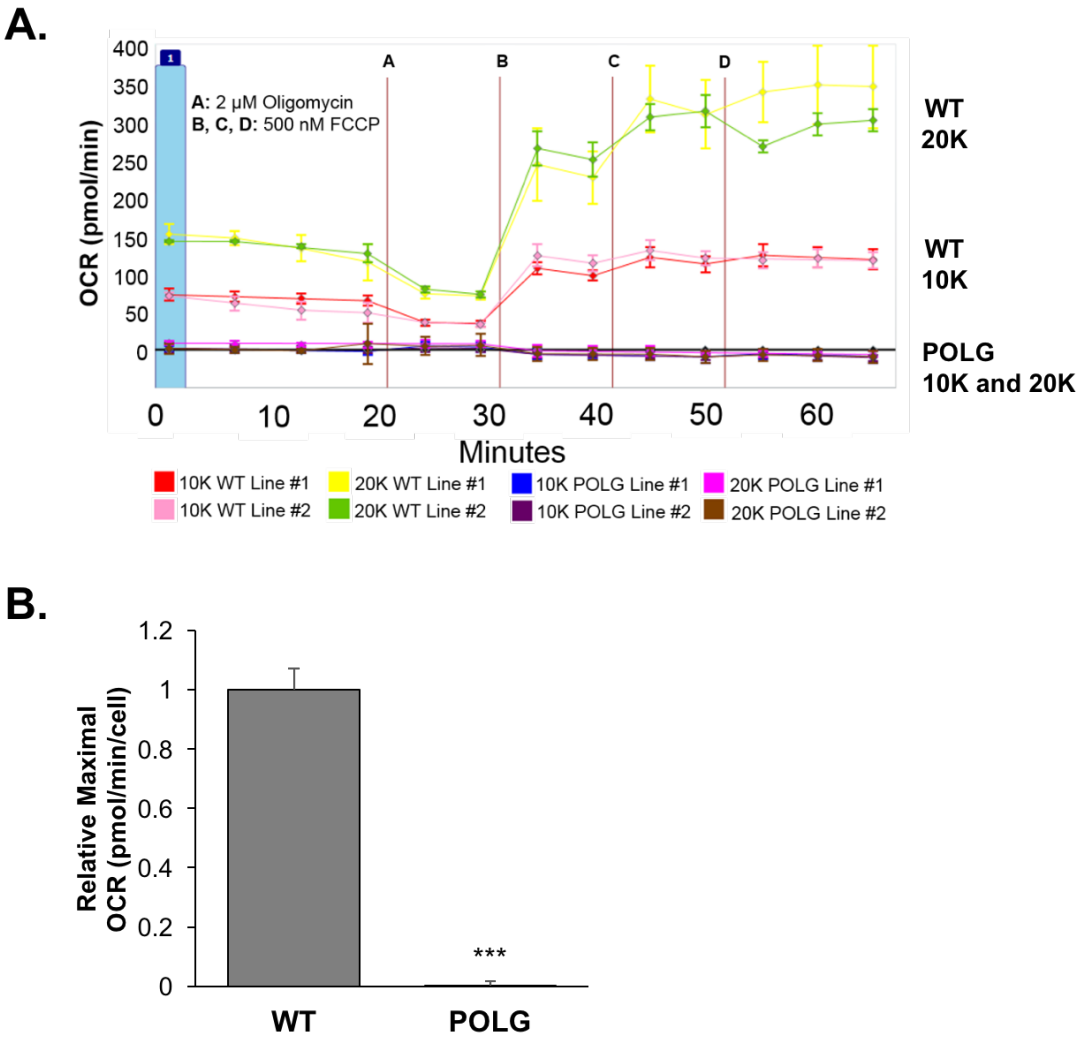

Figure 4.11: Mitochondrial respiration in WT and POLG CPCs. A. Mitochondrial respiration was measured in WT and POLG CPCs using a Seahorse XF Analyzer. **B.** Maximal oxygen consumption rate (OCR) was normalized to cell number (n=4). Cell seeding density: 10K = 10,000; 20K = 20,000. (***p<0.001)

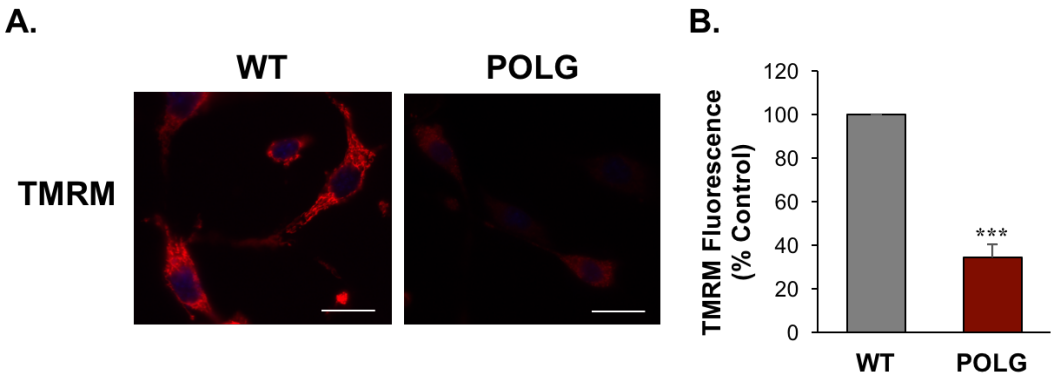

Figure 4.12: TMRM fluorescence is reduced in POLG CPCs. A. Representative fluorescent images of WT and POLG CPCs stained with tetramethylrhodamine methyl ester (TMRM). **B.** Quantitation of TMRM fluorescence in WT and POLG CPCs (n=3). Scale bar = 25 μm. (***p<0.001).

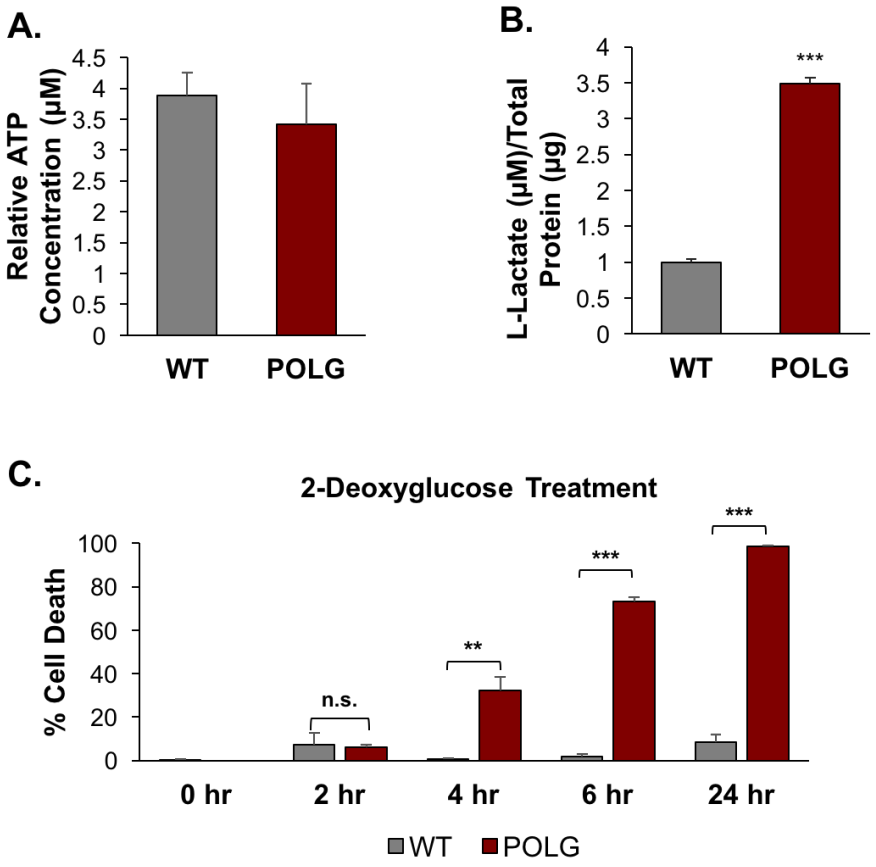

Figure 4.13: POLG CPCs rely on glycolysis to produce ATP. A. Analysis of cellular ATP content in WT and POLG CPCs (n=3). **B.** L-lactate present in growth medium was measured in WT and POLG CPCs (n=3). **C.** 2-deoxyglucose (10 nM) was added to the growth medium to inhibit glycolysis in WT and POLG CPCs. Cell death was assessed using YO-PRO-1 staining (n=3). (**p<0.01; ***p<0.001)

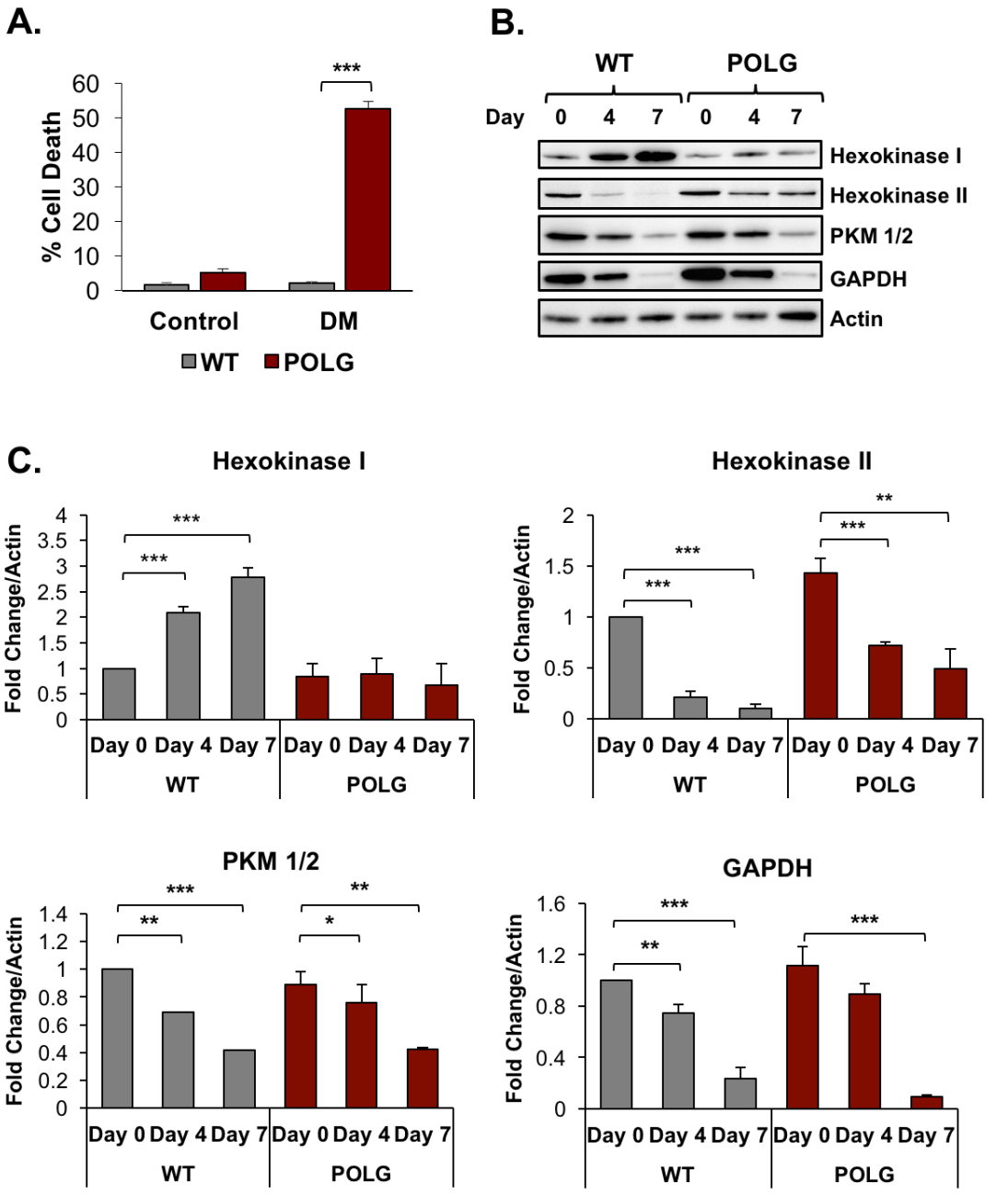

Figure 4.14: POLG CPCs downregulate glycolysis upon differentiation which leads to cell death. A. WT and POLG CPCs were incubated in differentiation medium and cell death was assessed using YO-PRO-1 staining 4 days later (n=3). **B.** Representative Western blots of glycolytic enzymes after incubation in DM. **C.** Quantitation of Hexokinase I, Hexokinase II, PKM1/2, and GAPDH at different time points after differentiation (n=3). (*p<0.05; **p<0.01; ***p<0.001)

CHAPTER 5: MITOCHONDRIAL AUTOPHAGY IS IMPORTANT FOR CARDIAC PROGENITOR CELL DIFFERENTIATION

Introduction

Accumulation of mtDNA mutations can lead to defects in proteins encoded by the mtDNA, resulting in mitochondrial dysfunction. Cells must maintain a healthy population of mitochondria to maintain optimal cellular function. Mitochondrial autophagy or mitophagy is a process that cells use to remove dysfunctional mitochondria. When the cell undergoes mitophagy, defective mitochondria are sequestered in autophagosomes and subsequently degraded in lysosomes (Kubli & Gustafsson, 2012). Mitophagy can occur through different mechanisms. The most well-characterized mechanism of mitophagy is Parkin-mediated. In this process, the E3 ubiquitin ligase Parkin translocates from the cytosol to damaged mitochondria, where it ubiquitinates protein substrates on the outer mitochondrial membrane. These ubiquitinated proteins are recognized by the adaptor protein p62, which then recruits LC3 II bound to the autophagosome membrane. The cargo is sequestered and the contents are degraded in the lysosome.

Another mechanism of mitophagy is mediated by mitophagy receptors such as BNIP3, BNIP3L/NIX, and FUNDC1. These receptors are found in the outer mitochondrial membrane (OMM) and directly bind to LC3 II on the

autophagosome membrane. This process does not require ubiquitin or adaptor proteins.

A recent study has reported that mitophagy is required for differentiation of skeletal myoblasts into mature myotubes (Sin et al., 2016). This study demonstrated that myoblasts activated mitophagy during early differentiation to remove old mitochondria. Mitochondrial biogenesis was activated simultaneously to re-populate cells with new and more functionally efficient mitochondria. Damage to mtDNA can impair mitochondrial quality control in various tissues such as skeletal muscle (Joseph et al., 2013). Erythrocytes from mice with the POLG mutation exhibit defects in mitochondrial clearance during erythroid maturation (Li-Harms et al., 2015; Ahlqvist et al., 2015).

Aging is associated with accumulation of mtDNA mutations and reduced autophagy (Larsson, 2010; Rubinsztein et al., 2011). I have shown that POLG CPCs accumulate defective mitochondria which results in impaired differentiation, suggesting that these cells could have impaired mitophagy. Here, I have examined whether mitophagy was increased or impaired in POLG CPCs under baseline conditions. I also investigated whether activation of mitophagy is required for CPC differentiation.

Results

POLG CPCs have increased mitophagy at baseline

I have shown in Chapter 4 that mitochondria from POLG CPCs had abnormal mitochondrial morphology and impaired mitochondrial respiration. These defects suggested the presence of dysfunctional and depolarized mitochondria, which have been shown to trigger mitophagy. Therefore, I examined whether POLG CPCs had increased levels of mitophagy at baseline in an attempt to clear the defective mitochondria. First, I assessed whether autophagic flux was altered in POLG CPCs at baseline. To assess flux, cells were treated with vehicle (DMSO) or bafilomycin A1 to inhibit the fusion between autophagosomes and lysosomes. The presence of bafilomycin A1 leads to accumulation of LC3 II-positive autophagosomes. I found that both WT and POLG CPCs accumulated similar levels of the autophagy marker LC3 II in the presence of bafilomycin A1 (Figure 5.1 A and B). This suggests that autophagic flux is not affected in POLG CPCs and that a similar number of autophagosomes are formed at a steady state in both WT and POLG CPCs. I also assessed whether there were differences in lysosomal activity by LAMP2 staining, but I found no significant differences in lysosomal content between WT and POLG CPCs (Figure 5.1 C and D). These data suggest that baseline autophagic flux is not altered in POLG CPCs.

Next, I assessed the level of mitophagy in WT and POLG CPCs at baseline by monitoring TOM20-labeled mitochondria sequestered in GFP-LC3-

positive autophagosomes. Cells were treated with bafilomycin A1 to prevent degradation of autophagosomes containing mitochondria, as observed by increased formation of GFP-LC3 puncta in both WT and POLG CPCs (Figure 5.2). In addition, I found that POLG CPCs exhibited a significantly higher number of GFP-LC3-positive autophagosomes that co-localized with TOM20-labeled mitochondria compared with WT (Figure 5.2). This suggests that the level of mitophagy is higher in POLG CPCs under baseline conditions.

POLG CPCs have intact mitophagy in response to stress

After characterizing mitophagy at baseline, I then assessed the ability of POLG CPCs to induce mitophagy in response to stress. CPCs were treated with the mitochondrial uncoupler FCCP, which induces mitochondrial depolarization and mitophagy. Other cell types such as HeLa and mouse embryonic fibroblasts (MEFs) require the presence of Parkin to clear mitochondria in response to mitochondrial uncouplers (Narendra et al., 2008; Geisler et al., 2010). Therefore, I also overexpressed Parkin in one set of CPCs to determine whether Parkin is required to activate autophagy in CPCs. I found that both WT and POLG CPCs accumulated similar levels of LC3 II after treatment with FCCP (Figure 5.3 A and B). I also found that Parkin overexpression did not enhance LC3 II accumulation when compared to cells expressing β-gal control. These results suggest that POLG CPCs can activate autophagy to the same extent as WT CPCs in response to FCCP.

Next, I examined whether mitochondrial clearance was induced in POLG CPCs by assessing protein levels of inner mitochondrial membrane protein TIM23 after FCCP treatment. I found that WT and POLG CPCs both had reduced TIM23 protein levels (Figure 5.4 A and B). These results suggest that the mitophagy response to FCCP-induced stress is intact in POLG CPCs and that overexpression of Parkin is not required for promoting mitochondrial degradation.

POLG CPCs have impaired mitophagy in response to differentiation

The data indicated that POLG CPCs still have intact autophagy and mitophagy pathways. Next, I assessed whether autophagy and mitophagy were activated in CPCs during differentiation. WT and POLG CPCs were infected with GFP-LC3 to monitor autophagosome formation during 3 days of incubation in DM. I found that LC3 puncta significantly increased at day 2 and day 3 of differentiation in WT CPCs (Figure 5.5 A and B). The number of LC3 puncta also increased in POLG CPCs but not to the same extent as WT CPCs (Figure 5.5 A and B), suggesting that POLG CPCs still activate autophagy during differentiation, but not as robustly as WT CPCs. To assess mitophagy, I also stained WT and POLG CPCs for TOM20 and visualized colocalization of TOM20-positive mitochondria with GFP-LC3 positive autophagosomes. I found that WT CPCs had significantly increased co-localization between mitochondria and autophagosomes over 3 days of incubation in DM. However, POLG CPCs

did not exhibit a significant increase in mitochondrial co-localization during the same time period (Figure 5.6 A and B). Overall, these data suggest that POLG CPCs have reduced activation of autophagy and are unable to activate mitophagy during differentiation.

Mitophagy receptors mediate mitophagy response during CPC differentiation

There are different pathways that can mediate mitophagy, so I sought to determine which pathway was involved in the mitophagy response during CPC differentiation. Since Parkin is a well-known regulator of mitophagy, I decided to assess changes in Parkin during CPC differentiation. Surprisingly, I found no detectable levels of Parkin protein by Western blotting in CPCs (Figure 5.7 A). Real-time qPCR confirmed that CPCs did not express Parkin and that it did not increase in response to differentiation (Figure 5.7 B). This suggests that Parkin is not involved in the mitophagy response during CPC differentiation. Next, I examined whether differentiation-stimulated mitophagy occurred via the mitophagy receptors. I examined transcript levels of three known mitophagy receptors, *Bnip3*, *Nix*, and *Fundc1* under baseline conditions and during differentiation. I found that *Bnip3* gene expression did not change in WT and POLG CPCs after 7 days of differentiation (Figure 5.8). On the other hand, *Nix* and *Fundc1* transcripts increased after 7 days in the WT CPCs but did not increase in the POLG CPCs (Figure 5.8). This suggests that NIX and FUNDC1

are involved in the mitophagy response during CPC differentiation, and the signals activating mitophagy during differentiation are impaired in POLG CPCs.

Discussion

Here, I demonstrated that the POLG CPCs had an increased level of mitophagy at baseline compared to WT, but this was not sufficient to rescue their impaired function. Although my initial hypothesis predicted that CPCs with POLG mutations had impaired mitophagy in general, my data showed that both autophagy and mitophagy in response to stress are fully functional. However, activation of mitophagy in response to differentiation was impaired in POLG CPCs. The data suggest that activation of mitophagy in POLG CPCs differs in response to stress versus differentiation.

Mitochondrial degradation is coupled to mitochondrial biogenesis (Andres et al., 2015), but the underlying mechanism of this cross-talk is still unclear. The data suggest that mitochondrial biogenesis is impaired in POLG CPCs. It is possible that reduced mitochondrial biogenesis also affects the rate of mitochondrial turnover and an imbalance may lead to inefficient turnover of dysfunctional mitochondria. The relationship between mitochondrial degradation and synthesis in POLG CPCs requires further investigation.

Surprisingly, Parkin was not expressed in CPCs at baseline and after differentiation, confirming that Parkin-mediated mitophagy is not involved in clearing defective mitochondria in CPCs. However, CPCs appeared to activate

other mitophagy receptors. NIX is involved in mitochondrial clearance in erythrocytes during maturation (Ahlqvist et al., 2015), but could also play a role in CPC/adult progenitor cell maturation. Future studies will address whether Nix plays a role in CPC differentiation and mitochondrial biogenesis. Since mitochondria are important for regulating stemness and differentiation in other stem cell populations (Joshi & Kundu, 2013) and in CPCs (Chapter 3), defects in mitophagy during differentiation may also affect the fate of differentiating CPCs.

Chapter 5, in part, was originally published in the *Journal of Biological Chemistry*. Orogo AM, Gonzalez ER, Kubli DA, Baptista IL, Ong SB, Prolla TA, Sussman MA, Murphy AN, Gustafsson ÅB. Accumulation of Mitochondrial DNA Mutations Disrupts Cardiac Progenitor Cell Function and Reduces Survival. *The Journal of Biological Chemistry*. 290(36):22061-75, 2015. © 2015 The American Society for Biochemistry and Molecular Biology. The dissertation author was the primary investigator and author of this paper.

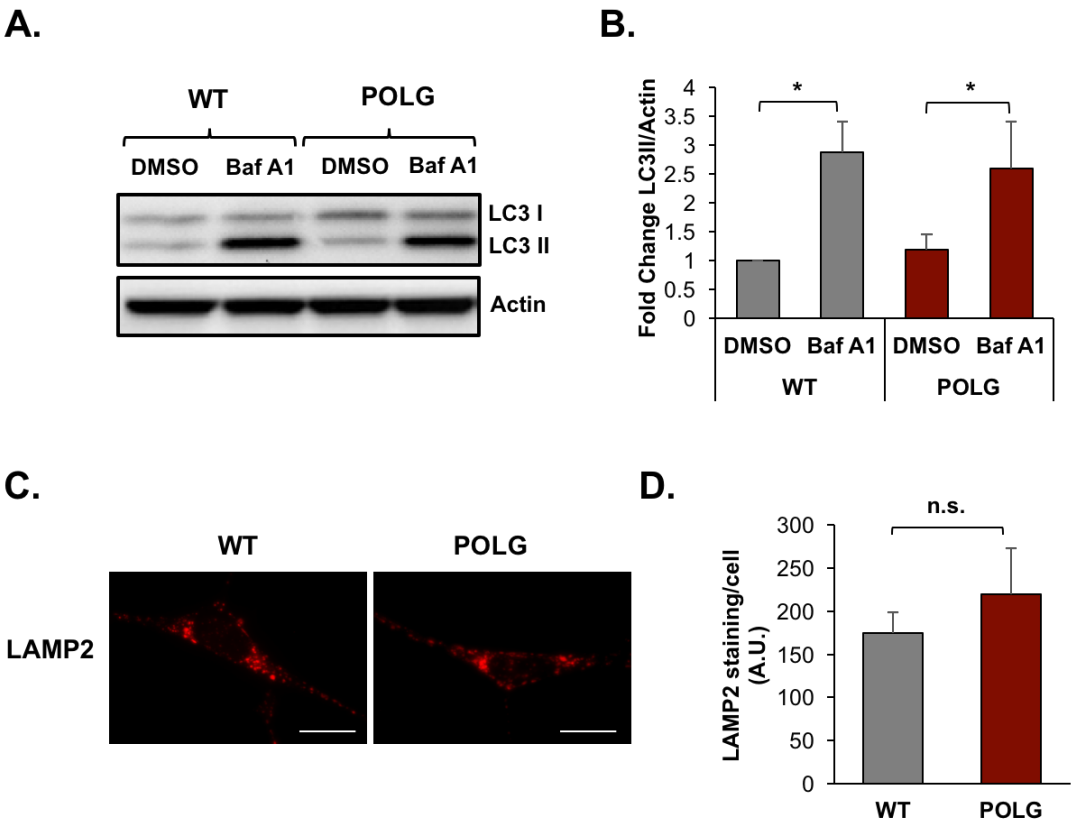

Figure 5.1: Baseline autophagic flux is not altered in POLG CPCs. A. Representative Western blot shows similar levels of LC3 II protein in both WT and POLG CPCs after treatment with 50 nM Bafilomycin A1 for 2 hours. **B.** Quantitation of LC3 II protein levels (n=3). **C.** Representative fluorescent images of LAMP2 staining in WT and POLG CPCs. Scale bar = 20 μm. **D.** Quantitation of LAMP2 staining in WT and POLG CPCs (n=3). A.U., arbitrary units. (*$p<0.05$; n.s., not significant)

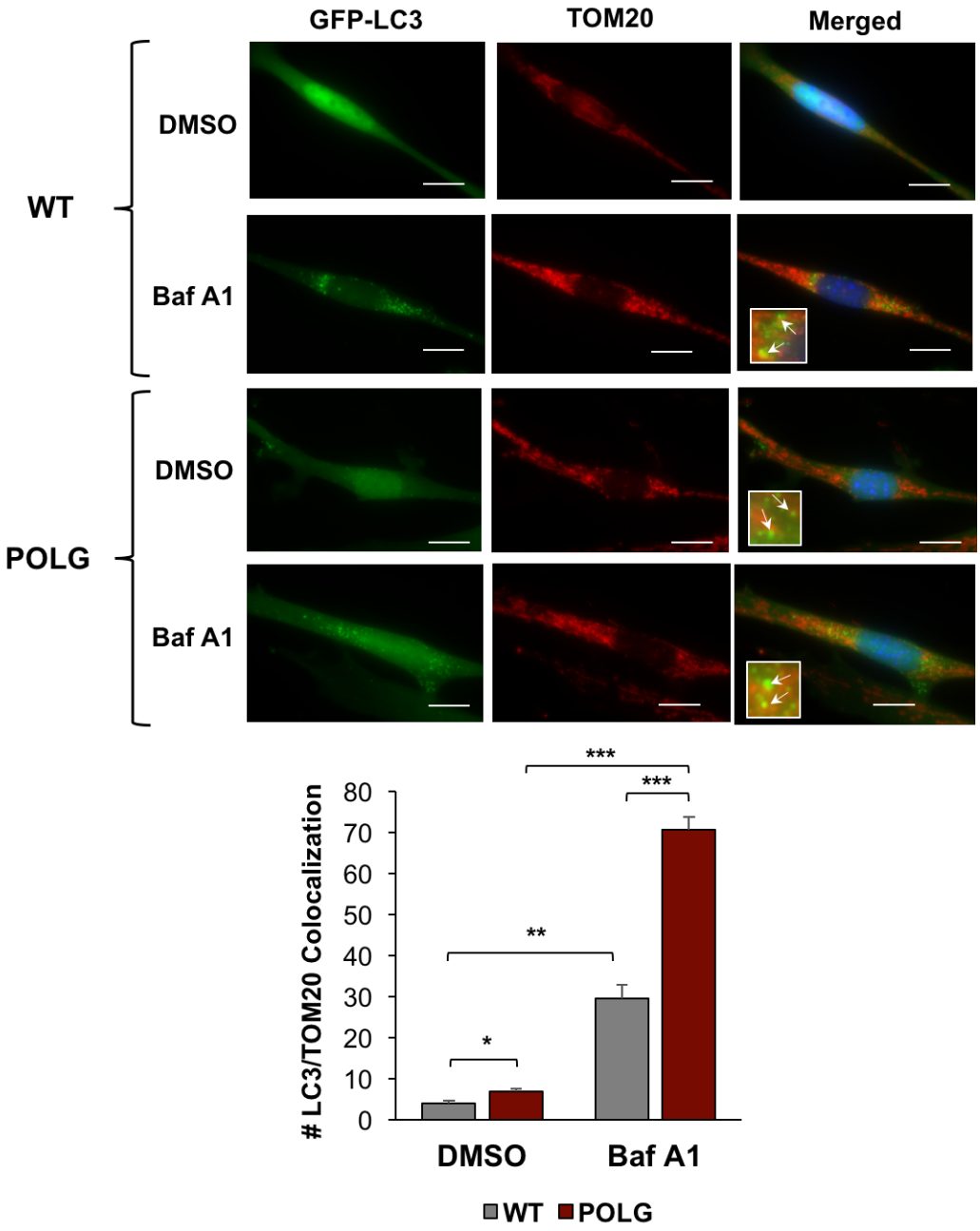

Figure 5.2: Baseline mitophagy is increased in POLG CPCs. Representative fluorescent images and quantitation of GFP-LC3 and TOM20 co-localization per cell in WT and POLG CPCs (n=3). Cells were treated with DMSO or 50 nM Bafilomycin A1 for 3 hours before fixation. Scale bar = 20 μm. (*p<0.05; **p<0.01; ***p<0.001)

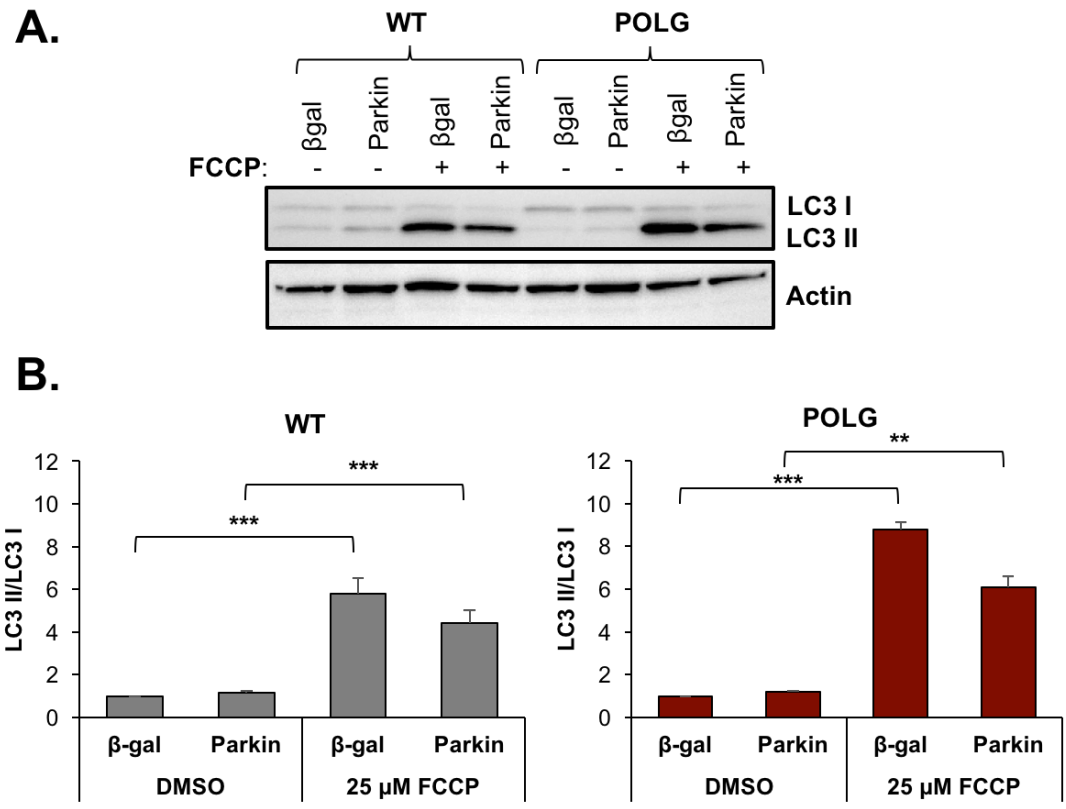

Figure 5.3: Activation of autophagy in response to FCCP in WT and POLG CPCs. A. Representative Western blot of LC3 I, LC3 II, and Actin levels in WT and POLG CPCs. **B.** Band quantitation of LC3 II/LC3 I ratios in WT (n=4) and POLG CPCs (n=3). Cells were infected with β-gal or mCherry-Parkin and treated with 25 μM FCCP for 24 hours. (**p<0.01; ***p<0.001)

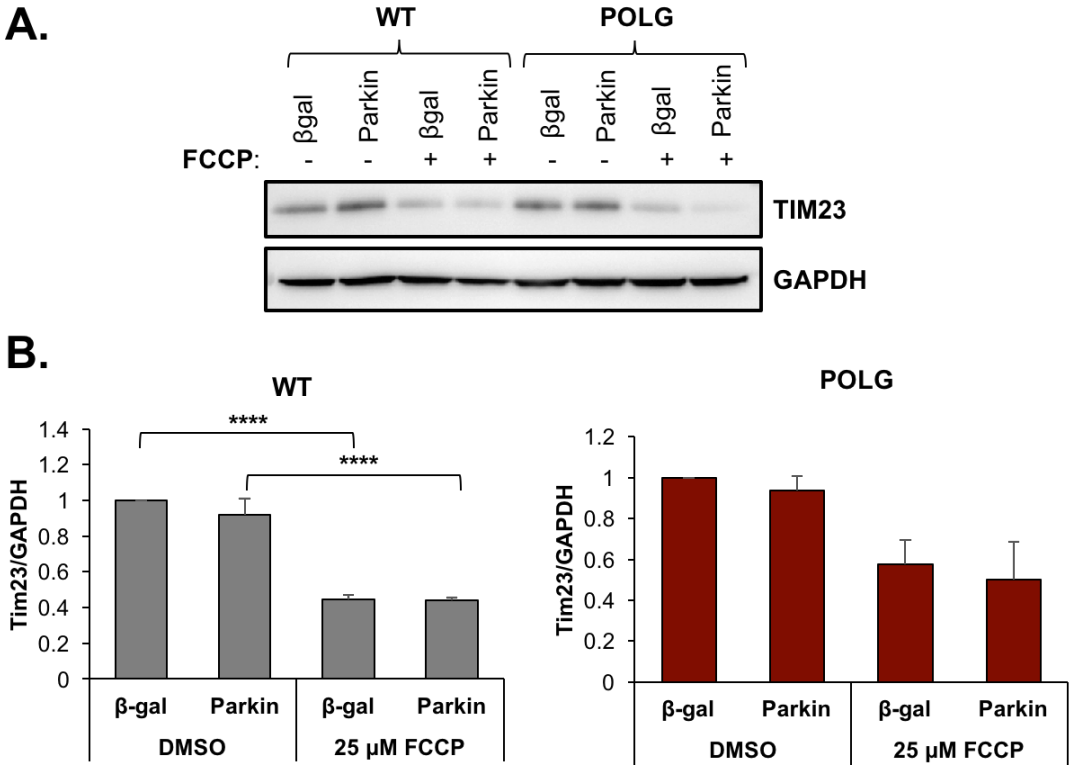

Figure 5.4: Mitophagy in response to FCCP in WT and POLG CPCs. A. Representative Western blot of TIM23 and GAPDH levels in WT and POLG CPCs. **B.** Band quantitation of TIM23/GAPDH ratios in WT (n=4) and POLG CPCs (n=4). Cells were infected with β-gal or mCherry-Parkin and treated with 25 μM FCCP for 24 hours. (****p<0.0001)

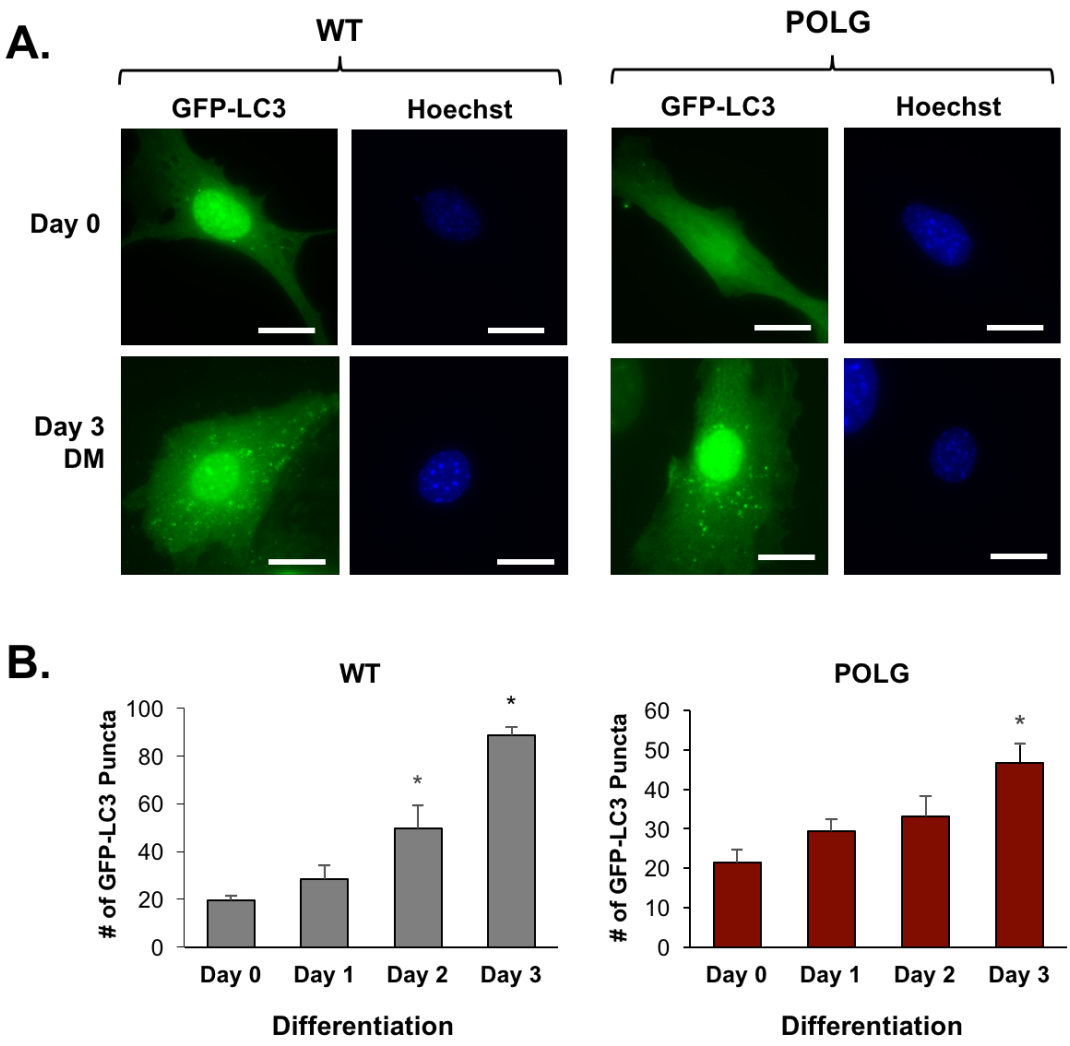

Figure 5.5: Activation of autophagy in response to differentiation in WT and POLG CPCs. A. Representative fluorescent images of GFP-LC3 in WT and POLG CPCs. Scale bar = 20 μm. **B.** Quantitation of number of GFP-LC3 puncta per cell in WT and POLG CPCs (n=3). (*p<0.05 vs. Day 0)

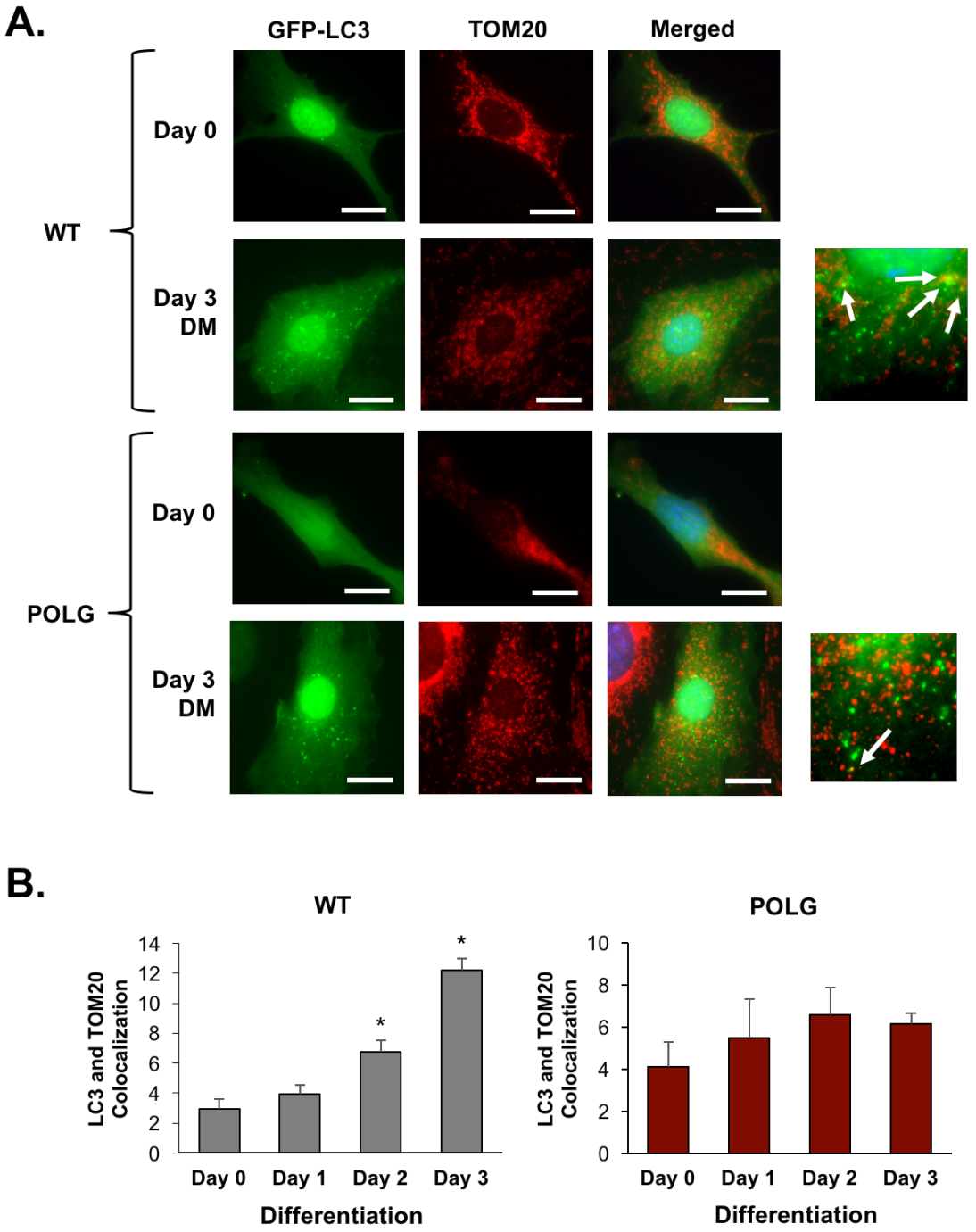

Figure 5.6: Mitophagy in response to differentiation in WT and POLG CPCs. A. Representative fluorescent images of GFP-LC3 and TOM20 in WT and POLG CPCs. Scale bar = 20 μm. **B.** Quantitation of GFP-LC3 and TOM20 colocalization per cell in WT and POLG CPCs (n=3). (*p<0.05 vs. Day 0)

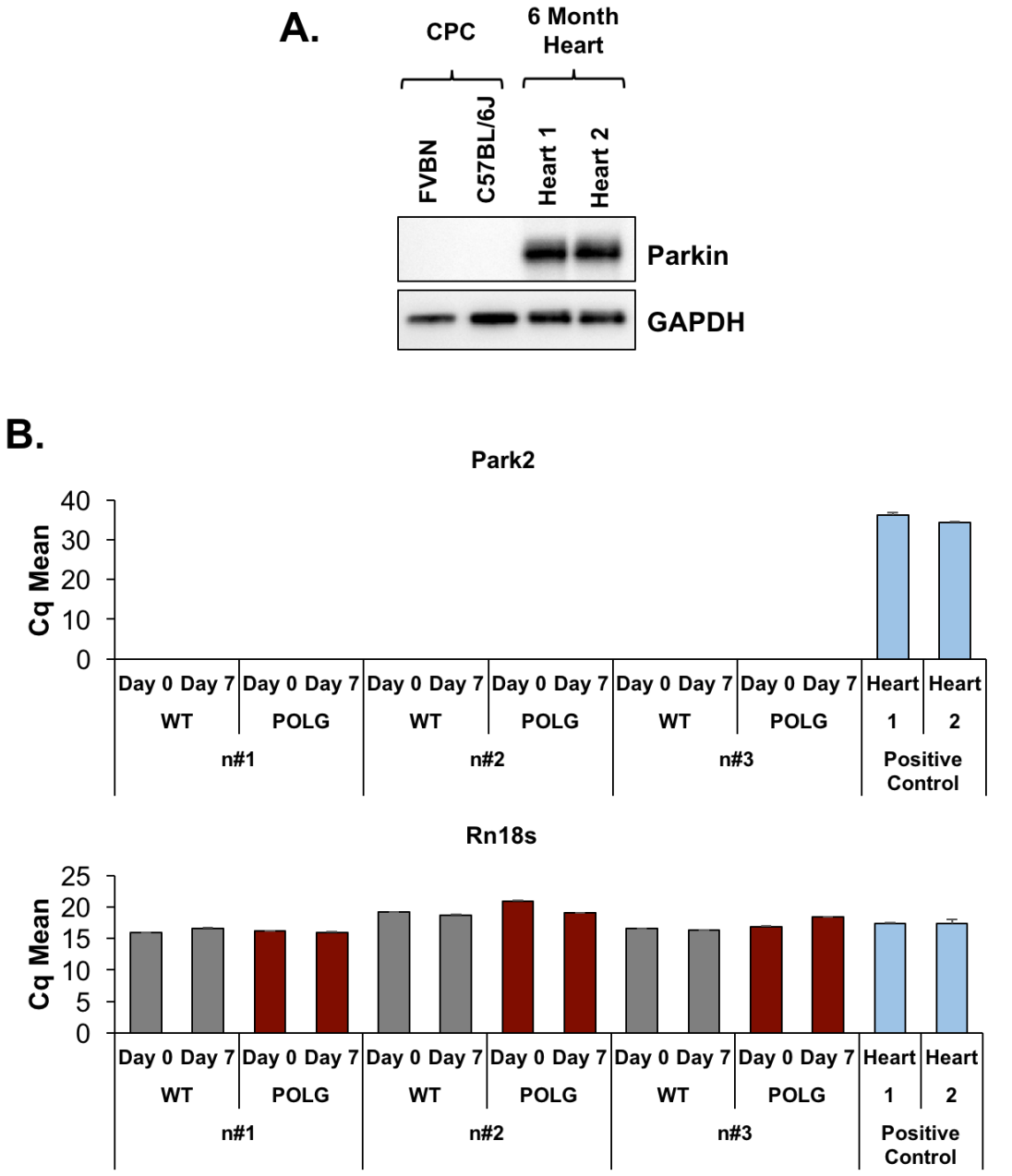

Figure 5.7: Western blot and qPCR of Parkin expression in CPCs. A. Western blot of Parkin and GAPDH expression in CPCs compared to whole heart lysates (positive control) (n=2). Parkin protein was not detected in CPCs. **B.** Real-time qPCR analysis of *Park2* and *Rn18s* (reference gene) transcript levels in CPCs (n=3) and heart tissue (positive control) (n=2). *Park2* transcripts were undetectable in CPCs.

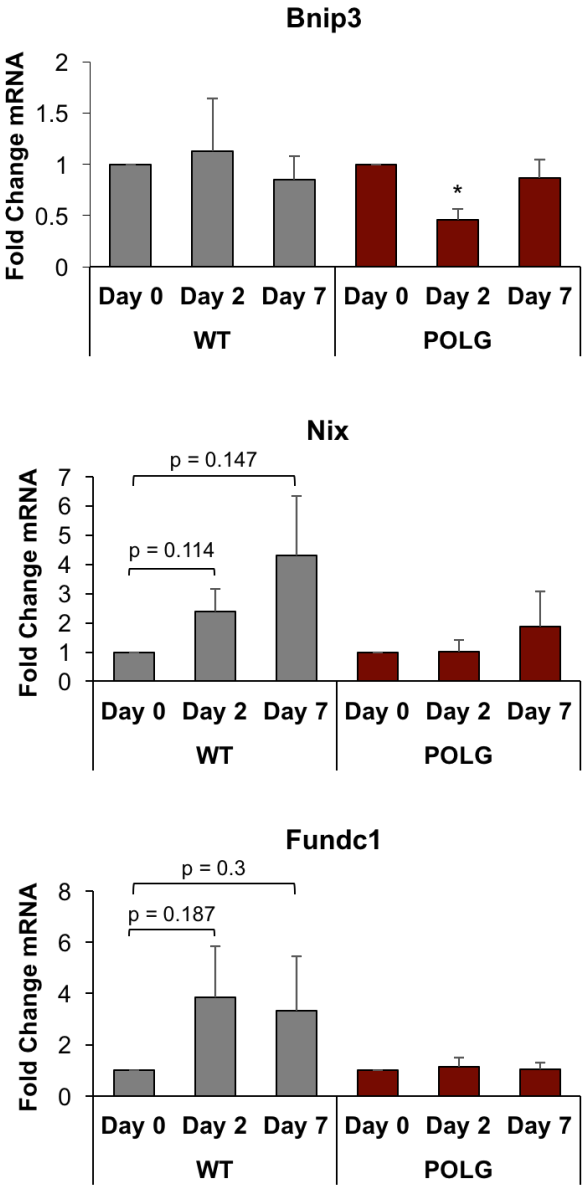

Figure 5.8: Real-time qPCR analysis of mitophagy receptors in WT and POLG CPCs. Expression of mitophagy receptors *Bnip3*, *Nix*, and *Fundc1* in WT and POLG CPCs after 7 days in DM (n=5). (*p<0.05 vs. Day 0)

CHAPTER 6: MITOCHONDRIAL DNA MUTATIONS AND PARKIN-MEDIATED MITOPHAGY

Introduction

Mice harboring the POLG^{D257A} mutation accumulate mtDNA mutations in tissues throughout the body and have been reported to display cardiac dysfunction after 13-14 months (Dai et al., 2010). Accumulation of mtDNA mutations can lead to dysfunctional mitochondria which must be cleared by the cell to maintain homeostasis and survival. Parkin is an E3 ubiquitin ligase that mediates mitophagy in cells and has been shown to play an important role in adapting to acute stress in the myocardium (Kubli et al., 2013). Parkin has also been reported to eliminate mitochondria with mutations in the mtDNA-encoded *Cox1* gene, suggesting that Parkin may facilitate clearance of mitochondria with mtDNA mutations (Suen et al., 2010).

I have shown that CPCs isolated from POLG mice show defects in survival, proliferation, and differentiation. These cells also have abnormal mitochondrial morphology and defective respiration. Therefore, I hypothesized that cardiomyocytes in the hearts of POLG mice would also accumulate mtDNA mutations at an accelerated rate, leading to accumulation of dysfunctional mitochondria. Thus, I predict that POLG mice will develop cardiac defects earlier than WT mice.

Accumulation of mtDNA damage with age can impair mitochondrial quality control in tissues such as skeletal muscle and hematopoietic cells (Joseph et al., 2013; Ahlqvist et al., 2015; Li-Harms et al., 2015). On the other hand, enhancing mitophagy can rescue aging phenotypes and lead to increased lifespan (Rana et al., 2013; LaRocca et al., 2014; Cui et al., 2013). This suggests that accumulation of mtDNA mutations with age may also lead to impaired mitophagy in the heart. However, the mechanism by which mtDNA mutations impair mitophagy is unclear. In this study, I investigated the role of Parkin-mediated mitophagy in the hearts of POLG mice. I generated POLG x Parkin TG and POLG x Parkin KO mice in parallel and monitored their cardiac function over 12 months to determine whether modulating Parkin levels in hearts with the POLG mutation will affect the development of age-related cardiac defects. I hypothesize that cardiac-specific Parkin overexpression will reduce the aging phenotype and Parkin deficiency will accelerate cardiac dysfunction in POLG hearts.

Results

Mice with the POLG mutation develop cardiac hypertrophy and have reduced Parkin

To investigate the effect of accumulating mtDNA mutations on the aging heart, WT and POLG mice were aged to 6 months. At this time point, I began to see modest differences in baseline cardiac parameters and mitochondrial

function. POLG mice had a small but significant reduction in body weight and increased heart weight/body weight ratios compared to age-matched WT mice (Figure 6.1 A). However, I observed no differences in lung weight/body weight ratios (Figure 6.1 A) or cardiac function assessed by echocardiography (Figure 6.1 B). Next, we measured respiration of isolated mitochondria from the hearts of WT and POLG mice using the Seahorse XF Analyzer. Different substrates were used to assess pyruvate, long-chain fatty acid, and succinate-driven respiration. There was a trend of reduced mitochondrial function in POLG mice, which was significant using pyruvate/malate as substrates (Figure 6.2 A). I compared mitochondrial OXPHOS proteins and found that COX I and COX IV protein subunits were significantly reduced in POLG mice at 6 months (Figure 6.2 B). These data indicate that POLG mice begin to develop cardiac hypertrophy and mitochondrial respiration defects at 6 months of age, but this did not seem to affect cardiac function.

The above data indicate that mitochondria were affected in POLG hearts at 6 months of age. Previous studies have reported that Parkin is upregulated in the heart in response to mitochondrial stress (Kubli et al., 2013; Kubli et al., 2015; Song et al., 2015). To investigate whether Parkin is upregulated in response to stress caused by accumulating mtDNA mutations, I investigated Parkin levels in 6 month WT and POLG hearts. I hypothesized that POLG hearts will upregulate Parkin expression to activate Parkin-mediated mitophagy and clear defective mitochondria. Consistent with this, I found that Parkin gene

expression increased at 6 months (Figure 6.3 A). Surprisingly, Parkin protein levels in the heart were significantly reduced in POLG mice (Figure 6.3 B). Parkin translocates to dysfunctional mitochondria to promote their clearance (Narendra et al., 2008; Kubli et al., 2013). I isolated mitochondria from the hearts of 6 month WT and POLG mice and found that Parkin protein levels were significantly reduced in the mitochondrial fraction of the POLG mice (Figure 6.3 C). These data suggest that accumulation of mtDNA mutations in the heart leads to upregulation of Parkin gene expression. However, increased mRNA message did not translate to increased protein. Reduced Parkin in the mitochondrial fraction of POLG hearts also suggests that accumulation of mtDNA mutations impairs Parkin recruitment to the mitochondria.

Aging POLG mice have increased levels of ROS and oxidative stress in their tissues (Logan et al., 2014; Dai et al., 2010). It has been reported that Parkin can be subjected to oxidative modification (Meng et al., 2011; Winklhofer et al., 2003; Wong et al., 2007), which leads to Parkin protein misfolding and aggregation. To examine whether reduced Parkin levels in POLG mouse hearts is due to increased misfolding and aggregation, I measured the presence of Parkin in soluble and insoluble fractions. I found insoluble Parkin present in both WT and POLG hearts (Figure 6.4 A and B). The percentage of total Parkin in the insoluble fraction was not different in WT and POLG hearts (Figure 6.4 B). The data suggest that the majority of Parkin does not end up in the insoluble fraction in POLG hearts. Thus, Parkin aggregation is not necessarily the cause

of reduced Parkin levels in POLG mice. There could be a defect in Parkin translation or increased Parkin degradation that leads to reduced Parkin protein.

Parkin-mediated mitophagy is impaired in POLG mice and Parkin overexpression does not enhance mitophagy

The data from the 6 month-old mice led to the hypothesis that accumulation of mtDNA mutations contributes to reduced Parkin-mediated mitophagy, which would lead to more rapid accumulation of damaged mitochondria. To examine if restoration of Parkin would enhance mitochondrial turnover and prevent cardiac aging, I generated a mouse line by crossing POLG mice with Parkin TG mice. I aged the mice for 12 months and analyzed their cardiac function at 2, 6, and 12 months. At 12 months, I found that both POLG and POLG/Parkin TG mice had reduced body weight and increased heart weight/body weight ratios compared to WT and Parkin TG (Figure 6.5 A). H&E staining of heart sections from 12 month mice revealed that POLG, Parkin TG, and POLG/Parkin TG mice had enlarged hearts compared to WT mice (Figure 6.5 B). Furthermore, these same groups appeared to upregulate gene expression of cardiac hypertrophy markers beta-myosin heavy chain (β-MHC) and atrial natriuretic peptide (ANP) (Figure 6.5 C).

The POLG, Parkin TG, and POLG/Parkin TG mice all developed cardiac hypertrophy at 12 months. When comparing cardiac function among the 4 genotypes, echocardiographic analysis showed that at 12 months, the POLG

and POLG/Parkin TG mice had significantly increased % fractional shortening (% FS) and % ejection fraction (% EF) compared to the other 2 groups (Table 6.1). This could be a compensatory mechanism to maintain cardiac contractility in response to increased mitochondrial damage caused by the POLG mutation. When examining the effect of age on cardiac parameters, the POLG/Parkin TG mice significantly increased % FS and % EF at 12 months compared to 2 months (Table 6.1). Interventricular septal thickness at diastole (IVS; d) and left ventricular posterior wall thickness at diastole (LVPW; d) are parameters used to assess left ventricular (LV) hypertrophy. IVS; d increased over 12 months in all groups, suggesting that aging leads to hypertrophy, even in WT hearts (Table 6.1). Left ventricular internal dimension at diastole (LVID; d) is used to assess left ventricular dilation, and the POLG and POLG/Parkin TG mice had increased LVID; d over 12 months (Table 6.1). These data show that aging leads to cardiac hypertrophy, and Parkin overexpression did not delay cardiac aging.

To determine whether Parkin overexpression will enhance the clearance of defective mitochondria in POLG mice, I assessed proteins involved in autophagy and mitophagy by Western blot in hearts of 12 month old mice. Parkin TG and POLG/Parkin TG mice had increased LC3 II levels compared to non-transgenic mice (Figure 6.6 A). Levels of adaptor protein p62 were reduced in POLG and POLG/Parkin TG mice (Figure 6.6 A). On the other hand, real-time qPCR of *Sqstm1* showed that hearts with the POLG mutation appeared to upregulate p62 (Figure 6.6 B), suggesting that more p62 is being produced as

other p62 proteins are being degraded via autophagy. Furthermore, transcripts for autophagy genes *Atg5* and *Atg7* also appeared to slightly increase in Parkin TG and POLG/Parkin TG (Figure 6.6 B), suggesting that transgenic mice had increased autophagy. Interestingly, transcripts for autophagy genes *Becn1* and *Rab7* increased in POLG and POLG/Parkin TG (Figure 6.6 B). BECLIN1 is involved in phagophore complex initiation (Kihara et al., 2001), while RAB7 plays a role in maturation of late autophagic vacuoles (Jager et al., 2004). These data suggest that autophagic flux is increased in POLG and POLG/Parkin TG hearts.

Next, I examined Parkin levels in the hearts of 12 month-old mice. I found that POLG hearts had reduced Parkin protein compared to WT hearts at 12 months (Figure 6.7 A). Parkin transgene overexpression in Parkin TG mice resulted in increased ubiquitinated proteins as expected (Figure 6.7 A). However, POLG mice overexpressing Parkin (POLG/Parkin TG) had reduced Parkin transgene protein levels and ubiquitination in the heart compared to Parkin TG mice (Figure 6.7 A). Interestingly, real-time qPCR data showed that endogenous Parkin (mouse *Park2*) was upregulated in POLG and POLG/Parkin TG hearts at 12 months (Figure 6.7 B). Parkin transgene (human *PARK2*) expression did not alter transcript levels of endogenous Parkin (Figure 6.7 B). These findings suggest that expression of the Parkin transgene did not enhance ubiquitination in hearts with the POLG mutation. In addition, the POLG mutation may regulate endogenous Parkin transcripts in the heart.

Although there was minimal Parkin aggregation in the POLG hearts at 6 months, I investigated whether accumulation of mtDNA mutations with age could lead to increased Parkin aggregation. In particular, I detected Parkin in both soluble and insoluble fractions of 12 month hearts (Figure 6.7 C). Soluble Parkin protein levels were lower in the POLG hearts compared to WT. However, the percentage of total Parkin in the insoluble fraction was similar in WT and POLG hearts (Figure 6.7 C). POLG/Parkin TG hearts had more soluble Parkin protein compared to POLG hearts (Figure 6.7 C). Interestingly, the percentage of total Parkin in the insoluble fraction was lower in the POLG/Parkin TG hearts compared to Parkin TG hearts (Figure 6.7 C), indicating that less Parkin ended up in the insoluble fraction in POLG/Parkin TG hearts. Thus, increased Parkin aggregation is unlikely to be the mechanism for reduced Parkin protein levels in mice with the POLG mutation. Because the Parkin transgenic protein is also low in hearts with the POLG mutation, it is possible that the POLG mutation leads to increased degradation of both endogenous and transgenic Parkin protein.

Next, I assessed whether increasing Parkin levels in the heart would enhance mitophagy by measuring proteins in the mitochondrial fraction from hearts of 12 month old mice. I observed that there was reduced Parkin translocation to the mitochondria and reduced ubiquitination of mitochondrial proteins in POLG/Parkin TG hearts compared to Parkin TG hearts (Figure 6.8 A). Furthermore, I found increased p62 protein in the mitochondrial fraction of Parkin TG hearts, but did not see the same increase in the POLG/Parkin TG

mitochondrial fraction (Figure 6.8 A). Even though POLG/Parkin TG hearts had reduced Parkin and p62 in the mitochondria compared to Parkin TG, LC3 II recruitment was not decreased (Figure 6.8 A).

PINK1 is a kinase that accumulates on the outer mitochondrial membrane (OMM), where it phosphorylates ubiquitin to recruit and activate Parkin (Nguyen et al., 2016). PINK1 also phosphorylates MFN2 and promotes Parkin-mediated ubiquitination of MFN2 in the heart (Chen & Dorn, 2013). Since PINK1 and MFN2 play a role in Parkin recruitment to the mitochondria, I determined whether levels of these proteins are altered in the hearts of 12 month mice. I assessed protein levels in the mitochondrial fraction by Western blot and found no differences in PINK1 accumulation in the mitochondria (Figure 6.8 B). However, Parkin receptor MFN2 was increased in the mitochondria of Parkin TG and POLG/Parkin TG (Figure 6.8 B). Hearts with the POLG mutation had increased *Pink1* and *Mfn2* transcripts (Figure 6.8 C). The data suggest that despite Parkin overexpression, hearts with the POLG mutation have reduced Parkin and p62 recruitment to the mitochondria, but this is not due to reduced PINK1 or MFN2. The presence of LC3 II in POLG/Parkin TG mitochondria suggest that these hearts can still utilize Parkin-independent mechanisms to recruit LC3 to defective mitochondria.

Since the data seemed to suggest that Parkin-mediated mitophagy was impaired in mice with POLG mutations, cardiomyocytes could utilize alternative mechanisms involving mitophagy receptors to compensate for the defect in

Parkin recruitment. I examined BNIP3 and NIX, which have been shown to mediate selective removal of mitochondria in cardiomyocytes (Quinsay et al., 2010; Kubli et al., 2015; Dorn, 2010). I saw no differences in BNIP3 and NIX protein in the mitochondrial fraction (Figure 6.9 A), but transcripts of *Bnip3* and *Bnip3l/Nix* increased in POLG and POLG/Parkin TG hearts (Figure 6.9 B). These data suggest that increased mitophagy might be occurring through BNIP3.

Parkin deficiency does not accelerate cardiac aging or impair mitophagy

To further explore the role of Parkin-mediated mitophagy in the heart, I generated another mouse line by crossing POLG mice with Parkin KO mice to investigate the effect of Parkin deficiency on cardiac aging. Similar to the POLG x Parkin TG line, I analyzed their cardiac function at 2, 6, and 12 months. At 12 months, I found that POLG and POLG/Parkin KO mice had reduced body weight and increased heart weight/body weight ratios compared to WT and Parkin KO mice (Figure 6.10 A). H&E staining showed cardiac hypertrophy in the POLG/Parkin KO heart compared to the smaller Parkin KO heart (Figure 6.10 B). Moreover, increased transcripts of *Myh7* (β-MHC) and *Nppa* (ANP) in 12 month POLG and POLG/Parkin KO hearts confirm that the POLG mutation leads to activation of cardiac hypertrophy (Figure 6.10 C), consistent with data from the POLG x Parkin TG line.

Next, I measured cardiac function by echocardiography and saw no differences in % FS and % EF between the 4 genotypes at 12 months of age (Table 6.2), indicating that Parkin deficiency did not accelerate cardiac dysfunction. Interestingly, POLG mice had increased IVS; d over 12 months, while values for the other 3 genotypes remained similar after 12 months (Table 6.2). LVID; d increased in all groups with age, and was significant in Parkin KO and POLG/Parkin KO mice. At 12 months, LVID; d was higher in POLG and POLG/Parkin KO mice than the other 2 groups (Table 6.2). This data suggests that aging leads to cardiac dilation which is more pronounced in Parkin-deficient mice. However, at 12 months, hearts with the POLG mutation were more dilated than hearts without the POLG mutation (Table 6.2).

Next, I determined whether Parkin deficiency will reduce autophagy in aging hearts with the POLG mutation. I examined autophagy proteins in whole heart lysates from 12 month old mice and saw no differences in LC3 II (Figure 6.11 A) suggesting no impairment in autophagosome formation in Parkin-deficient hearts. However, there was a slight reduction of p62 levels in POLG and POLG/Parkin KO (Figure 6.11 A). Real-time qPCR showed no differences in transcript levels of *Atg5*, *Atg 7*, and *Becn1* (Figure 6.11 B). Interestingly, there was a significant increase in *Rab7* transcripts in the POLG/Parkin KO hearts (Figure 6.11 A). These data confirm that autophagic flux is increased in mice with the POLG mutation.

Next, I assessed mitophagy by measuring protein levels in the mitochondrial fraction of 12 month hearts. Levels of LC3 II and p62 were similar (Figure 6.12 A) There was reduced PINK1 protein in the mitochondria of Parkin KO hearts, but *Pink1* and *Mfn2* transcripts were similar among all groups (Figure 6.12 B). The reduced PINK1 protein in the mitochondria of Parkin KO hearts could be due to lack of Parkin.

Because Parkin-deficient hearts with the POLG mutation can still recruit LC3 II and p62 to the mitochondria, this suggests that other mechanisms can mediate mitophagy independently of Parkin. I assessed protein levels of mitophagy receptor BNIP3 and found that levels were similar among all groups (Figure 6.12 A). However, *Bnip3* transcripts appeared to increase only in POLG and POLG/Parkin KO hearts (Figure 6.12 B), suggesting that mitochondria with POLG mutations mainly rely on BNIP3-mediated mitophagy to clear defective mitochondria. Interestingly, *Bnip3l/Nix* transcripts were significantly increased only in POLG/Parkin KO mice (Figure 6.12 B). Since BNIP3 and NIX are both involved in mitochondrial clearance and serve redundant functions (Dorn, 2010), the data suggest that Parkin does not play a role in clearing these dysfunctional mitochondria. Instead, mitophagy receptors might be involved in clearing excessive dysfunctional mitochondria caused by mtDNA mutations. Data from the POLG x Parkin KO mice show that Parkin deficiency did not accelerate cardiac dysfunction in aging mice with the POLG mutation.

Discussion

The present study demonstrates that the POLG mutation leads to impaired Parkin-mediated mitophagy, and that Parkin does not play a major role in clearing defective mitochondria in aging hearts. This is a novel and surprising finding in contrast to Parkin's established role in adapting to acute cardiac stress such as after an MI (Kubli et al., 2013). POLG mice with cardiac-specific Parkin transgene overexpression still had reduced Parkin protein levels, suggesting that the POLG mutation somehow affects Parkin protein stability and/or degradation. Accumulation of mtDNA mutations lead to increased mitochondrial ROS production, which could lead to Parkin misfolding and protein aggregation. However, the data showed that Parkin aggregates did not accumulate in the insoluble fraction, ruling out this potential mechanism for reduced Parkin levels. Future studies will examine mechanisms of Parkin degradation to determine how mtDNA mutations and aging may affect Parkin protein function.

Since Parkin is a well-known regulator of mitophagy in cardiomyocytes, Parkin deficiency was predicted to accelerate cardiac aging in mice with the POLG mutation. However, I did not see worsening cardiac function in POLG/Parkin KO mice compared to POLG mice alone. In addition, hearts from Parkin-deficient mice still had intact mitophagy, and *Bnip3* and *Bnip3l/Nix* transcripts increased in hearts with the POLG mutation, indicating that these hearts rely on Parkin-independent mechanisms to clear dysfunctional mitochondria due to accumulating mtDNA mutations.

Overall, these data show that Parkin-mediated mitophagy is not the primary mechanism that the aging heart utilizes to clear mitochondria with accumulating mtDNA mutations. Neither overexpression nor lack of Parkin affected clearance of mitochondria with mtDNA mutations, suggesting that Parkin protein function is affected by the POLG mutation, rather than Parkin functioning upstream to regulate clearance of dysfunctional mitochondria with mtDNA mutations.

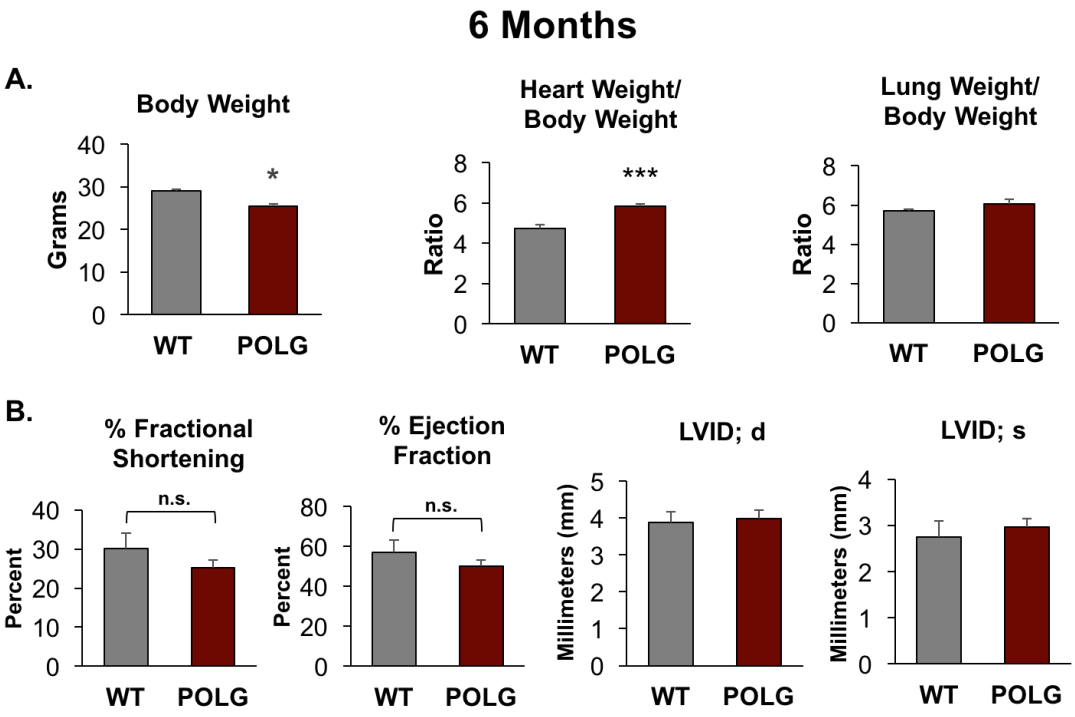

Figure 6.1: Baseline parameters and echocardiography of WT and POLG mice at 6 months. A. Average body weight, heart weight/body weight, and lung weight/body weight ratios of WT and POLG mice at 6 months of age (n=6-9). **B.** Echocardiographic analysis of % fractional shortening, % ejection fraction, left ventricular internal dimension at diastole, and left ventricular internal dimension at systole (n=5-6). (*p<0.05; ***p<0.001; n.s., not significant)

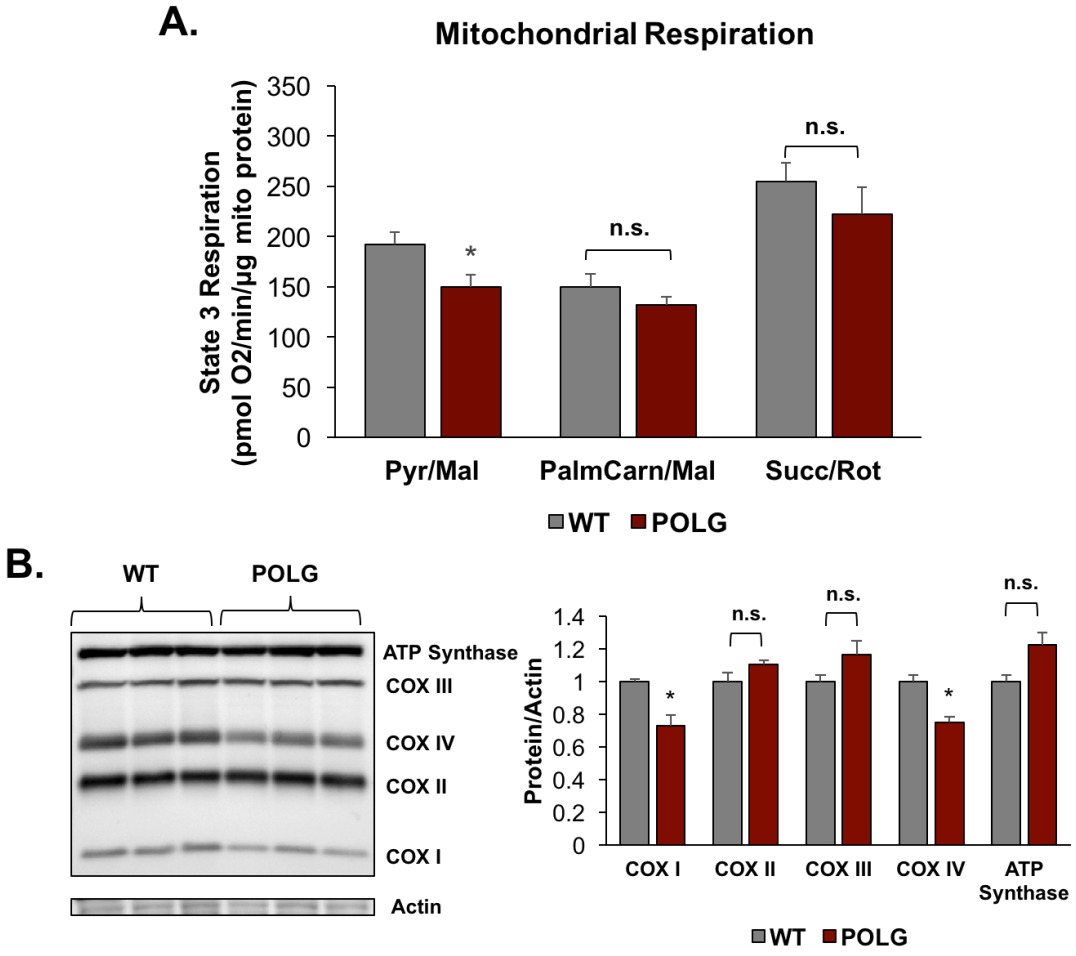

Figure 6.2: Mitochondrial respiration and OXPHOS proteins in WT and POLG mouse hearts at 6 months. A. Mitochondria were isolated from the hearts of 6 month-old WT and POLG mice. Substrates and inhibitors to measure glucose metabolism, fatty acid oxidation, and Complex II activity were added and oxygen consumption was measured using the Seahorse XF96 Analyzer. (n=3). **B.** Western blot and quantitation of mitochondrial OXPHOS proteins from hearts of WT and POLG mice at 6 months of age showed reduced levels of COX I and COX IV in POLG mice (n=3). (*$p<0.05$; n.s., not significant)

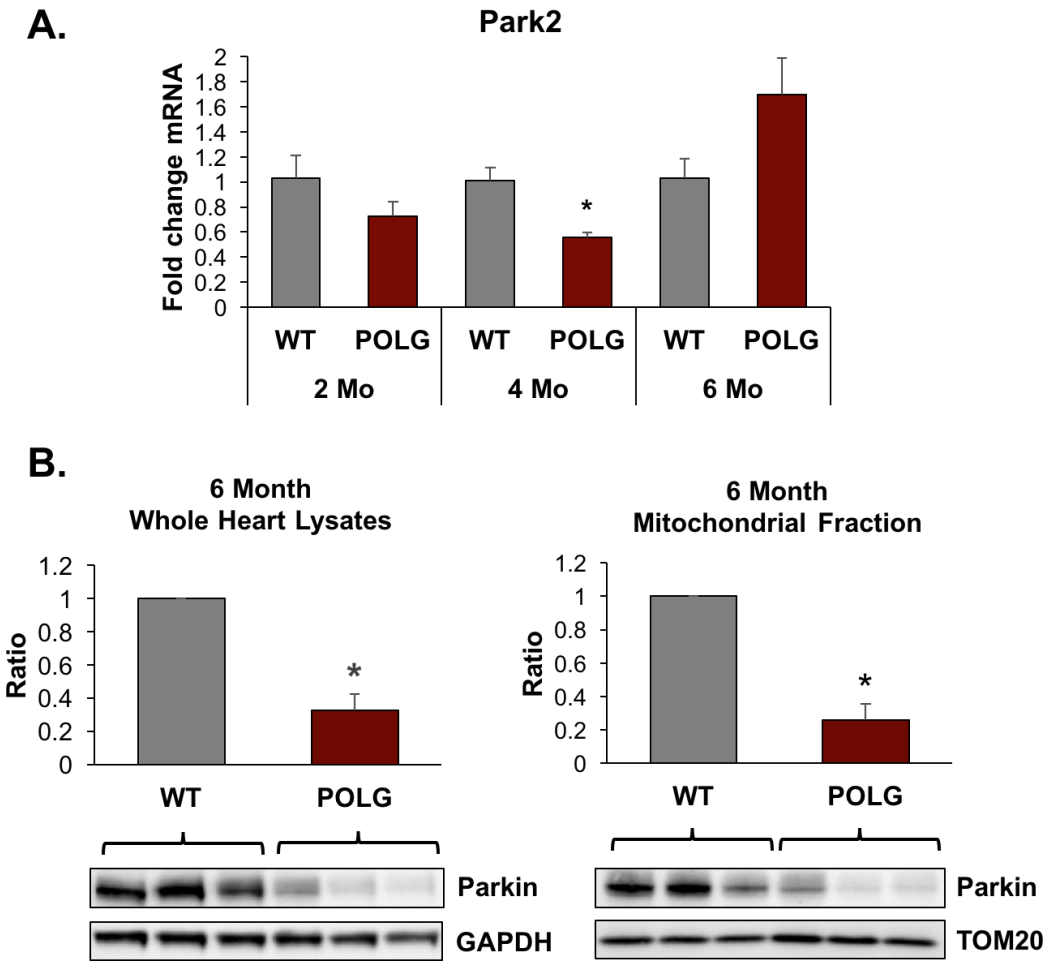

Figure 6.3: Real-time qPCR and Western blot of Parkin in WT and POLG mouse hearts at 6 months. A. Real-time qPCR analysis of *Park2* (Parkin) gene expression in hearts of 2, 4, and 6 month-old WT and POLG mice (n=3). **B.** Western blot and quantitation of Parkin protein levels from whole heart lysates and mitochondrial fraction of hearts from 6 month-old WT and POLG mice (n=3). (*p<0.05)

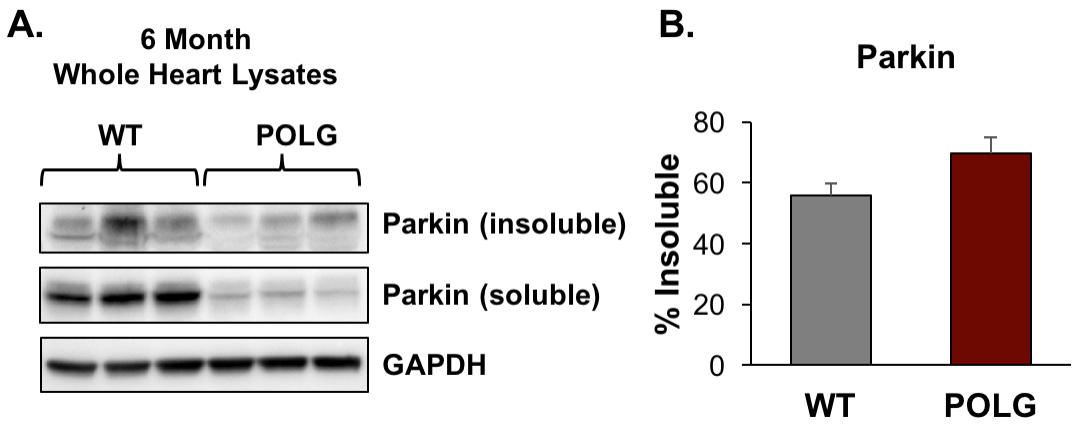

Figure 6.4: Soluble and insoluble Parkin in hearts of WT and POLG mice at 6 months. A. Western blot of soluble and insoluble Parkin protein levels from whole heart lysates of 6 month-old WT and POLG mice (n=3). **B.** Quantitation of % insoluble Parkin in WT and POLG whole heart lysates (n=3).

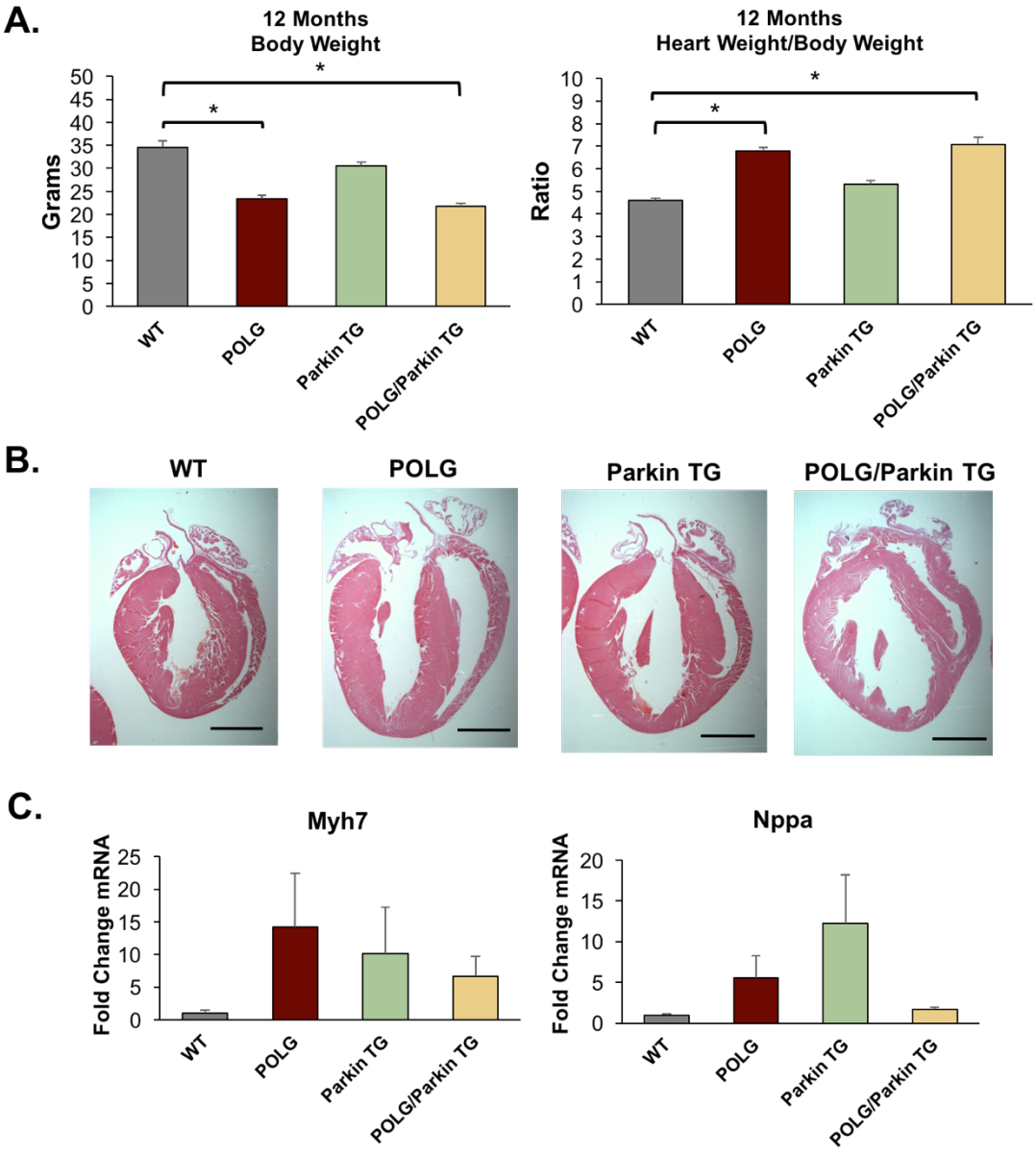

Figure 6.5: Characterization of baseline parameters and cardiac hypertrophy in POLG x Parkin TG mice at 12 months. A. Body weight and heart weight/body weight ratios of POLG x Parkin TG mice at 12 months (n=6-11). **B.** H&E staining of 12 month POLG x Parkin TG hearts. **C.** Real-time qPCR analysis of β-MHC (*Myh7)* and Atrial Natriuretic Peptide (*Nppa)* in hearts of 12 month-old POLG x Parkin TG mice (n=4). Scale Bar = 2 mm. (*p<0.05)

Table 6.1: Echocardiography of POLG x Parkin TG mouse heart function. WT n=3-6, POLG n=7-11, Parkin TG n=5-7, POLG/Parkin TG n=5-11. (*p<0.05 vs. 2 months, ^ vs. 6 months, # vs. WT, $ vs. POLG, & vs. Parkin TG)

	Mean Value ± SEM			
		2 Months	**6 Months**	**12 Months**
% FS	WT	31.82 ± 1.64	30.47 ± 2.16	28.87 ± 0.64
	POLG	32.25 ± 1.69	32.92 ± 1.01	35.98 ± 1.39 #
	Parkin TG	35.15 ± 2.80	32.46 ± 1.96	31.43 ± 1.34
	POLG/Parkin TG	34.79 ± 1.85	32.87 ± 1.15	38.30 ± 1.56 ^#&
% EF	WT	60.11 ± 2.30	57.88 ± 3.25	55.58 ± 0.93
	POLG	60.75 ± 2.40	61.57 ± 1.46	65.29 ± 1.81 #
	Parkin TG	64.60 ± 3.79	60.96 ± 2.84	59.53 ± 1.96
	POLG/Parkin TG	64.34 ± 2.53	58.54 ± 2.65	68.43 ± 1.89 ^#&
IVS;d (mm)	WT	0.80 ± 0.07	0.87 ± 0.03	0.99 ± 0.02 *
	POLG	0.75 ± 0.03	0.84 ± 0.03	1.08 ± 0.03 *^
	Parkin TG	0.76 ± 0.06	0.87 ± 0.04	1.06 ± 0.05 *
	POLG/Parkin TG	0.74 ± 0.05	0.89 ± 0.03 *	1.08 ± 0.04 *^
IVS;s (mm)	WT	1.20 ± 0.14	1.15 ± 0.07	1.36 ± 0.04
	POLG	1.16 ± 0.05	1.23 ± 0.03	1.49 ± 0.03 *^
	Parkin TG	1.23 ± 0.05	1.20 ± 0.08	1.43 ± 0.08 ^
	POLG/Parkin TG	1.13 ± 0.06	1.19 ± 0.03	1.59 ± 0.07 *^#
LVID;d (mm)	WT	4.29 ± 0.17	4.31 ± 0.08	4.57 ± 0.06
	POLG	4.08 ± 0.08	4.32 ± 0.08	4.70 ± 0.10 *^
	Parkin TG	4.01 ± 0.16	4.07 ± 0.10	4.24 ± 0.09 $
	POLG/Parkin TG	4.04 ± 0.12	4.08 ± 0.07	4.57 ± 0.10 *^
LVID;s (mm)	WT	2.92 ± 0.12	3.00 ± 0.13	3.25 ± 0.03
	POLG	2.77 ± 0.11	2.91 ± 0.08	3.02 ± 0.12
	Parkin TG	2.62 ± 0.21	2.75 ± 0.12	2.91 ± 0.10
	POLG/Parkin TG	2.64 ± 0.12	2.75 ± 0.08	2.76 ± 0.10 #
LVPW;d (mm)	WT	0.70 ± 0.05	0.76 ± 0.03	0.74 ± 0.03
	POLG	0.72 ± 0.02	0.81 ± 0.04	0.74 ± 0.03
	Parkin TG	0.70 ± 0.06	0.81 ± 0.05	0.87 ± 0.05 *
	POLG/Parkin TG	0.72 ± 0.01	0.81 ± 0.02	0.82 ± 0.04
LVPW;s (mm)	WT	1.01 ± 0.06	1.11 ± 0.06	1.11 ± 0.04
	POLG	1.10 ± 0.04	1.18 ± 0.02	1.19 ± 0.05
	Parkin TG	1.07 ± 0.04	1.18 ± 0.03	1.25 ± 0.07
	POLG/Parkin TG	1.10 ± 0.02	1.15 ± 0.03	1.30 ± 0.06 *^
MV E/A ratio	WT	1.63 ± 0.17	1.66 ± 0.17	1.54 ± 0.12
	POLG	1.68 ± 0.11	1.55 ± 0.09	1.70 ± 0.11
	Parkin TG	1.68 ± 0.06	2.01 ± 0.19	1.96 ± 0.23
	POLG/Parkin TG	1.57 ± 0.05	1.70 ± 0.08	1.97 ± 0.28

FS indicates fractional shortening; EF, ejection fraction; IVS;d, interventricular septal thickness at diastole; IVS;s, interventricular septal thickness at systole; LVID;d, left ventricular internal dimension at diastole; LVID;s, left ventricular internal dimension at systole; LVPW;d, left ventricular posterior wall thickness at diastole; LVPW;s, left ventricular posterior wall thickness at systole; MV E/A ratio, mitral valve early peak velocity/atrial peak velocity.

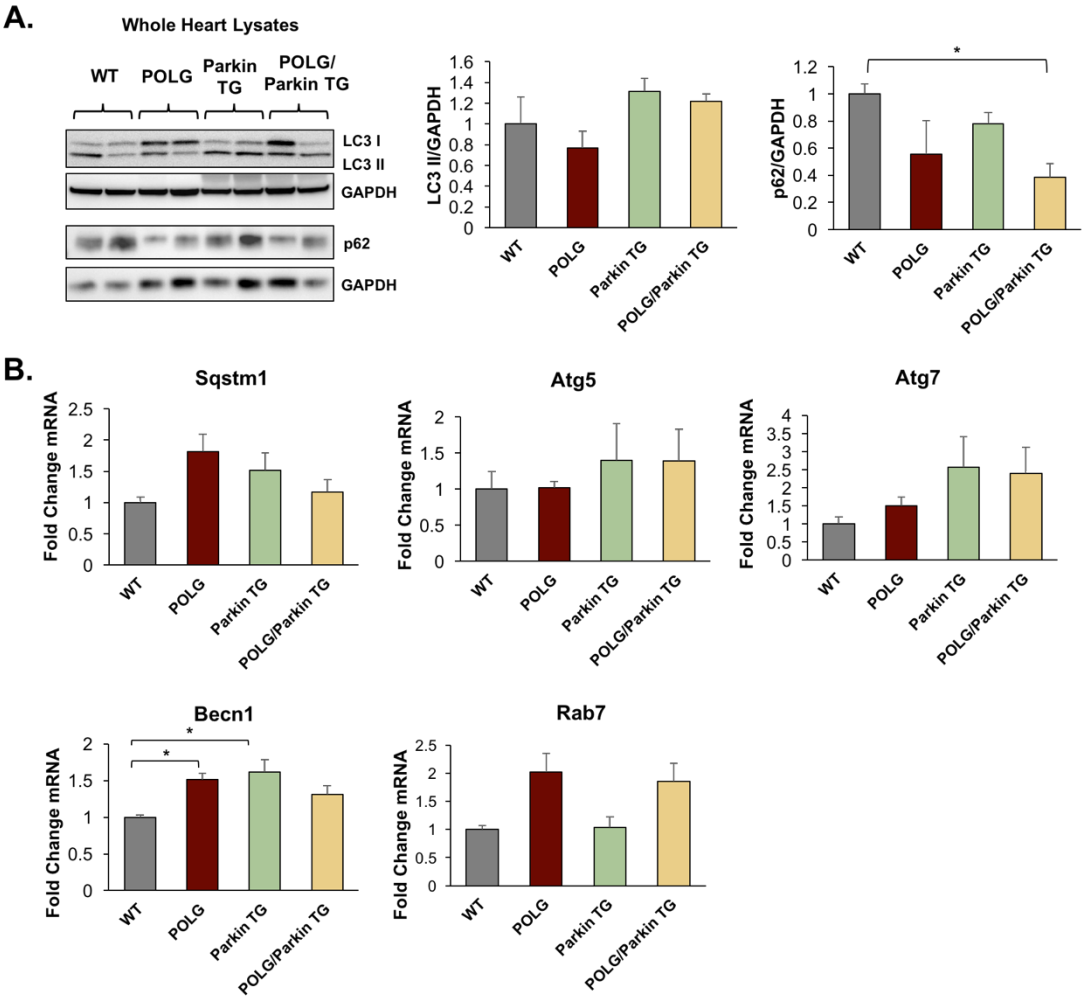

Figure 6.6: Autophagy in POLG x Parkin TG mouse hearts at 12 months. **A.** Representative Western blots and quantitation of LC3 and p62 expression from whole heart lysates of 12 month POLG x Parkin TG mice (n=4). **B.** Real-time qPCR of *Sqstm1*, *Atg5*, *Atg7*, *Becn1*, and *Rab7* in 12 month POLG x Parkin TG mouse hearts (n=4). (*p<0.05)

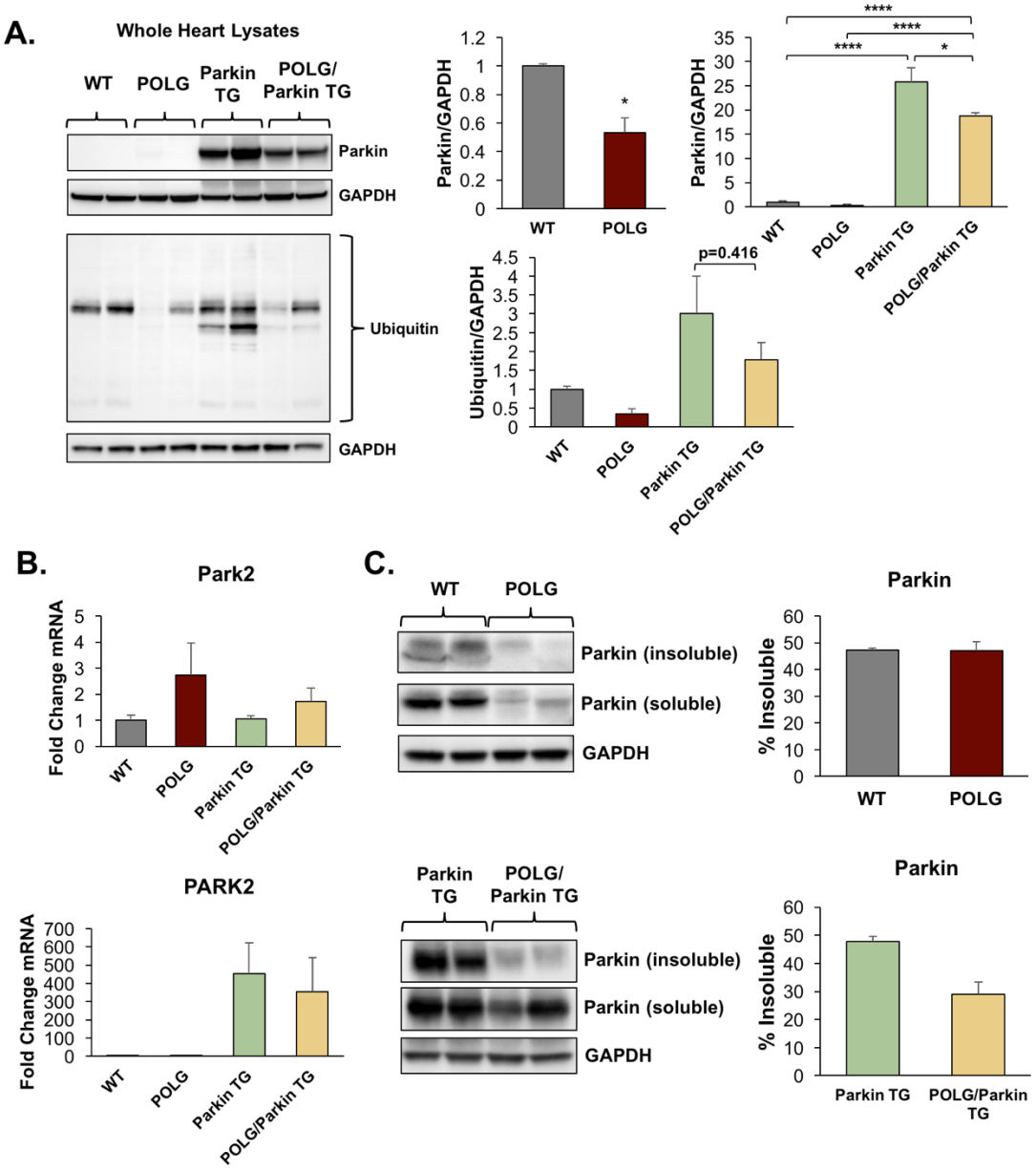

Figure 6.7: Parkin expression in POLG x Parkin TG mouse hearts at 12 months. A. Representative Western blots and quantitation of Parkin and ubiquitin expression from whole heart lysates of 12 month POLG x Parkin TG mice (n=4). **B.** Real-time qPCR of mouse *Park2* and human *PARK2* transcripts in 12 month POLG x Parkin TG mouse hearts (n=4). **C.** Western blots of soluble and insoluble Parkin protein levels and quantitation of % insoluble Parkin from whole heart lysates of 12 month-old POLG x Parkin TG mice (n=2). (*p<0.05; ****p<0.0001)

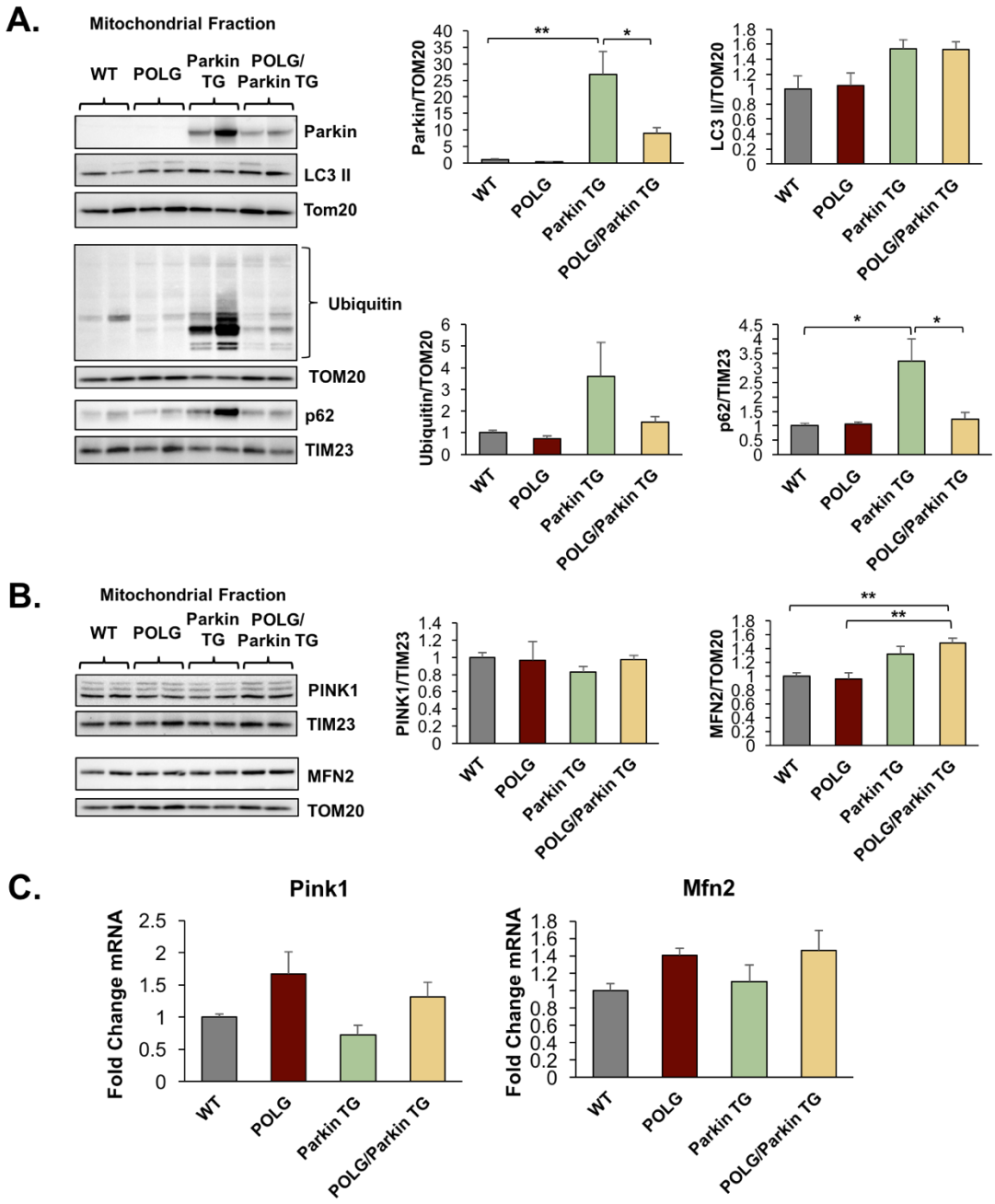

Figure 6.8: Mitophagy in POLG x Parkin TG mouse hearts at 12 months. A. Representative Western blots and quantitation of Parkin, ubiquitin, LC3, and p62 expression in isolated mitochondria from hearts of 12 month POLG x Parkin TG mice (n=4). **B.** Representative Western blots and quantitation of PINK1 and MFN2 expression in isolated mitochondria from the hearts of 12 month POLG x Parkin TG mice (n=4). **C.** Real-time qPCR analysis of *Pink1* and *Mfn2* gene expression in hearts of 12 month-old POLG x Parkin TG mice (n=4). (*p<0.05; **p<0.01)

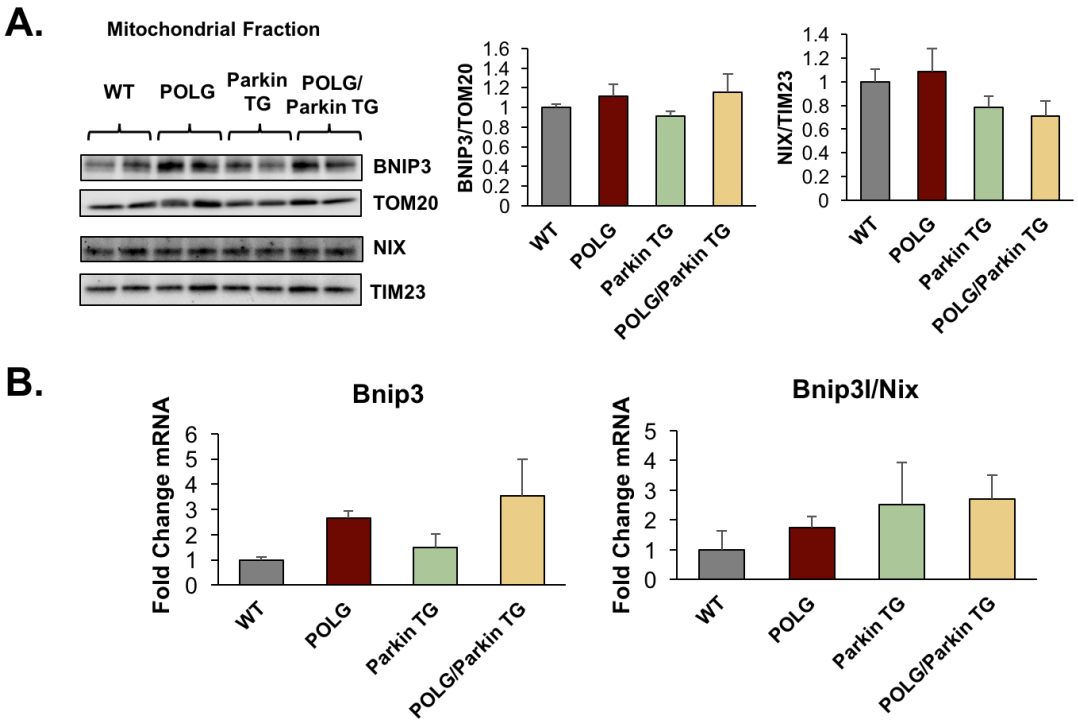

Figure 6.9: Mitophagy receptors in POLG x Parkin TG mouse hearts at 12 months. A. Representative Western blots and quantitation of BNIP3 and NIX expression in isolated mitochondria from hearts of 12 month POLG x Parkin TG mice (n=4). **B.** Real-time qPCR analysis of *Bnip3* and *Bnip3l/Nix* gene expression in hearts of 12 month-old POLG x Parkin TG mice (n=4).

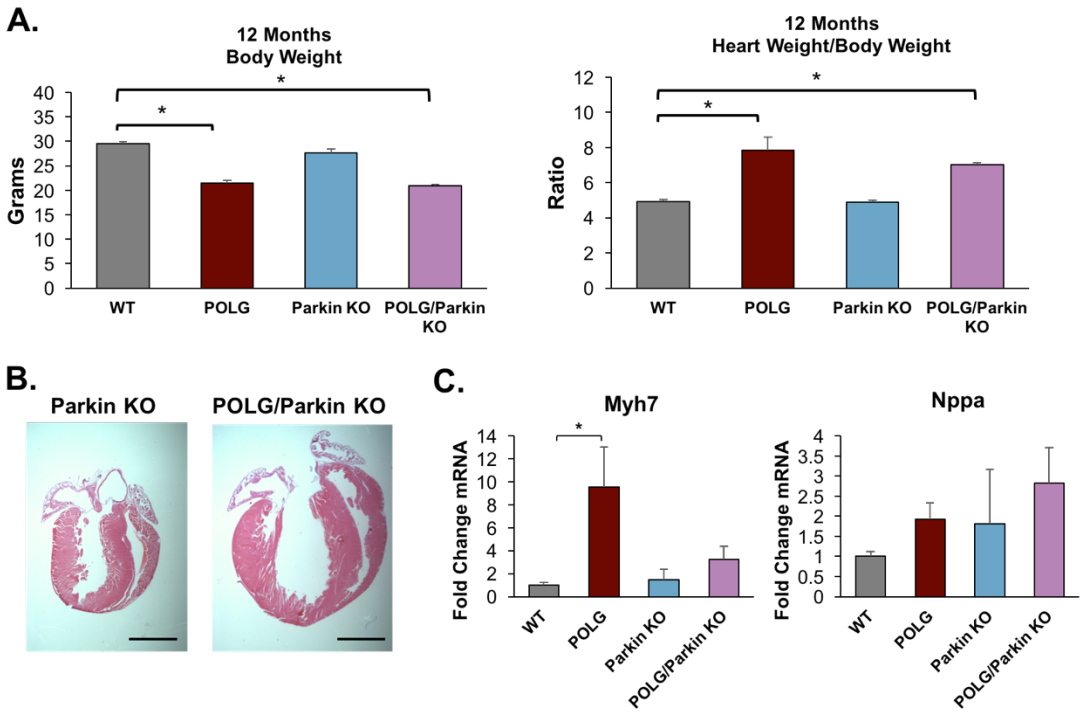

Figure 6.10: Characterization of baseline parameters and cardiac hypertrophy in POLG x Parkin KO mice at 12 months. A. Body weight and heart weight/body weight ratios of POLG x Parkin KO mice at 12 months (n=5-7). **B.** H&E staining of 12 month Parkin KO and POLG/Parkin KO hearts. **C.** Real-time qPCR analysis of β-MHC (*Myh7)* and Atrial Natriuretic Peptide (*Nppa)* in hearts of 12 month old POLG x Parkin TG mice (n=4). Scale Bar = 2 mm. (*p<0.05)

Table 6.2: Echocardiography of POLG x Parkin KO mouse heart function.
WT n=6, POLG n=5, Parkin KO n=6-7, POLG/Parkin KO n=6-7.
(*p<0.05 vs. 2 months, ^ vs. 6 months, # vs. WT, $ vs. POLG, & vs. Parkin KO)

		Mean Value ± SEM		
		2 Months	**6 Months**	**12 Months**
% FS	WT	35.20 ± 3.02	34.67 ± 0.23	35.96 ± 1.81
	POLG	31.80 ± 1.53	32.64 ± 2.52	35.03 ± 1.01
	Parkin KO	36.95 ± 1.73	37.47 ± 1.08	35.89 ± 3.02
	POLG/Parkin KO	34.79 ± 1.15	30.81 ± 1.15 &	33.37 ± 2.10
% EF	WT	64.56 ± 3.85	64.16 ± 0.32	65.67 ± 2.42
	POLG	60.22 ± 2.20	61.05 ± 3.46	64.46 ± 1.42
	Parkin KO	67.61 ± 2.23	68.02 ± 1.33	65.19 ± 4.52
	POLG/Parkin KO	65.05 ± 1.59	58.78 ± 1.63 &	61.98 ± 3.02
IVS;d (mm)	WT	0.95 ± 0.09	0.92 ± 0.03	0.97 ± 0.02
	POLG	0.75 ± 0.02	0.92 ± 0.04	1.13 ± 0.07 *
	Parkin KO	1.15 ± 0.10 $	0.89 ± 0.04 *	0.94 ± 0.05 $
	POLG/Parkin KO	0.91 ± 0.11	0.85 ± 0.04	0.89 ± 0.05 $
IVS;s (mm)	WT	1.38 ± 0.10	1.28 ± 0.06	1.35 ± 0.04
	POLG	1.21 ± 0.04	1.28 ± 0.03	1.56 ± 0.09 *^
	Parkin KO	1.45 ± 0.07	1.26 ± 0.06	1.39 ± 0.08
	POLG/Parkin KO	1.29 ± 0.11	1.16 ± 0.06	1.18 ± 0.06 $
LVID;d (mm)	WT	3.91 ± 0.09	4.27 ± 0.13	4.25 ± 0.06
	POLG	4.07 ± 0.09	4.23 ± 0.13	4.44 ± 0.10
	Parkin KO	3.54 ± 0.16 $	3.97 ± 0.13 *	4.08 ± 0.12 *
	POLG/Parkin KO	3.41 ± 0.07 #$	4.11 ± 0.08 *	4.40 ± 0.12 *&
LVID;s (mm)	WT	2.53 ± 0.14	2.79 ± 0.08	2.72 ± 0.09
	POLG	2.77 ± 0.10	2.88 ± 0.14	2.89 ± 0.10
	Parkin KO	2.24 ± 0.14 $	2.48 ± 0.08 $	2.63 ± 0.20
	POLG/Parkin KO	2.22 ± 0.07 $	2.84 ± 0.08 *&	2.95 ± 0.17 *
LVPW;d (mm)	WT	0.88 ± 0.08	0.76 ± 0.05	0.85 ± 0.03
	POLG	0.71 ± 0.04	0.69 ± 0.04	0.78 ± 0.05
	Parkin KO	0.94 ± 0.06	0.80 ± 0.05	0.71 ± 0.02 *#
	POLG/Parkin KO	0.92 ± 0.11	0.75 ± 0.02	0.77 ± 0.04
LVPW;s (mm)	WT	1.32 ± 0.14	1.22 ± 0.04	1.34 ± 0.03
	POLG	1.08 ± 0.05	1.10 ± 0.05	1.26 ± 0.08
	Parkin KO	1.11 ± 0.05	1.21 ± 0.05	1.21 ± 0.05
	POLG/Parkin KO	1.25 ± 0.15	1.19 ± 0.05	1.27 ± 0.07

FS indicates fractional shortening; EF, ejection fraction; IVS;d, interventricular septal thickness at diastole; IVS;s, interventricular septal thickness at systole; LVID;d, left ventricular internal dimension at diastole; LVID;s, left ventricular internal dimension at systole; LVPW;d, left ventricular posterior wall thickness at diastole; LVPW;s, left ventricular posterior wall thickness at systole.

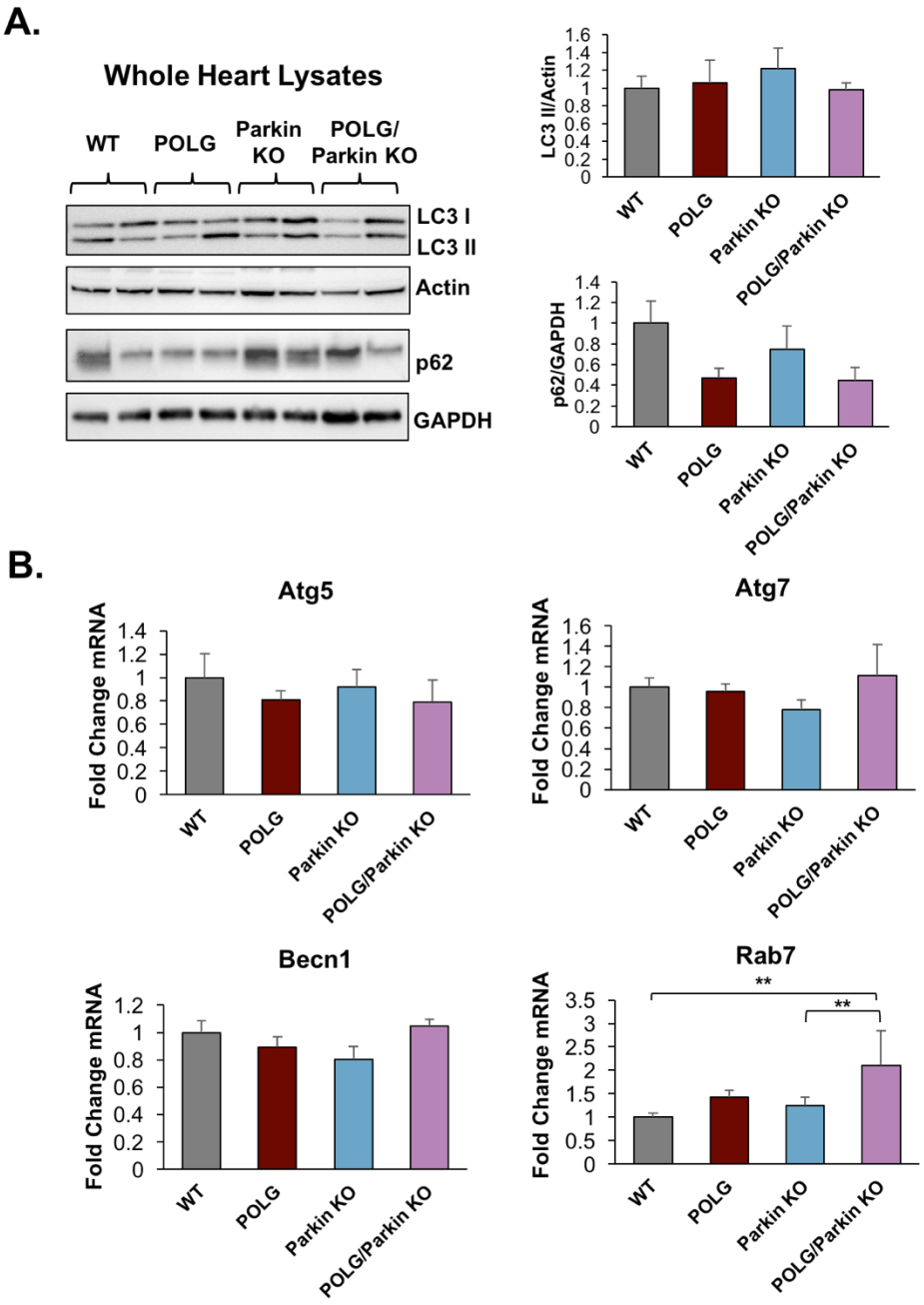

Figure 6.11: Autophagy in POLG x Parkin KO mouse hearts at 12 months. **A.** Representative Western blots and quantitation of LC3 and p62 expression from whole heart lysates of 12 month POLG x Parkin KO mice (n=4). **B.** Real-time qPCR of *Atg5*, *Atg7*, *Becn1*, and *Rab7* in 12 month POLG x Parkin KO mouse hearts (n=4). (*p<0.05; **p<0.01)

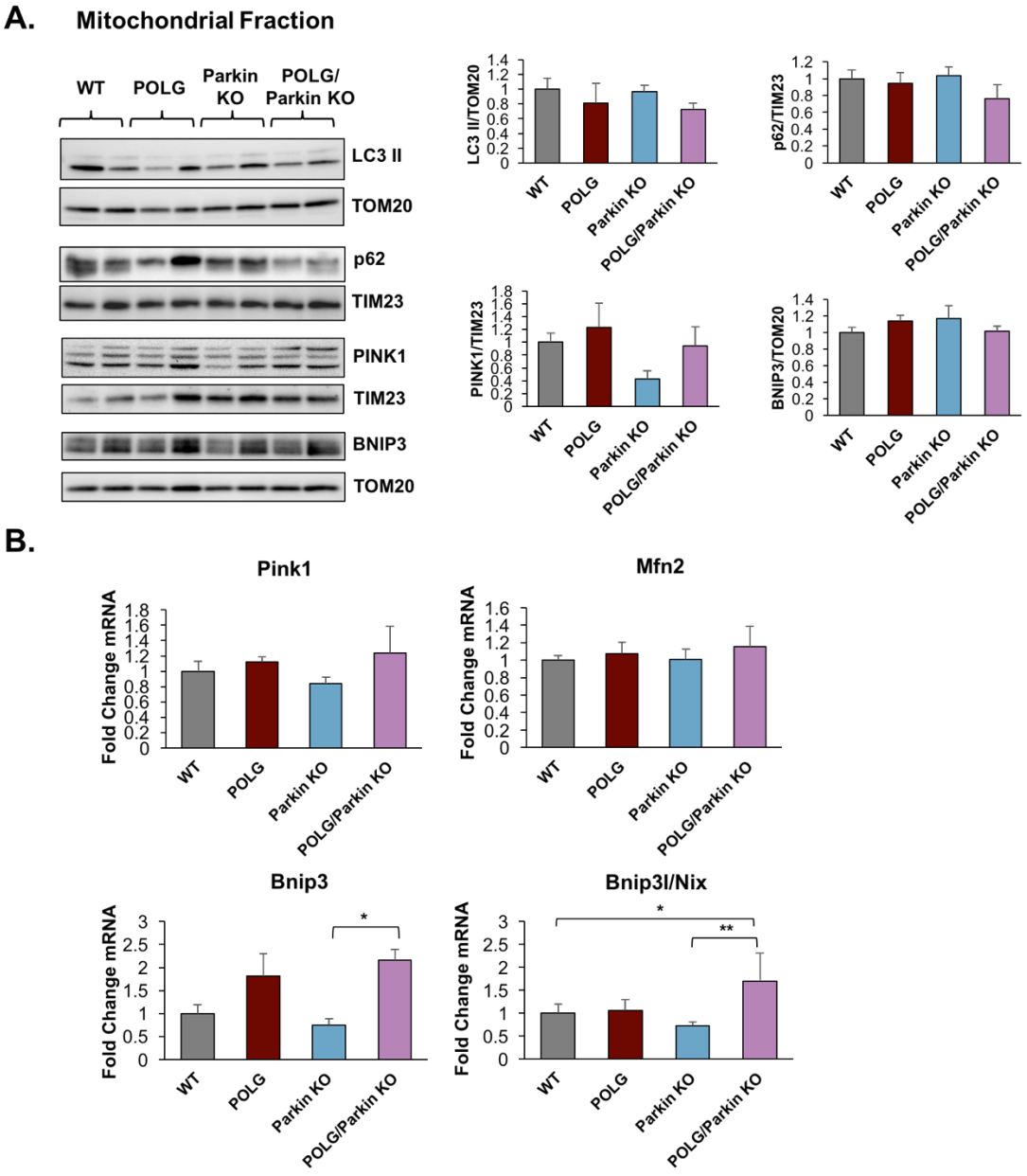

Figure 6.12: Mitophagy in POLG x Parkin KO mouse hearts at 12 months. **A.** Representative Western blots and quantitation of LC3, p62, PINK1, and BNIP3 expression in isolated mitochondria from hearts of 12 month POLG x Parkin KO mice (n=4). **B.** Real-time qPCR analysis of *Pink1, Mfn2, Bnip3, and Bnip3l/Nix* gene expression in hearts of 12 month-old POLG x Parkin KO mice (n=4). (*p<0.05; **p<0.01)

CHAPTER 7: DISCUSSION

Introduction

My dissertation research addresses the role of mitochondrial quality control in regulating cardiac progenitor cell function and cardiac aging. My studies demonstrate that mitochondrial biogenesis and network expansion occur during CPC lineage commitment, and that accumulation of mtDNA mutations impairs CPC survival, proliferation, and differentiation. Both WT and POLG CPCs activate autophagy and mitophagy in response to acute stress. However, POLG CPCs exhibited impaired mitophagy activation in response to differentiation. Gene expression of mitophagy receptors NIX and FUNDC1, not Parkin, increase during differentiation and may play a role in mediating the mitophagy in CPCs. In contrast to the CPCs, the myocardium is remarkably resistant to the POLG mutation. Parkin has been shown to play a critical role in cardiomyocytes by promoting removal of damaged mitochondria in response to acute stress. My studies investigated the role of Parkin in clearing damaged mitochondria due to accumulating mtDNA mutations. I found that aging led to cardiac hypertrophy, and modifying Parkin levels by cardiac-specific overexpression or genetic ablation did not affect autophagy, mitophagy, and cardiac function in POLG mice. My data suggest that Parkin-mediated mitophagy is impaired and is not the primary mechanism that aging hearts utilize to clear mitochondria with accumulating mtDNA mutations. Thus, my findings

from both CPCs and hearts with the POLG mutation suggest that Parkin-mediated mitophagy does not play a role in clearing mitochondria with accumulating mtDNA mutations.

Mitochondrial biogenesis and network expansion correlate with cardiac progenitor cell differentiation

Mitochondria regulate stemness, self-renewal, and differentiation in many stem cell populations (Rehman, 2010; Ito & Suda, 2014; Kasahara & Scorrano, 2014). My studies show that mitochondria also play an important role in CPC differentiation. Activation of AMPK and PGC-1α leads to activation of mitochondrial biogenesis and expansion of mitochondria along the microtubule network, which correlates with lineage commitment.

The differentiation stimuli and upstream signals that regulate mitochondrial reprogramming and activate mitochondrial expansion in CPCs have not been fully elucidated. Although I show that AMPK and PGC-1α are activated in CPCs, it is not clear whether lineage commitment precedes mitochondrial expansion, or whether mitochondrial biogenesis occurs before differentiation. It is also possible that these two events occur simultaneously. Signaling pathways that have been reported to regulate CPC proliferation and differentiation include Pim1 (Samse et al., 2015), Notch1 (Boni et al., 2008; Gude et al., 2015), stem cell factor (SCF) (Vajravelu et al., 2015), sphingosine 1-phosphate (S1P) (Castaldi et al., 2016), and CAMKII (Quijada, Hariharan, et

al., 2015). It will be important to determine what signals originating from cells in the border zone stimulate CPCs to proliferate and differentiate, and how these signaling pathways affect mitochondrial reprogramming. Expansion of the mitochondrial network is important because it allows cells to adjust to the increased energy demand. Failure of stem cells to undergo a metabolic transition could lead to reduced survival, which could negatively affect their repair potential when injected into patients. Elucidating the potential signals that regulate mitochondrial expansion could identify targets that may improve the quality of CPCs and other stem cells used in the clinic.

Accumulation of mtDNA mutations impairs CPC survival, proliferation, and differentiation

Mitochondrial quality control is important in many stem cell populations (Joshi & Kundu, 2013; Vazquez-Martin et al., 2016), so it is not surprising that my studies also show the importance of maintaining a healthy population of mitochondria in CPCs. I demonstrate that accumulation of mtDNA mutations leads to mitochondrial dysfunction, which impairs cell survival, proliferation and differentiation. I also show that POLG CPCs rely on glycolysis for energy production and are unable to transition to mitochondrial respiration upon activation of differentiation.

Aging is associated with accumulation of mtDNA damage in tissues including the heart (Kujoth et al., 2007). The susceptibility to mtDNA mutations

can differ between cells within the same organ. It is likely that CPCs from young 2 month-old mice are more sensitive to accumulation of mtDNA mutations than cardiomyocytes because they are proliferative and constantly replicating mitochondria during cell division. In contrast, hearts from mice of the same age do not show any cardiac or mitochondrial dysfunction due to the senescent phenotype of cardiomyocytes.

Accumulating mtDNA mutations can also have differential effects depending on the type of stem cells and differentiation state. POLG CPCs rely on glycolysis and are able to survive at baseline conditions, although they proliferate less efficiently. However, they are sensitive to stress and differentiation stimulus, and are unable to transition to mitochondrial OXPHOS which leads to cell death. Similarly, iPSCs derived from fibroblasts and aged in culture also have abnormal mitochondria and fail to undergo neurogenesis (Masotti et al., 2014). In contrast, iPS cells generated from POLG mice exhibit hyperactive glycolytic activity during differentiation to compensate for OXPHOS defects (Wahlestedt et al., 2014). It is interesting that the failure to undergo the metabolic switch from glycolysis to mitochondrial OXPHOS leads to severe consequences (cell death) in an adult progenitor cell population such as CPCs, but only leads to increased glycolysis and arrested differentiation in iPS cells. These findings suggest that reprogramming somatic cells into iPS cells may yield a pluripotent phenotype but does not take into account changes in mitochondria that regulate cell differentiation. Thus, it is important to deepen our

understanding of mitochondrial biology in CPCs and other stem cells if they are to be used clinically.

Autophagy is reduced with age and failure to clear defective mitochondria could lead to impaired cell function (Rubinsztein et al., 2011). Cells utilize mitophagy to clear dysfunctional mitochondria (Kubli & Gustafsson, 2012), and replacement of old mitochondria with new mitochondria has been shown to be required for myoblast differentiation (Sin et al., 2016). I have found that the mitophagy response is intact in POLG CPCs at baseline and when exposed to acute stress such as FCCP, but is impaired with differentiation. I have also found that the mitophagy response in CPCs does not involve Parkin and is likely mediated by BNIP3L/NIX and FUNDC1. These findings indicate that mitophagy is a mechanism used by CPCs to maintain mitochondrial homeostasis, respond to stress, and adapt to energy-requiring stimuli such as differentiation. I have also shown that AMPK activation is important for CPC differentiation and proper formation of the mitochondrial network. AMPK has been shown to phosphorylate ULK1 to activate mitophagy (Egan et al., 2011). It is possible that the upstream signals to activate mitophagy in POLG CPCs are also impaired in iPS cells, and could explain why these stem cells cannot proceed to differentiation. These observations further support the important role of mitochondria in regulating stem cell function. Therefore, continued study of mitophagy in stem cells will contribute to our knowledge of stem cell biology.

Defective POLG is expected to produce errors only in mtDNA-encoded genes, but these defects can consequently affect not only mitochondrial function but also overall cellular function. Although nuclear-to-mitochondrial (anterograde) signaling is well-studied, mitochondrial-to-nuclear (retrograde) signaling has not been fully explored in mammalian cells and has mainly been studied in yeast (Liu & Butow, 2006). Changes in mitochondrial function that lead to changes in nuclear gene expression and cell function could have implications for stem cell differentiation and aging. Mitochondrial retrograde signaling due to mtDNA mutations and changes in mtDNA copy number have been studied in tumorigenesis (Guha & Avadhani, 2013). A recent study also demonstrates that mitochondrial dynamics regulate the fate of neural stem cells via ROS and NRF2-mediated retrograde signaling (Khacho et al., 2016). Nuclear factor, erythroid 2-like 2 (NRF2) is a transcription factor that is normally sequestered in the cytoplasm and translocates to the nucleus in response to oxidative stress (Dinkova-Kostova & Abramov, 2015). NRF2 can activate downstream target genes to regulate antioxidant response and has been shown to regulate self-renewal and stemness in hESCs (Jang et al., 2014). It is possible that retrograde signaling also plays a role in regulating the fate of CPCs and other stem cell populations.

The RTG pathway, identified in yeast, involves Rtg protein complexes which are transcriptional activators that translocate from mitochondria to cytosol to nucleus and activate expression of genes involved in metabolic

reprogramming (Liu & Butow, 2006). More recently, different branches of the RTG pathway have been shown to activate different gene targets, suggesting that mitochondrial status can promote divergent metabolic reprogramming and affect distinct cellular processes (Palkova & Vachova, 2016). Due to its similarities to the RTG pathway in yeast, NFκB has been postulated to mediate the retrograde signaling pathway in mammalian cells (Jazwinski & Kriete, 2012). Further investigation of the role of NFκB in CPCs and other stem cells may provide valuable insight on regulation of stem cell function.

Parkin-mediated mitophagy does not play a role in clearing dysfunctional mitochondria in aging hearts with accumulating mtDNA mutations

The heart cannot efficiently regenerate after stress or injury and relies on organelle quality control to maintain homeostasis and optimal function. Cardiomyocytes depend on mitochondria to generate ATP for contractile function, and utilize mitophagy to remove dysfunctional mitochondria induced by acute stress (Kubli & Gustafsson, 2012). Parkin-mediated mitophagy is the most well-characterized mechanism for clearing depolarized and dysfunctional mitochondria. Many studies have investigated the role of Parkin in the context of neurodegenerative disorders such as Parkinson's, Alzheimer's, and Huntington's disease (Khalil et al., 2015; Ye et al., 2015; Shaltouki et al., 2015), and others have studied its role in the heart (Chen & Dorn, 2013; Kubli et al., 2013; Song et al., 2015).

If defects in mitophagy lead to disease, and if Parkin-mediated mitophagy is the primary pathway, then lack of Parkin would be expected to have detrimental effects. However, my data does not support this prediction. Interestingly, genetic animal models of Parkin deficiency do not have dopaminergic or behavioral defects and do not recapitulate symptoms of Parkinson's disease (Goldberg et al., 2003; Perez & Palmiter, 2005). A recent study investigated the role of Parkin *in vivo* by crossing Parkin-deficient mice with POLG mice (Pickrell et al., 2015). Although they reported degeneration of dopaminergic neurons and some mild behavioral defects in 12 month old mice, they did not observe differences in the number of somatic mtDNA mutations, indicating that Parkin is not necessarily involved in selectively removing mitochondria with accumulating mtDNA mutations (Pickrell et al., 2015).

To my knowledge, my studies are the first to explore the role of Parkin-mediated mitophagy in hearts of aging mice with accumulating mtDNA mutations. Although Parkin plays a critical role in adapting to acute stress such as an MI, my findings show that Parkin is not the only protein that facilitates mitophagy in the heart. Hearts with the POLG mutation appear to upregulate BNIP3 and NIX, suggesting that these mitophagy receptors are important for removing mitochondria with mtDNA mutations. Data from the Parkin-deficient mice also show that BNIP3 and NIX can mediate mitophagy in the absence of Parkin. These data suggest that stress-induced mitophagy is mediated by Parkin, and maintenance of mitochondrial quality is likely mediated by

mitophagy receptors BNIP3 and NIX. In addition, data from the CPCs show that mitophagy receptors NIX and FUNDC1 are likely involved in baseline mitochondrial maintenance and differentiation-induced mitophagy, consistent with the essential role of NIX in removal of mitochondria during erythroid differentiation (Sandoval et al., 2008).

The presence of the POLG mutation increases the probability of generating mitochondria with many errors. Cardiac-specific Parkin overexpression was predicted to clear these mitochondria so the cells retain only the healthy mitochondria, and rescue cardiac dysfunction caused by the POLG mutation. However, my findings show that Parkin overexpression in POLG hearts did not affect cardiac function when compared to POLG hearts.

Cells must maintain a balance between mitophagy and mitochondrial biogenesis, and failure to do so can lead to accumulation of dysfunctional mitochondria and development of disease (Andres et al., 2015). POLG CPCs exhibited impaired mitochondrial biogenesis during differentiation, and it is possible that mitochondrial biogenesis could also be impaired in cardiomoyocytes with the POLG mutation. In contrast to the previous hypothesis of Parkin overexpression rescuing cardiac dysfunction, an alternate outcome is that excessive Parkin-mediated mitophagy in POLG hearts could potentially deplete the remaining mitochondria and lead to cell death. However, my data do not show that POLG/Parkin TG hearts had worsening cardiac function compared to POLG mice alone. Thus, cardiac function was mainly

affected by the presence of the POLG mutation, not by the absence or presence of Parkin.

Future studies

There is continued interest in gaining a deeper understanding of mechanisms of myocardial regeneration after pathological injury (Broughton & Sussman, 2016). Various examples of engineered CPCs have been shown to improve CPC function (Mohsin et al., 2012; Mohsin et al., 2013; Quijada, Salunga, et al., 2015). Future studies will address other upstream regulators of mitochondrial biogenesis in CPCs to determine what other pathways could be targeted for therapeutic value.

Since Parkin is not expressed in CPCs, future studies will continue to investigate the role of other mitophagy receptors in mediating mitophagy in CPCs. *Bnip3l/Nix* and *Fundc1* gene expression appeared to increase with differentiation, suggesting that they play a role in differentiating CPCs. Silencing gene expression by siRNA will determine whether these proteins are critical for differentiation and mitochondrial biogenesis. Conversely, overexpressing NIX and FUNDC1 in POLG CPCs will determine if defects in mitophagy can be rescued and if this will restore CPC function.

Parkin levels are reduced in the hearts of POLG mice, and it will be important to determine whether the reduced Parkin is due to increased proteasomal degradation. There is also less Parkin recruited to mitochondria,

even though PINK1 and MFN2 are present, suggesting that there could be defects in Parkin protein, PINK1 or MFN2 activity, or impaired signals from the mitochondria. Future studies will assess cardiomyocyte hypertrophy, pathological remodeling, and apoptosis in the hearts of POLG x Parkin TG and POLG x Parkin KO mice to further confirm cardiac defects. My data only provides information regarding cardiac function at baseline, but does not address the effect of stress on cardiac function. Thus, future studies will induce MI in mice to determine whether Parkin plays a role in adapting to acute cardiac stress. These studies will provide insight on whether aging POLG mice are more sensitive to acute stress and if Parkin overexpression will improve cardiac function in this setting. If Parkin is activated in an MI stress model, Parkin activity can be measured by blotting for phosphorylated ubiquitin and phosphorylated Parkin.

Mitochondrial DNA sequencing is in progress to determine if cardiomyocytes accumulate mtDNA mutations over time, and if POLG hearts have increased mutation rates compared to WT. In addition, mitochondrial respiration will be assessed in the hearts of 12 month old mice to determine if accumulating mtDNA mutations impair mitochondrial function. Furthermore, mitochondrial OXPHOS protein levels and PGC1α (*Ppargc1a*) and PGC-1β (*Ppargc1b*) transcripts will be assessed to determine if mitochondrial biogenesis is impaired in cardiomyocytes with the POLG mutation.

Proposed model and potential mechanisms regulating mitophagy in the aging heart

Although Parkin is involved in regulating mitophagy after acute stress, it is not involved in clearing mitochondria with mtDNA mutations. Based on my findings, I propose a model of the mechanism of clearance of mitochondria with mtDNA mutations. In this model, acute stress causes mitochondrial membrane depolarization and recruits Parkin to damaged mitochondria, where it facilitates clearance by autophagy (Figure 7.1). With aging, mtDNA mutations accumulate, which induces chronic stress. The signals that recruit Parkin to the mitochondria may be impaired in cardiomyocytes with the POLG mutation. My data from CPCs and hearts of mice with the POLG mutation show that Parkin is not important in age-related mitophagy, and cells instead upregulate mitophagy receptors BNIP3 and NIX to clear these defective mitochondria (Figure 7.1). Tissues with the POLG mutation produce ROS which are involved in various signaling pathways. It is possible that mtDNA mutations increase ROS which can affect Parkin protein folding and function, or mtDNA mutations can stimulate mitochondrial retrograde signaling that may regulate nuclear gene expression to modify Parkin's activity.

Therapeutic relevance

Despite the controversy about the exact contribution of CPCs in cardiac regeneration (van Berlo & Molkentin, 2016), CPCs have been shown to migrate

to the border zone after MI (Fransioli et al., 2008) and are thought to assist in repair by secreting paracrine factors. A recent study tested multiple injections of CPCs in rat hearts and found cumulative beneficial effects on cardiac structure and function (Tokita et al., 2016). However, the exact mechanism by which CPCs induced repair and improvement in this model was not explored. CPCs used in the SCIPIO clinical trial led to modest cardiac improvement despite unknown mechanism (Chugh et al., 2012). There is also continued interested in using CPCs in clinical trials. The CONCERT-HF trial combines CPCs and mesenchymal stem cells (MSCs) and is currently recruiting patients for Phase II (ClinicalTrials.gov, 2016). Thus, several important questions need to be addressed regarding CPCs: 1) why is the heart unable to efficiently regenerate after pathological injury, 2) why do stem cells engraft poorly and only induce modest improvement, and 3) what signals (either endogenous or exogenous) and pathways can be targeted to robustly activate CPCs and other repair mechanisms? It is possible that repeated dosing of CPCs in the injured heart enhances repair due to increased retention, and positive feedback signals from the engrafted CPCs enhance the survival of incoming CPCs.

POLG CPCs had impaired survival, proliferation, and differentiation, and these findings suggest that there are limitations to using CPCs or other stem cells derived from aging patients. Even though using autologous CPCs may be advantageous because they avoid an immune response, these CPCs may not be the most optimal cells to use in regenerative therapy. CPCs from aging

hearts will not survive the hostile environment of the failing heart and have reduced probability of survival and engraftment (Quijada & Sussman, 2014). Thus, it is important to learn more about the biology of these cells so that we can develop protocols to select only the youngest and healthiest cells with optimal function. In addition, we can also modify signaling pathways to rejuvenate these CPCs and enhance their regenerative potential (Mohsin et al., 2013; Hariharan et al., 2015). Therefore, understanding the mitochondrial biology of CPCs will increase our knowledge of stem cell biology, which could lead to strategies to improve therapies for heart disease.

Autophagy is a potential target for development of new therapies for cardiovascular disease (Orogo & Gustafsson, 2015). Parkin is an established regulator of mitophagy, and targeting Parkin is believed to increase mitophagy and improve mitochondrial quality control. More studies are clarifying the role of Parkin in clearing defective mitochondria and emerging evidence suggests that Parkin is involved in a mitophagy pathway that responds to acute cardiac injury, and this is distinct from alternative mitophagy pathways that promote mitochondrial quality control under homeostatic conditions (Dorn, 2016). My findings are in agreement with this conclusion.

Acute stress from an MI is distinct from chronic stress such as accumulating mtDNA mutations. Therefore, strategies to target autophagy and mitophagy should take into consideration that many factors such as aging can lead to development of cardiovascular disease, and these different factors could

induce different stress responses that involve distinct signaling pathways. Targeting Parkin-mediated mitophagy may be insufficient to remove dysfunctional mitochondria, or may lead to excessive mitochondrial removal and detrimental effects. Thus, Parkin may not be the best target to prevent or delay age-related heart disease.

Mitochondrial dysfunction is implicated in the pathogenesis of Parkinson's disease (Exner et al., 2012; Yamano et al., 2016), and impairment of Parkin-mediated mitophagy leads to mitochondrial dysfunction and neuronal degeneration (Cai et al., 2012; Ashrafi et al., 2014). Although Parkin plays a neuroprotective role in the brains of aging mice with mtDNA mutations (Pickrell et al., 2015), my data suggest that Parkin is not important in age-related mitophagy in the heart. Thus, the mechanisms executing mitophagy in the heart and brain might be different, and this observation could have important implications for designing therapies that are specific to each organ.

Concluding remarks

My findings have implications for the therapeutic potential of CPCs. Mitochondria are critical for stem self-renewal and differentiation, and using the most optimal stem cells in the clinic will improve their therapeutic potential. Autophagy and mitophagy are potential targets for heart disease, but because it is such fundamental cellular process, interventions that target a specific protein or pathway could have unintended consequences. Mitochondrial quality

control is essential for cell homeostasis and survival. Therefore, it is critical to understand the mechanisms that regulate this process in stem cells and the heart in order to pave the way for new therapies for heart disease.

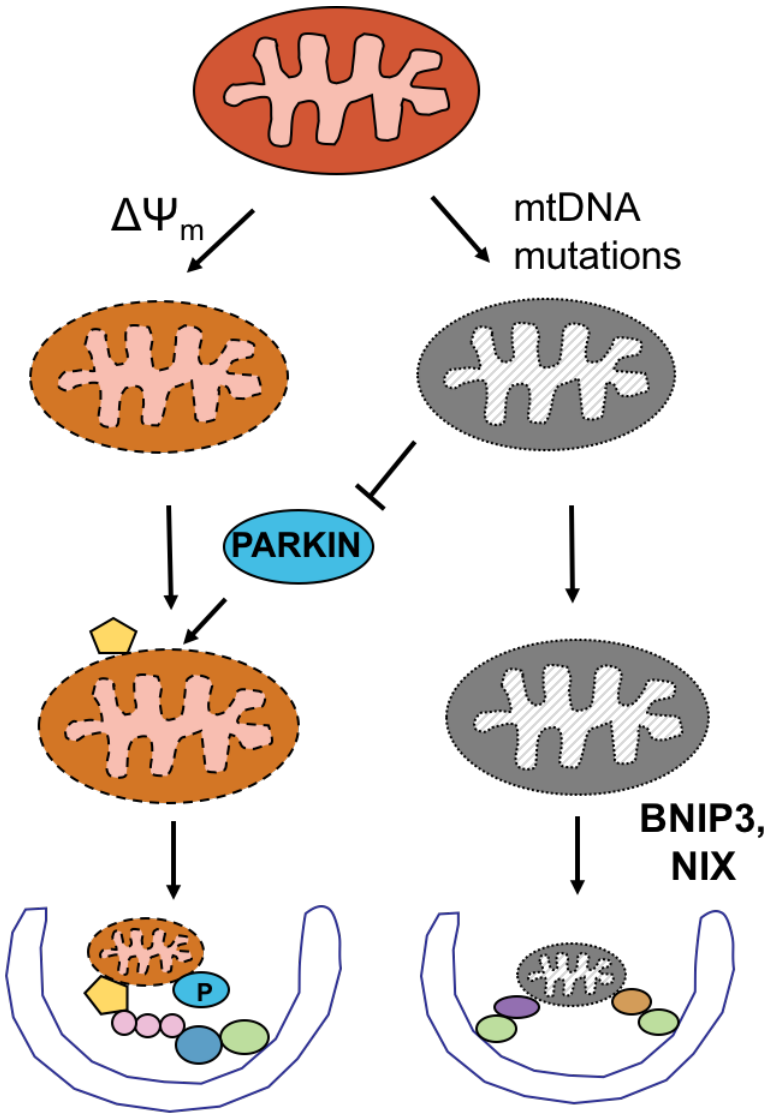

Figure 7.1: Proposed model of mitophagy in cardiomyocytes with mtDNA mutations. Acute stress, such as an MI, causes mitochondrial membrane depolarization. Parkin is recruited to the OMM, where it ubiquitinates proteins and facilitates mitophagy. With aging, mtDNA mutations accumulate and lead to chronic stress in the mitochondria. This could impair Parkin protein function or impair signals that lead to Parkin recruitment. Mitochondria rely on mitophagy receptors to clear dysfunctional mitochondria due to mtDNA mutations.

REFERENCES

Ahlqvist, K. J., Leoncini, S., Pecorelli, A., Wortmann, S. B., Ahola, S., Forsstrom, S., Guerranti, R., De Felice, C., Smeitink, J., Ciccoli, L., Hamalainen, R. H., & Suomalainen, A. (2015). MtDNA mutagenesis impairs elimination of mitochondria during erythroid maturation leading to enhanced erythrocyte destruction. *Nat Commun, 6*, 6494. doi:10.1038/ncomms7494

Andres, A. M., Stotland, A., Queliconi, B. B., & Gottlieb, R. A. (2015). A time to reap, a time to sow: mitophagy and biogenesis in cardiac pathophysiology. *J Mol Cell Cardiol, 78*, 62-72. doi:10.1016/j.yjmcc.2014.10.003

Anesti, V., & Scorrano, L. (2006). The relationship between mitochondrial shape and function and the cytoskeleton. *Biochim Biophys Acta, 1757*(5-6), 692-699. doi:10.1016/j.bbabio.2006.04.013

Ashrafi, G., Schlehe, J. S., LaVoie, M. J., & Schwarz, T. L. (2014). Mitophagy of damaged mitochondria occurs locally in distal neuronal axons and requires PINK1 and Parkin. *J Cell Biol, 206*(5), 655-670. doi:10.1083/jcb.201401070

Atamna, H. (2004). Heme, iron, and the mitochondrial decay of ageing. *Ageing Res Rev, 3*(3), 303-318. doi:10.1016/j.arr.2004.02.002

Bartunek, J., Behfar, A., Dolatabadi, D., Vanderheyden, M., Ostojic, M., Dens, J., El Nakadi, B., Banovic, M., Beleslin, B., Vrolix, M., Legrand, V., Vrints, C., Vanoverschelde, J. L., Crespo-Diaz, R., Homsy, C., Tendera, M., Waldman, S., Wijns, W., & Terzic, A. (2013). Cardiopoietic stem cell therapy in heart failure: the C-CURE (Cardiopoietic stem Cell therapy in heart failURE) multicenter randomized trial with lineage-specified biologics. *J Am Coll Cardiol, 61*(23), 2329-2338. doi:10.1016/j.jacc.2013.02.071

Bartunek, J., Davison, B., Sherman, W., Povsic, T., Henry, T. D., Gersh, B., Metra, M., Filippatos, G., Hajjar, R., Behfar, A., Homsy, C., Cotter, G., Wijns, W., Tendera, M., & Terzic, A. (2016). Congestive Heart Failure Cardiopoietic Regenerative Therapy (CHART-1) trial design. *Eur J Heart Fail, 18*(2), 160-168. doi:10.1002/ejhf.434

Beltrami, A. P., Barlucchi, L., Torella, D., Baker, M., Limana, F., Chimenti, S., Kasahara, H., Rota, M., Musso, E., Urbanek, K., Leri, A., Kajstura, J., Nadal-Ginard, B., & Anversa, P. (2003). Adult cardiac stem cells are multipotent and support myocardial regeneration. *Cell, 114*(6), 763-776.

Bolli, R., Chugh, A. R., D'Amario, D., Loughran, J. H., Stoddard, M. F., Ikram, S., Beache, G. M., Wagner, S. G., Leri, A., Hosoda, T., Sanada, F., Elmore, J. B., Goichberg, P., Cappetta, D., Solankhi, N. K., Fahsah, I., Rokosh, D. G., Slaughter, M. S., Kajstura, J., & Anversa, P. (2011). Cardiac stem cells in patients with ischaemic cardiomyopathy (SCIPIO): initial results of a randomised phase 1 trial. *Lancet, 378*(9806), 1847-1857. doi:10.1016/S0140-6736(11)61590-0

Boni, A., Urbanek, K., Nascimbene, A., Hosoda, T., Zheng, H., Delucchi, F., Amano, K., Gonzalez, A., Vitale, S., Ojaimi, C., Rizzi, R., Bolli, R., Yutzey, K. E., Rota, M., Kajstura, J., Anversa, P., & Leri, A. (2008). Notch1 regulates the fate of cardiac progenitor cells. *Proc Natl Acad Sci U S A, 105*(40), 15529-15534. doi:10.1073/pnas.0808357105

Bratic, A., & Larsson, N. G. (2013). The role of mitochondria in aging. *J Clin Invest, 123*(3), 951-957. doi:10.1172/JCI64125

Broughton, K. M., & Sussman, M. A. (2016). Empowering Adult Stem Cells for Myocardial Regeneration V2.0: Success in Small Steps. *Circ Res, 118*(5), 867-880. doi:10.1161/CIRCRESAHA.115.305227

Cai, Q., Zakaria, H. M., Simone, A., & Sheng, Z. H. (2012). Spatial parkin translocation and degradation of damaged mitochondria via mitophagy in live cortical neurons. *Curr Biol, 22*(6), 545-552. doi:10.1016/j.cub.2012.02.005

Castaldi, A., Chesini, G. P., Taylor, A. E., Sussman, M. A., Brown, J. H., & Purcell, N. H. (2016). Sphingosine 1-phosphate elicits RhoA-dependent proliferation and MRTF-A mediated gene induction in CPCs. *Cell Signal, 28*(8), 871-879. doi:10.1016/j.cellsig.2016.04.006

CDC. (2015, August 10, 2015). Heart Disease Facts. *Heart Disease Statistics and Maps.* Retrieved from http://www.cdc.gov/heartdisease/facts.htm

Chakravarty, T., Makkar, R. R., Ascheim, D., Traverse, J. H., Schatz, R., DeMaria, A., Francis, G. S., Povsic, T. J., Smith, R., Lima, J. A., Pogoda, J. M., Marban, L., & Henry, T. D. (2016). ALLogeneic Heart STem Cells to Achieve Myocardial Regeneration (ALLSTAR) trial: Rationale & Design. *Cell Transplant*. doi:10.3727/096368916X692933

Chen, C. T., Shih, Y. R., Kuo, T. K., Lee, O. K., & Wei, Y. H. (2008). Coordinated changes of mitochondrial biogenesis and antioxidant enzymes during osteogenic differentiation of human mesenchymal stem cells. *Stem Cells, 26*(4), 960-968. doi:10.1634/stemcells.2007-0509

Chen, Y., & Dorn, G. W., 2nd. (2013). PINK1-phosphorylated mitofusin 2 is a Parkin receptor for culling damaged mitochondria. *Science, 340*(6131), 471-475. doi:10.1126/science.1231031

Cho, Y. M., Kwon, S., Pak, Y. K., Seol, H. W., Choi, Y. M., Park do, J., Park, K. S., & Lee, H. K. (2006). Dynamic changes in mitochondrial biogenesis and antioxidant enzymes during the spontaneous differentiation of human embryonic stem cells. *Biochem Biophys Res Commun, 348*(4), 1472-1478. doi:10.1016/j.bbrc.2006.08.020

Chugh, A. R., Beache, G. M., Loughran, J. H., Mewton, N., Elmore, J. B., Kajstura, J., Pappas, P., Tatooles, A., Stoddard, M. F., Lima, J. A., Slaughter, M. S., Anversa, P., & Bolli, R. (2012). Administration of cardiac stem cells in patients with ischemic cardiomyopathy: the SCIPIO trial: surgical aspects and interim analysis of myocardial function and viability by magnetic resonance. *Circulation, 126*(11 Suppl 1), S54-64. doi:10.1161/CIRCULATIONAHA.112.092627

Chung, S., Arrell, D. K., Faustino, R. S., Terzic, A., & Dzeja, P. P. (2010). Glycolytic network restructuring integral to the energetics of embryonic stem cell cardiac differentiation. *J Mol Cell Cardiol, 48*(4), 725-734. doi:10.1016/j.yjmcc.2009.12.014

Chung, S., Dzeja, P. P., Faustino, R. S., Perez-Terzic, C., Behfar, A., & Terzic, A. (2007). Mitochondrial oxidative metabolism is required for the cardiac differentiation of stem cells. *Nat Clin Pract Cardiovasc Med, 4 Suppl 1*, S60-67. doi:10.1038/ncpcardio0766

ClinicalTrials.gov. (2016, September 14, 2016). Combination of Mesenchymal and C-kit+ Cardiac Stem Cells as Regenerative Therapy for Heart Failure (CONCERT-HF). Retrieved from https://clinicaltrials.gov/ct2/show/NCT02501811

Corral-Debrinski, M., Horton, T., Lott, M. T., Shoffner, J. M., Beal, M. F., & Wallace, D. C. (1992). Mitochondrial DNA deletions in human brain: regional variability and increase with advanced age. *Nat Genet, 2*(4), 324-329. doi:10.1038/ng1292-324

Corral-Debrinski, M., Shoffner, J. M., Lott, M. T., & Wallace, D. C. (1992). Association of mitochondrial DNA damage with aging and coronary atherosclerotic heart disease. *Mutat Res, 275*(3-6), 169-180.

Cui, J., Shi, S., Sun, X., Cai, G., Cui, S., Hong, Q., Chen, X., & Bai, X. Y. (2013). Mitochondrial autophagy involving renal injury and aging is modulated by caloric intake in aged rat kidneys. *PLoS One, 8*(7), e69720. doi:10.1371/journal.pone.0069720

D'Amario, D., Fiorini, C., Campbell, P. M., Goichberg, P., Sanada, F., Zheng, H., Hosoda, T., Rota, M., Connell, J. M., Gallegos, R. P., Welt, F. G., Givertz, M. M., Mitchell, R. N., Leri, A., Kajstura, J., Pfeffer, M. A., & Anversa, P. (2011). Functionally competent cardiac stem cells can be isolated from endomyocardial biopsies of patients with advanced cardiomyopathies. *Circ Res, 108*(7), 857-861. doi:10.1161/CIRCRESAHA.111.241380

Dai, D. F., Chen, T., Wanagat, J., Laflamme, M., Marcinek, D. J., Emond, M. J., Ngo, C. P., Prolla, T. A., & Rabinovitch, P. S. (2010). Age-dependent cardiomyopathy in mitochondrial mutator mice is attenuated by overexpression of catalase targeted to mitochondria. *Aging Cell, 9*(4), 536-544. doi:10.1111/j.1474-9726.2010.00581.x

Dai, D. F., Santana, L. F., Vermulst, M., Tomazela, D. M., Emond, M. J., MacCoss, M. J., Gollahon, K., Martin, G. M., Loeb, L. A., Ladiges, W. C., & Rabinovitch, P. S. (2009). Overexpression of catalase targeted to mitochondria attenuates murine cardiac aging. *Circulation, 119*(21), 2789-2797. doi:10.1161/CIRCULATIONAHA.108.822403

De Angelis, A., Piegari, E., Cappetta, D., Marino, L., Filippelli, A., Berrino, L., Ferreira-Martins, J., Zheng, H., Hosoda, T., Rota, M., Urbanek, K., Kajstura, J., Leri, A., Rossi, F., & Anversa, P. (2010). Anthracycline cardiomyopathy is mediated by depletion of the cardiac stem cell pool and is rescued by restoration of progenitor cell function. *Circulation, 121*(2), 276-292. doi:10.1161/CIRCULATIONAHA.109.895771

Dinkova-Kostova, A. T., & Abramov, A. Y. (2015). The emerging role of Nrf2 in mitochondrial function. *Free Radic Biol Med, 88*(Pt B), 179-188. doi:10.1016/j.freeradbiomed.2015.04.036

Dorn, G. W., 2nd. (2010). Mitochondrial pruning by Nix and BNip3: an essential function for cardiac-expressed death factors. *J Cardiovasc Transl Res, 3*(4), 374-383. doi:10.1007/s12265-010-9174-x

Dorn, G. W., 2nd. (2016). Parkin-dependent mitophagy in the heart. *J Mol Cell Cardiol, 95*, 42-49. doi:10.1016/j.yjmcc.2015.11.023

Egan, D. F., Shackelford, D. B., Mihaylova, M. M., Gelino, S., Kohnz, R. A., Mair, W., Vasquez, D. S., Joshi, A., Gwinn, D. M., Taylor, R., Asara, J. M., Fitzpatrick, J., Dillin, A., Viollet, B., Kundu, M., Hansen, M., & Shaw, R. J. (2011). Phosphorylation of ULK1 (hATG1) by AMP-activated protein kinase connects energy sensing to mitophagy. *Science, 331*(6016), 456-461. doi:10.1126/science.1196371

Ellison, G. M., Vicinanza, C., Smith, A. J., Aquila, I., Leone, A., Waring, C. D., Henning, B. J., Stirparo, G. G., Papait, R., Scarfo, M., Agosti, V., Viglietto, G., Condorelli, G., Indolfi, C., Ottolenghi, S., Torella, D., & Nadal-Ginard, B. (2013). Adult c-kit(pos) cardiac stem cells are necessary and sufficient for functional cardiac regeneration and repair. *Cell, 154*(4), 827-842. doi:10.1016/j.cell.2013.07.039

Exner, N., Lutz, A. K., Haass, C., & Winklhofer, K. F. (2012). Mitochondrial dysfunction in Parkinson's disease: molecular mechanisms and pathophysiological consequences. *EMBO J, 31*(14), 3038-3062. doi:10.1038/emboj.2012.170

Finck, B. N., & Kelly, D. P. (2006). PGC-1 coactivators: inducible regulators of energy metabolism in health and disease. *J Clin Invest, 116*(3), 615-622. doi:10.1172/JCI27794

Fischer, K. M., Cottage, C. T., Wu, W., Din, S., Gude, N. A., Avitabile, D., Quijada, P., Collins, B. L., Fransioli, J., & Sussman, M. A. (2009). Enhancement of myocardial regeneration through genetic engineering of cardiac progenitor cells expressing Pim-1 kinase. *Circulation, 120*(21), 2077-2087. doi:10.1161/CIRCULATIONAHA.109.884403

Folmes, C. D., Dzeja, P. P., Nelson, T. J., & Terzic, A. (2012). Metabolic plasticity in stem cell homeostasis and differentiation. *Cell Stem Cell, 11*(5), 596-606. doi:10.1016/j.stem.2012.10.002

Fransioli, J., Bailey, B., Gude, N. A., Cottage, C. T., Muraski, J. A., Emmanuel, G., Wu, W., Alvarez, R., Rubio, M., Ottolenghi, S., Schaefer, E., & Sussman, M. A. (2008). Evolution of the c-kit-positive cell response to pathological challenge in the myocardium. *Stem Cells, 26*(5), 1315-1324. doi:10.1634/stemcells.2007-0751

Frerichs, F. C., Dingemans, K. P., & Brinkman, K. (2002). Cardiomyopathy with mitochondrial damage associated with nucleoside reverse-transcriptase inhibitors. *N Engl J Med, 347*(23), 1895-1896. doi:10.1056/NEJM200212053472320

Freude, B., Masters, T. N., Robicsek, F., Fokin, A., Kostin, S., Zimmermann, R., Ullmann, C., Lorenz-Meyer, S., & Schaper, J. (2000). Apoptosis is initiated by myocardial ischemia and executed during reperfusion. *J Mol Cell Cardiol, 32*(2), 197-208. doi:10.1006/jmcc.1999.1066

Gaspar, J. A., Doss, M. X., Hengstler, J. G., Cadenas, C., Hescheler, J., & Sachinidis, A. (2014). Unique metabolic features of stem cells, cardiomyocytes, and their progenitors. *Circ Res, 114*(8), 1346-1360. doi:10.1161/CIRCRESAHA.113.302021

Gatica, D., Chiong, M., Lavandero, S., & Klionsky, D. J. (2015). Molecular mechanisms of autophagy in the cardiovascular system. *Circ Res, 116*(3), 456-467. doi:10.1161/CIRCRESAHA.114.303788

Geisler, S., Holmstrom, K. M., Skujat, D., Fiesel, F. C., Rothfuss, O. C., Kahle, P. J., & Springer, W. (2010). PINK1/Parkin-mediated mitophagy is dependent on VDAC1 and p62/SQSTM1. *Nat Cell Biol, 12*(2), 119-131. doi:10.1038/ncb2012

Goichberg, P., Kannappan, R., Cimini, M., Bai, Y., Sanada, F., Sorrentino, A., Signore, S., Kajstura, J., Rota, M., Anversa, P., & Leri, A. (2013). Age-associated defects in EphA2 signaling impair the migration of human cardiac progenitor cells. *Circulation, 128*(20), 2211-2223. doi:10.1161/CIRCULATIONAHA.113.004698

Goldberg, M. S., Fleming, S. M., Palacino, J. J., Cepeda, C., Lam, H. A., Bhatnagar, A., Meloni, E. G., Wu, N., Ackerson, L. C., Klapstein, G. J., Gajendiran, M., Roth, B. L., Chesselet, M. F., Maidment, N. T., Levine, M. S., & Shen, J. (2003). Parkin-deficient mice exhibit nigrostriatal deficits but not loss of dopaminergic neurons. *J Biol Chem, 278*(44), 43628-43635. doi:10.1074/jbc.M308947200

Greene, A. W., Grenier, K., Aguileta, M. A., Muise, S., Farazifard, R., Haque, M. E., McBride, H. M., Park, D. S., & Fon, E. A. (2012). Mitochondrial processing peptidase regulates PINK1 processing, import and Parkin recruitment. *EMBO Rep, 13*(4), 378-385. doi:10.1038/embor.2012.14

Gude, N., Joyo, E., Toko, H., Quijada, P., Villanueva, M., Hariharan, N., Sacchi, V., Truffa, S., Joyo, A., Voelkers, M., Alvarez, R., & Sussman, M. A. (2015). Notch activation enhances lineage commitment and protective signaling in cardiac progenitor cells. *Basic Res Cardiol, 110*(3), 29. doi:10.1007/s00395-015-0488-3

Guha, M., & Avadhani, N. G. (2013). Mitochondrial retrograde signaling at the crossroads of tumor bioenergetics, genetics and epigenetics. *Mitochondrion, 13*(6), 577-591. doi:10.1016/j.mito.2013.08.007

Hanna, R. A., Quinsay, M. N., Orogo, A. M., Giang, K., Rikka, S., & Gustafsson, A. B. (2012). Microtubule-associated protein 1 light chain 3 (LC3) interacts with Bnip3 protein to selectively remove endoplasmic reticulum and mitochondria via autophagy. *J Biol Chem, 287*(23), 19094-19104. doi:10.1074/jbc.M111.322933

Hare, J. M., Fishman, J. E., Gerstenblith, G., DiFede Velazquez, D. L., Zambrano, J. P., Suncion, V. Y., Tracy, M., Ghersin, E., Johnston, P. V., Brinker, J. A., Breton, E., Davis-Sproul, J., Schulman, I. H., Byrnes, J., Mendizabal, A. M., Lowery, M. H., Rouy, D., Altman, P., Wong Po Foo, C., Ruiz, P., Amador, A., Da Silva, J., McNiece, I. K., Heldman, A. W., George, R., & Lardo, A. (2012). Comparison of allogeneic vs autologous bone marrow-derived mesenchymal stem cells delivered by transendocardial injection in patients with ischemic cardiomyopathy: the POSEIDON randomized trial. *JAMA, 308*(22), 2369-2379. doi:10.1001/jama.2012.25321

Hariharan, N., Quijada, P., Mohsin, S., Joyo, A., Samse, K., Monsanto, M., De La Torre, A., Avitabile, D., Ormachea, L., McGregor, M. J., Tsai, E. J., & Sussman, M. A. (2015). Nucleostemin rejuvenates cardiac progenitor cells and antagonizes myocardial aging. *J Am Coll Cardiol, 65*(2), 133-147. doi:10.1016/j.jacc.2014.09.086

Hatefi, Y. (1985). The mitochondrial electron transport and oxidative phosphorylation system. *Annu Rev Biochem, 54*, 1015-1069. doi:10.1146/annurev.bi.54.070185.005055

Heldman, A. W., DiFede, D. L., Fishman, J. E., Zambrano, J. P., Trachtenberg, B. H., Karantalis, V., Mushtaq, M., Williams, A. R., Suncion, V. Y., McNiece, I. K., Ghersin, E., Soto, V., Lopera, G., Miki, R., Willens, H., Hendel, R., Mitrani, R., Pattany, P., Feigenbaum, G., Oskouei, B., Byrnes, J., Lowery, M. H., Sierra, J., Pujol, M. V., Delgado, C., Gonzalez, P. J., Rodriguez, J. E., Bagno, L. L., Rouy, D., Altman, P., Foo, C. W., da Silva, J., Anderson, E., Schwarz, R., Mendizabal, A., & Hare, J. M. (2014). Transendocardial mesenchymal stem cells and mononuclear bone marrow cells for ischemic cardiomyopathy: the TAC-HFT randomized trial. *JAMA, 311*(1), 62-73. doi:10.1001/jama.2013.282909

Huang, C., Zhang, X., Ramil, J. M., Rikka, S., Kim, L., Lee, Y., Gude, N. A., Thistlethwaite, P. A., Sussman, M. A., Gottlieb, R. A., & Gustafsson, A. B. (2010). Juvenile exposure to anthracyclines impairs cardiac progenitor cell function and vascularization resulting in greater susceptibility to stress-induced myocardial injury in adult mice. *Circulation, 121*(5), 675-683. doi:10.1161/CIRCULATIONAHA.109.902221

Ichimura, Y., Kirisako, T., Takao, T., Satomi, Y., Shimonishi, Y., Ishihara, N., Mizushima, N., Tanida, I., Kominami, E., Ohsumi, M., Noda, T., & Ohsumi, Y.

(2000). A ubiquitin-like system mediates protein lipidation. *Nature, 408*(6811), 488-492. doi:10.1038/35044114

Ide, T., Tsutsui, H., Hayashidani, S., Kang, D., Suematsu, N., Nakamura, K., Utsumi, H., Hamasaki, N., & Takeshita, A. (2001). Mitochondrial DNA damage and dysfunction associated with oxidative stress in failing hearts after myocardial infarction. *Circ Res, 88*(5), 529-535.

Ito, K., & Suda, T. (2014). Metabolic requirements for the maintenance of self-renewing stem cells. *Nat Rev Mol Cell Biol, 15*(4), 243-256. doi:10.1038/nrm3772

Iwata, J., Ezaki, J., Komatsu, M., Yokota, S., Ueno, T., Tanida, I., Chiba, T., Tanaka, K., & Kominami, E. (2006). Excess peroxisomes are degraded by autophagic machinery in mammals. *J Biol Chem, 281*(7), 4035-4041. doi:10.1074/jbc.M512283200

Jager, S., Bucci, C., Tanida, I., Ueno, T., Kominami, E., Saftig, P., & Eskelinen, E. L. (2004). Role for Rab7 in maturation of late autophagic vacuoles. *J Cell Sci, 117*(Pt 20), 4837-4848. doi:10.1242/jcs.01370

Jang, J., Wang, Y., Kim, H. S., Lalli, M. A., & Kosik, K. S. (2014). Nrf2, a regulator of the proteasome, controls self-renewal and pluripotency in human embryonic stem cells. *Stem Cells, 32*(10), 2616-2625. doi:10.1002/stem.1764

Jazwinski, S. M., & Kriete, A. (2012). The yeast retrograde response as a model of intracellular signaling of mitochondrial dysfunction. *Front Physiol, 3*, 139. doi:10.3389/fphys.2012.00139

Jin, S. M., & Youle, R. J. (2013). The accumulation of misfolded proteins in the mitochondrial matrix is sensed by PINK1 to induce PARK2/Parkin-mediated mitophagy of polarized mitochondria. *Autophagy, 9*(11), 1750-1757. doi:10.4161/auto.26122

Joseph, A. M., Adhihetty, P. J., Wawrzyniak, N. R., Wohlgemuth, S. E., Picca, A., Kujoth, G. C., Prolla, T. A., & Leeuwenburgh, C. (2013). Dysregulation of mitochondrial quality control processes contribute to sarcopenia in a mouse

model of premature aging. *PLoS One, 8*(7), e69327. doi:10.1371/journal.pone.0069327

Joshi, A., & Kundu, M. (2013). Mitophagy in hematopoietic stem cells: the case for exploration. *Autophagy, 9*(11), 1737-1749. doi:10.4161/auto.26681

Kaguni, L. S. (2004). DNA polymerase gamma, the mitochondrial replicase. *Annu Rev Biochem, 73*, 293-320. doi:10.1146/annurev.biochem.72.121801.161455

Kasahara, A., & Scorrano, L. (2014). Mitochondria: from cell death executioners to regulators of cell differentiation. *Trends Cell Biol, 24*(12), 761-770. doi:10.1016/j.tcb.2014.08.005

Kazlauskaite, A., Kondapalli, C., Gourlay, R., Campbell, D. G., Ritorto, M. S., Hofmann, K., Alessi, D. R., Knebel, A., Trost, M., & Muqit, M. M. (2014). Parkin is activated by PINK1-dependent phosphorylation of ubiquitin at Ser65. *Biochem J, 460*(1), 127-139. doi:10.1042/BJ20140334

Khacho, M., Clark, A., Svoboda, D. S., Azzi, J., MacLaurin, J. G., Meghaizel, C., Sesaki, H., Lagace, D. C., Germain, M., Harper, M. E., Park, D. S., & Slack, R. S. (2016). Mitochondrial Dynamics Impacts Stem Cell Identity and Fate Decisions by Regulating a Nuclear Transcriptional Program. *Cell Stem Cell, 19*(2), 232-247. doi:10.1016/j.stem.2016.04.015

Khaidakov, M., Heflich, R. H., Manjanatha, M. G., Myers, M. B., & Aidoo, A. (2003). Accumulation of point mutations in mitochondrial DNA of aging mice. *Mutat Res, 526*(1-2), 1-7.

Khalil, B., El Fissi, N., Aouane, A., Cabirol-Pol, M. J., Rival, T., & Lievens, J. C. (2015). PINK1-induced mitophagy promotes neuroprotection in Huntington's disease. *Cell Death Dis, 6*, e1617. doi:10.1038/cddis.2014.581

Kihara, A., Kabeya, Y., Ohsumi, Y., & Yoshimori, T. (2001). Beclin-phosphatidylinositol 3-kinase complex functions at the trans-Golgi network. *EMBO Rep, 2*(4), 330-335. doi:10.1093/embo-reports/kve061

Kondapalli, C., Kazlauskaite, A., Zhang, N., Woodroof, H. I., Campbell, D. G., Gourlay, R., Burchell, L., Walden, H., Macartney, T. J., Deak, M., Knebel, A., Alessi, D. R., & Muqit, M. M. (2012). PINK1 is activated by mitochondrial membrane potential depolarization and stimulates Parkin E3 ligase activity by phosphorylating Serine 65. *Open Biol, 2*(5), 120080. doi:10.1098/rsob.120080

Koyano, F., Okatsu, K., Kosako, H., Tamura, Y., Go, E., Kimura, M., Kimura, Y., Tsuchiya, H., Yoshihara, H., Hirokawa, T., Endo, T., Fon, E. A., Trempe, J. F., Saeki, Y., Tanaka, K., & Matsuda, N. (2014). Ubiquitin is phosphorylated by PINK1 to activate parkin. *Nature, 510*(7503), 162-166. doi:10.1038/nature13392

Kubli, D. A., Cortez, M. Q., Moyzis, A. G., Najor, R. H., Lee, Y., & Gustafsson, A. B. (2015). PINK1 Is Dispensable for Mitochondrial Recruitment of Parkin and Activation of Mitophagy in Cardiac Myocytes. *PLoS One, 10*(6), e0130707. doi:10.1371/journal.pone.0130707

Kubli, D. A., & Gustafsson, A. B. (2012). Mitochondria and mitophagy: the yin and yang of cell death control. *Circ Res, 111*(9), 1208-1221. doi:10.1161/CIRCRESAHA.112.265819

Kubli, D. A., Zhang, X., Lee, Y., Hanna, R. A., Quinsay, M. N., Nguyen, C. K., Jimenez, R., Petrosyan, S., Murphy, A. N., & Gustafsson, A. B. (2013). Parkin protein deficiency exacerbates cardiac injury and reduces survival following myocardial infarction. *J Biol Chem, 288*(2), 915-926. doi:10.1074/jbc.M112.411363

Kujoth, G. C., Bradshaw, P. C., Haroon, S., & Prolla, T. A. (2007). The role of mitochondrial DNA mutations in mammalian aging. *PLoS Genet, 3*(2), e24. doi:10.1371/journal.pgen.0030024

Kujoth, G. C., Hiona, A., Pugh, T. D., Someya, S., Panzer, K., Wohlgemuth, S. E., Hofer, T., Seo, A. Y., Sullivan, R., Jobling, W. A., Morrow, J. D., Van Remmen, H., Sedivy, J. M., Yamasoba, T., Tanokura, M., Weindruch, R., Leeuwenburgh, C., & Prolla, T. A. (2005). Mitochondrial DNA mutations, oxidative stress, and apoptosis in mammalian aging. *Science, 309*(5733), 481-484. doi:10.1126/science.1112125

Lamark, T., Kirkin, V., Dikic, I., & Johansen, T. (2009). NBR1 and p62 as cargo receptors for selective autophagy of ubiquitinated targets. *Cell Cycle, 8*(13), 1986-1990.

LaRocca, T. J., Hearon, C. M., Jr., Henson, G. D., & Seals, D. R. (2014). Mitochondrial quality control and age-associated arterial stiffening. *Exp Gerontol, 58*, 78-82. doi:10.1016/j.exger.2014.07.008

Larsson, N. G. (2010). Somatic mitochondrial DNA mutations in mammalian aging. *Annu Rev Biochem, 79*, 683-706. doi:10.1146/annurev-biochem-060408-093701

Lebrecht, D., & Walker, U. A. (2007). Role of mtDNA lesions in anthracycline cardiotoxicity. *Cardiovasc Toxicol, 7*(2), 108-113. doi:10.1007/s12012-007-0009-1

Leri, A., Kajstura, J., & Anversa, P. (2011). Role of cardiac stem cells in cardiac pathophysiology: a paradigm shift in human myocardial biology. *Circ Res, 109*(8), 941-961. doi:10.1161/CIRCRESAHA.111.243154

Li, Q., Guo, Y., Ou, Q., Chen, N., Wu, W. J., Yuan, F., O'Brien, E., Wang, T., Luo, L., Hunt, G. N., Zhu, X., & Bolli, R. (2011). Intracoronary administration of cardiac stem cells in mice: a new, improved technique for cell therapy in murine models. *Basic Res Cardiol, 106*(5), 849-864. doi:10.1007/s00395-011-0180-1

Li-Harms, X., Milasta, S., Lynch, J., Wright, C., Joshi, A., Iyengar, R., Neale, G., Wang, X., Wang, Y. D., Prolla, T. A., Thompson, J. E., Opferman, J. T., Green, D. R., Schuetz, J., & Kundu, M. (2015). Mito-protective autophagy is impaired in erythroid cells of aged mtDNA-mutator mice. *Blood, 125*(1), 162-174. doi:10.1182/blood-2014-07-586396

Liu, L., Feng, D., Chen, G., Chen, M., Zheng, Q., Song, P., Ma, Q., Zhu, C., Wang, R., Qi, W., Huang, L., Xue, P., Li, B., Wang, X., Jin, H., Wang, J., Yang, F., Liu, P., Zhu, Y., Sui, S., & Chen, Q. (2012). Mitochondrial outer-membrane protein FUNDC1 mediates hypoxia-induced mitophagy in mammalian cells. *Nat Cell Biol, 14*(2), 177-185. doi:10.1038/ncb2422

Liu, Q., Yang, R., Huang, X., Zhang, H., He, L., Zhang, L., Tian, X., Nie, Y., Hu, S., Yan, Y., Zhang, L., Qiao, Z., Wang, Q. D., Lui, K. O., & Zhou, B. (2016). Genetic lineage tracing identifies in situ Kit-expressing cardiomyocytes. *Cell Res, 26*(1), 119-130. doi:10.1038/cr.2015.143

Liu, Z., & Butow, R. A. (2006). Mitochondrial retrograde signaling. *Annu Rev Genet, 40*, 159-185. doi:10.1146/annurev.genet.40.110405.090613

Logan, A., Shabalina, I. G., Prime, T. A., Rogatti, S., Kalinovich, A. V., Hartley, R. C., Budd, R. C., Cannon, B., & Murphy, M. P. (2014). In vivo levels of mitochondrial hydrogen peroxide increase with age in mtDNA mutator mice. *Aging Cell, 13*(4), 765-768. doi:10.1111/acel.12212

Masotti, A., Celluzzi, A., Petrini, S., Bertini, E., Zanni, G., & Compagnucci, C. (2014). Aged iPSCs display an uncommon mitochondrial appearance and fail to undergo in vitro neurogenesis. *Aging (Albany NY), 6*(12), 1094-1108. doi:10.18632/aging.100708

Matsui, J., Wakabayashi, T., Asada, M., Yoshimatsu, K., & Okada, M. (2004). Stem cell factor/c-kit signaling promotes the survival, migration, and capillary tube formation of human umbilical vein endothelial cells. *J Biol Chem, 279*(18), 18600-18607. doi:10.1074/jbc.M311643200

Meng, F., Yao, D., Shi, Y., Kabakoff, J., Wu, W., Reicher, J., Ma, Y., Moosmann, B., Masliah, E., Lipton, S. A., & Gu, Z. (2011). Oxidation of the cysteine-rich regions of parkin perturbs its E3 ligase activity and contributes to protein aggregation. *Mol Neurodegener, 6*, 34. doi:10.1186/1750-1326-6-34

Mizushima, N. (2007). Autophagy: process and function. *Genes Dev, 21*(22), 2861-2873. doi:10.1101/gad.1599207

Mohsin, S., Khan, M., Nguyen, J., Alkatib, M., Siddiqi, S., Hariharan, N., Wallach, K., Monsanto, M., Gude, N., Dembitsky, W., & Sussman, M. A. (2013). Rejuvenation of human cardiac progenitor cells with Pim-1 kinase. *Circ Res, 113*(10), 1169-1179. doi:10.1161/CIRCRESAHA.113.302302

Mohsin, S., Khan, M., Toko, H., Bailey, B., Cottage, C. T., Wallach, K., Nag, D., Lee, A., Siddiqi, S., Lan, F., Fischer, K. M., Gude, N., Quijada, P., Avitabile, D.,

Truffa, S., Collins, B., Dembitsky, W., Wu, J. C., & Sussman, M. A. (2012). Human cardiac progenitor cells engineered with Pim-I kinase enhance myocardial repair. *J Am Coll Cardiol, 60*(14), 1278-1287. doi:10.1016/j.jacc.2012.04.047

Mushtaq, M., DiFede, D. L., Golpanian, S., Khan, A., Gomes, S. A., Mendizabal, A., Heldman, A. W., & Hare, J. M. (2014). Rationale and design of the Percutaneous Stem Cell Injection Delivery Effects on Neomyogenesis in Dilated Cardiomyopathy (the POSEIDON-DCM study): a phase I/II, randomized pilot study of the comparative safety and efficacy of transendocardial injection of autologous mesenchymal stem cell vs. allogeneic mesenchymal stem cells in patients with non-ischemic dilated cardiomyopathy. *J Cardiovasc Transl Res, 7*(9), 769-780. doi:10.1007/s12265-014-9594-0

Nakai, A., Yamaguchi, O., Takeda, T., Higuchi, Y., Hikoso, S., Taniike, M., Omiya, S., Mizote, I., Matsumura, Y., Asahi, M., Nishida, K., Hori, M., Mizushima, N., & Otsu, K. (2007). The role of autophagy in cardiomyocytes in the basal state and in response to hemodynamic stress. *Nat Med, 13*(5), 619-624. doi:10.1038/nm1574

Nakano, A., Kato, H., Watanabe, T., Min, K. D., Yamazaki, S., Asano, Y., Seguchi, O., Higo, S., Shintani, Y., Asanuma, H., Asakura, M., Minamino, T., Kaibuchi, K., Mochizuki, N., Kitakaze, M., & Takashima, S. (2010). AMPK controls the speed of microtubule polymerization and directional cell migration through CLIP-170 phosphorylation. *Nat Cell Biol, 12*(6), 583-590. doi:10.1038/ncb2060

Narendra, D., Kane, L. A., Hauser, D. N., Fearnley, I. M., & Youle, R. J. (2010). p62/SQSTM1 is required for Parkin-induced mitochondrial clustering but not mitophagy; VDAC1 is dispensable for both. *Autophagy, 6*(8), 1090-1106.

Narendra, D., Tanaka, A., Suen, D. F., & Youle, R. J. (2008). Parkin is recruited selectively to impaired mitochondria and promotes their autophagy. *J Cell Biol, 183*(5), 795-803. doi:10.1083/jcb.200809125

Narendra, D. P., Jin, S. M., Tanaka, A., Suen, D. F., Gautier, C. A., Shen, J., Cookson, M. R., & Youle, R. J. (2010). PINK1 is selectively stabilized on impaired mitochondria to activate Parkin. *PLoS Biol, 8*(1), e1000298. doi:10.1371/journal.pbio.1000298

Nguyen, T. N., Padman, B. S., & Lazarou, M. (2016). Deciphering the Molecular Signals of PINK1/Parkin Mitophagy. *Trends Cell Biol, 26*(10), 733-744. doi:10.1016/j.tcb.2016.05.008

NHLBI. (2015, June 22, 2015). How Is Heart Failure Treated? *Health Topics - Heart Failure.* Retrieved from https://www.nhlbi.nih.gov/health/health-topics/topics/hf/treatment

Nishino, I., Fu, J., Tanji, K., Yamada, T., Shimojo, S., Koori, T., Mora, M., Riggs, J. E., Oh, S. J., Koga, Y., Sue, C. M., Yamamoto, A., Murakami, N., Shanske, S., Byrne, E., Bonilla, E., Nonaka, I., DiMauro, S., & Hirano, M. (2000). Primary LAMP-2 deficiency causes X-linked vacuolar cardiomyopathy and myopathy (Danon disease). *Nature, 406*(6798), 906-910. doi:10.1038/35022604

Novak, I., Kirkin, V., McEwan, D. G., Zhang, J., Wild, P., Rozenknop, A., Rogov, V., Lohr, F., Popovic, D., Occhipinti, A., Reichert, A. S., Terzic, J., Dotsch, V., Ney, P. A., & Dikic, I. (2010). Nix is a selective autophagy receptor for mitochondrial clearance. *EMBO Rep, 11*(1), 45-51. doi:10.1038/embor.2009.256

Nunnari, J., & Suomalainen, A. (2012). Mitochondria: in sickness and in health. *Cell, 148*(6), 1145-1159. doi:10.1016/j.cell.2012.02.035

Ochocki, J. D., & Simon, M. C. (2013). Nutrient-sensing pathways and metabolic regulation in stem cells. *J Cell Biol, 203*(1), 23-33. doi:10.1083/jcb.201303110

Orogo, A. M., & Gustafsson, A. B. (2015). Therapeutic targeting of autophagy: potential and concerns in treating cardiovascular disease. *Circ Res, 116*(3), 489-503. doi:10.1161/CIRCRESAHA.116.303791

Palkova, Z., & Vachova, L. (2016). Mitochondria in aging cell differentiation. *Aging (Albany NY), 8*(7), 1287-1288. doi:10.18632/aging.100993

Perez, F. A., & Palmiter, R. D. (2005). Parkin-deficient mice are not a robust model of parkinsonism. *Proc Natl Acad Sci U S A, 102*(6), 2174-2179. doi:10.1073/pnas.0409598102

Pickrell, A. M., Huang, C. H., Kennedy, S. R., Ordureau, A., Sideris, D. P., Hoekstra, J. G., Harper, J. W., & Youle, R. J. (2015). Endogenous Parkin Preserves Dopaminergic Substantia Nigral Neurons following Mitochondrial DNA Mutagenic Stress. *Neuron, 87*(2), 371-381. doi:10.1016/j.neuron.2015.06.034

Pikkarainen, S., Tokola, H., Kerkela, R., & Ruskoaho, H. (2004). GATA transcription factors in the developing and adult heart. *Cardiovasc Res, 63*(2), 196-207. doi:10.1016/j.cardiores.2004.03.025

Quijada, P., Hariharan, N., Cubillo, J. D., Bala, K. M., Emathinger, J. M., Wang, B. J., Ormachea, L., Bers, D. M., Sussman, M. A., & Poizat, C. (2015). Nuclear Calcium/Calmodulin-dependent Protein Kinase II Signaling Enhances Cardiac Progenitor Cell Survival and Cardiac Lineage Commitment. *J Biol Chem, 290*(42), 25411-25426. doi:10.1074/jbc.M115.657775

Quijada, P., Salunga, H. T., Hariharan, N., Cubillo, J. D., El-Sayed, F. G., Moshref, M., Bala, K. M., Emathinger, J. M., De La Torre, A., Ormachea, L., Alvarez, R., Jr., Gude, N. A., & Sussman, M. A. (2015). Cardiac Stem Cell Hybrids Enhance Myocardial Repair. *Circ Res, 117*(8), 695-706. doi:10.1161/CIRCRESAHA.115.306838

Quijada, P., & Sussman, M. A. (2014). Making it stick: chasing the optimal stem cells for cardiac regeneration. *Expert Rev Cardiovasc Ther, 12*(11), 1275-1288. doi:10.1586/14779072.2014.972941

Quinsay, M. N., Thomas, R. L., Lee, Y., & Gustafsson, A. B. (2010). Bnip3-mediated mitochondrial autophagy is independent of the mitochondrial permeability transition pore. *Autophagy, 6*(7), 855-862.

Rana, A., Rera, M., & Walker, D. W. (2013). Parkin overexpression during aging reduces proteotoxicity, alters mitochondrial dynamics, and extends lifespan. *Proc Natl Acad Sci U S A, 110*(21), 8638-8643. doi:10.1073/pnas.1216197110

Rehman, J. (2010). Empowering self-renewal and differentiation: the role of mitochondria in stem cells. *J Mol Med (Berl), 88*(10), 981-986. doi:10.1007/s00109-010-0678-2

Richter, C., Park, J. W., & Ames, B. N. (1988). Normal oxidative damage to mitochondrial and nuclear DNA is extensive. *Proc Natl Acad Sci U S A, 85*(17), 6465-6467.

Rikka, S., Quinsay, M. N., Thomas, R. L., Kubli, D. A., Zhang, X., Murphy, A. N., & Gustafsson, A. B. (2011). Bnip3 impairs mitochondrial bioenergetics and stimulates mitochondrial turnover. *Cell Death Differ, 18*(4), 721-731. doi:10.1038/cdd.2010.146

Rogers, G. W., Brand, M. D., Petrosyan, S., Ashok, D., Elorza, A. A., Ferrick, D. A., & Murphy, A. N. (2011). High throughput microplate respiratory measurements using minimal quantities of isolated mitochondria. *PLoS One, 6*(7), e21746. doi:10.1371/journal.pone.0021746

Rowe, G. C., Jiang, A., & Arany, Z. (2010). PGC-1 coactivators in cardiac development and disease. *Circ Res, 107*(7), 825-838. doi:10.1161/CIRCRESAHA.110.223818

Rubinsztein, D. C., Marino, G., & Kroemer, G. (2011). Autophagy and aging. *Cell, 146*(5), 682-695. doi:10.1016/j.cell.2011.07.030

Samse, K., Emathinger, J., Hariharan, N., Quijada, P., Ilves, K., Volkers, M., Ormachea, L., De La Torre, A., Orogo, A. M., Alvarez, R., Din, S., Mohsin, S., Monsanto, M., Fischer, K. M., Dembitsky, W. P., Gustafsson, A. B., & Sussman, M. A. (2015). Functional Effect of Pim1 Depends upon Intracellular Localization in Human Cardiac Progenitor Cells. *J Biol Chem, 290*(22), 13935-13947. doi:10.1074/jbc.M114.617431

Sandoval, H., Thiagarajan, P., Dasgupta, S. K., Schumacher, A., Prchal, J. T., Chen, M., & Wang, J. (2008). Essential role for Nix in autophagic maturation of erythroid cells. *Nature, 454*(7201), 232-235. doi:10.1038/nature07006

Sarraf, S. A., Raman, M., Guarani-Pereira, V., Sowa, M. E., Huttlin, E. L., Gygi, S. P., & Harper, J. W. (2013). Landscape of the PARKIN-dependent ubiquitylome in response to mitochondrial depolarization. *Nature, 496*(7445), 372-376. doi:10.1038/nature12043

Senyo, S. E., Steinhauser, M. L., Pizzimenti, C. L., Yang, V. K., Cai, L., Wang, M., Wu, T. D., Guerquin-Kern, J. L., Lechene, C. P., & Lee, R. T. (2013). Mammalian heart renewal by pre-existing cardiomyocytes. *Nature, 493*(7432), 433-436. doi:10.1038/nature11682

Shaltouki, A., Sivapatham, R., Pei, Y., Gerencser, A. A., Momcilovic, O., Rao, M. S., & Zeng, X. (2015). Mitochondrial alterations by PARKIN in dopaminergic neurons using PARK2 patient-specific and PARK2 knockout isogenic iPSC lines. *Stem Cell Reports, 4*(5), 847-859. doi:10.1016/j.stemcr.2015.02.019

Shi, J., Fung, G., Deng, H., Zhang, J., Fiesel, F. C., Springer, W., Li, X., & Luo, H. (2015). NBR1 is dispensable for PARK2-mediated mitophagy regardless of the presence or absence of SQSTM1. *Cell Death Dis, 6*, e1943. doi:10.1038/cddis.2015.278

Shirakabe, A., Ikeda, Y., Sciarretta, S., Zablocki, D. K., & Sadoshima, J. (2016). Aging and Autophagy in the Heart. *Circ Res, 118*(10), 1563-1576. doi:10.1161/CIRCRESAHA.116.307474

Sin, J., Andres, A. M., Taylor, D. J., Weston, T., Hiraumi, Y., Stotland, A., Kim, B. J., Huang, C., Doran, K. S., & Gottlieb, R. A. (2016). Mitophagy is required for mitochondrial biogenesis and myogenic differentiation of C2C12 myoblasts. *Autophagy, 12*(2), 369-380. doi:10.1080/15548627.2015.1115172

Song, M., Gong, G., Burelle, Y., Gustafsson, A. B., Kitsis, R. N., Matkovich, S. J., & Dorn, G. W., 2nd. (2015). Interdependence of Parkin-Mediated Mitophagy and Mitochondrial Fission in Adult Mouse Hearts. *Circ Res, 117*(4), 346-351. doi:10.1161/CIRCRESAHA.117.306859

Spitkovsky, D., Sasse, P., Kolossov, E., Bottinger, C., Fleischmann, B. K., Hescheler, J., & Wiesner, R. J. (2004). Activity of complex III of the mitochondrial electron transport chain is essential for early heart muscle cell differentiation. *FASEB J, 18*(11), 1300-1302. doi:10.1096/fj.03-0520fje

St John, J. C., Ramalho-Santos, J., Gray, H. L., Petrosko, P., Rawe, V. Y., Navara, C. S., Simerly, C. R., & Schatten, G. P. (2005). The expression of mitochondrial DNA transcription factors during early cardiomyocyte in vitro differentiation from human embryonic stem cells. *Cloning Stem Cells, 7*(3), 141-153. doi:10.1089/clo.2005.7.141

Suen, D. F., Narendra, D. P., Tanaka, A., Manfredi, G., & Youle, R. J. (2010). Parkin overexpression selects against a deleterious mtDNA mutation in heteroplasmic cybrid cells. *Proc Natl Acad Sci U S A, 107*(26), 11835-11840. doi:10.1073/pnas.0914569107

Sultana, N., Zhang, L., Yan, J., Chen, J., Cai, W., Razzaque, S., Jeong, D., Sheng, W., Bu, L., Xu, M., Huang, G. Y., Hajjar, R. J., Zhou, B., Moon, A., & Cai, C. L. (2015). Resident c-kit(+) cells in the heart are not cardiac stem cells. *Nat Commun, 6*, 8701. doi:10.1038/ncomms9701

Taneike, M., Yamaguchi, O., Nakai, A., Hikoso, S., Takeda, T., Mizote, I., Oka, T., Tamai, T., Oyabu, J., Murakawa, T., Nishida, K., Shimizu, T., Hori, M., Komuro, I., Takuji Shirasawa, T. S., Mizushima, N., & Otsu, K. (2010). Inhibition of autophagy in the heart induces age-related cardiomyopathy. *Autophagy, 6*(5), 600-606. doi:10.4161/auto.6.5.11947

Tokita, Y., Tang, X. L., Li, Q., Wysoczynski, M., Hong, K. U., Nakamura, S., Wu, W. J., Xie, W., Li, D., Hunt, G., Ou, Q., Stowers, H., & Bolli, R. (2016). Repeated Administrations of Cardiac Progenitor Cells Are Markedly More Effective Than a Single Administration: A New Paradigm in Cell Therapy. *Circ Res, 119*(5), 635-651. doi:10.1161/CIRCRESAHA.116.308937

Trifunovic, A., Wredenberg, A., Falkenberg, M., Spelbrink, J. N., Rovio, A. T., Bruder, C. E., Bohlooly, Y. M., Gidlof, S., Oldfors, A., Wibom, R., Tornell, J., Jacobs, H. T., & Larsson, N. G. (2004). Premature ageing in mice expressing defective mitochondrial DNA polymerase. *Nature, 429*(6990), 417-423. doi:10.1038/nature02517

Vajravelu, B. N., Hong, K. U., Al-Maqtari, T., Cao, P., Keith, M. C., Wysoczynski, M., Zhao, J., Moore, J. B. t., & Bolli, R. (2015). C-Kit Promotes Growth and Migration of Human Cardiac Progenitor Cells via the PI3K-AKT and MEK-ERK Pathways. *PLoS One, 10*(10), e0140798. doi:10.1371/journal.pone.0140798

van Berlo, J. H., Kanisicak, O., Maillet, M., Vagnozzi, R. J., Karch, J., Lin, S. C., Middleton, R. C., Marban, E., & Molkentin, J. D. (2014). c-kit+ cells minimally contribute cardiomyocytes to the heart. *Nature, 509*(7500), 337-341. doi:10.1038/nature13309

van Berlo, J. H., & Molkentin, J. D. (2016). Most of the Dust Has Settled: cKit+ Progenitor Cells Are an Irrelevant Source of Cardiac Myocytes In Vivo. *Circ Res, 118*(1), 17-19. doi:10.1161/CIRCRESAHA.115.307934

Vazquez-Martin, A., Van den Haute, C., Cufi, S., Corominas-Faja, B., Cuyas, E., Lopez-Bonet, E., Rodriguez-Gallego, E., Fernandez-Arroyo, S., Joven, J., Baekelandt, V., & Menendez, J. A. (2016). Mitophagy-driven mitochondrial rejuvenation regulates stem cell fate. *Aging (Albany NY), 8*(7), 1330-1352. doi:10.18632/aging.100976

Wahlestedt, M., Ameur, A., Moraghebi, R., Norddahl, G. L., Sten, G., Woods, N. B., & Bryder, D. (2014). Somatic cells with a heavy mitochondrial DNA mutational load render induced pluripotent stem cells with distinct differentiation defects. *Stem Cells, 32*(5), 1173-1182. doi:10.1002/stem.1630

Wanagat, J., Wolff, M. R., & Aiken, J. M. (2002). Age-associated changes in function, structure and mitochondrial genetic and enzymatic abnormalities in the Fischer 344 x Brown Norway F(1) hybrid rat heart. *J Mol Cell Cardiol, 34*(1), 17-28. doi:10.1006/jmcc.2001.1483

Wanet, A., Arnould, T., Najimi, M., & Renard, P. (2015). Connecting Mitochondria, Metabolism, and Stem Cell Fate. *Stem Cells Dev, 24*(17), 1957-1971. doi:10.1089/scd.2015.0117

Wang, W., Osenbroch, P., Skinnes, R., Esbensen, Y., Bjoras, M., & Eide, L. (2010). Mitochondrial DNA integrity is essential for mitochondrial maturation during differentiation of neural stem cells. *Stem Cells, 28*(12), 2195-2204. doi:10.1002/stem.542

Wencker, D., Chandra, M., Nguyen, K., Miao, W., Garantziotis, S., Factor, S. M., Shirani, J., Armstrong, R. C., & Kitsis, R. N. (2003). A mechanistic role for cardiac myocyte apoptosis in heart failure. *J Clin Invest, 111*(10), 1497-1504. doi:10.1172/JCI17664

Whelan, R. S., Kaplinskiy, V., & Kitsis, R. N. (2010). Cell death in the pathogenesis of heart disease: mechanisms and significance. *Annu Rev Physiol, 72*, 19-44. doi:10.1146/annurev.physiol.010908.163111

Wild, P., Farhan, H., McEwan, D. G., Wagner, S., Rogov, V. V., Brady, N. R., Richter, B., Korac, J., Waidmann, O., Choudhary, C., Dotsch, V., Bumann, D., & Dikic, I. (2011). Phosphorylation of the autophagy receptor optineurin restricts Salmonella growth. *Science, 333*(6039), 228-233. doi:10.1126/science.1205405

Winklhofer, K. F., Henn, I. H., Kay-Jackson, P. C., Heller, U., & Tatzelt, J. (2003). Inactivation of parkin by oxidative stress and C-terminal truncations: a protective role of molecular chaperones. *J Biol Chem, 278*(47), 47199-47208. doi:10.1074/jbc.M306769200

Wong, E. S., Tan, J. M., Wang, C., Zhang, Z., Tay, S. P., Zaiden, N., Ko, H. S., Dawson, V. L., Dawson, T. M., & Lim, K. L. (2007). Relative sensitivity of parkin and other cysteine-containing enzymes to stress-induced solubility alterations. *J Biol Chem, 282*(16), 12310-12318. doi:10.1074/jbc.M609466200

Wong, Y. C., & Holzbaur, E. L. (2014). Optineurin is an autophagy receptor for damaged mitochondria in parkin-mediated mitophagy that is disrupted by an ALS-linked mutation. *Proc Natl Acad Sci U S A, 111*(42), E4439-4448. doi:10.1073/pnas.1405752111

Writing Group, M., Mozaffarian, D., Benjamin, E. J., Go, A. S., Arnett, D. K., Blaha, M. J., Cushman, M., Das, S. R., de Ferranti, S., Despres, J. P., Fullerton, H. J., Howard, V. J., Huffman, M. D., Isasi, C. R., Jimenez, M. C., Judd, S. E., Kissela, B. M., Lichtman, J. H., Lisabeth, L. D., Liu, S., Mackey, R. H., Magid, D. J., McGuire, D. K., Mohler, E. R., 3rd, Moy, C. S., Muntner, P., Mussolino, M. E., Nasir, K., Neumar, R. W., Nichol, G., Palaniappan, L., Pandey, D. K., Reeves, M. J., Rodriguez, C. J., Rosamond, W., Sorlie, P. D., Stein, J., Towfighi, A., Turan, T. N., Virani, S. S., Woo, D., Yeh, R. W., Turner, M. B., American Heart Association Statistics, C., & Stroke Statistics, S. (2016a). Executive Summary: Heart Disease and Stroke Statistics--2016 Update: A Report From the American Heart Association. *Circulation, 133*(4), 447-454. doi:10.1161/CIR.0000000000000366

Writing Group, M., Mozaffarian, D., Benjamin, E. J., Go, A. S., Arnett, D. K., Blaha, M. J., Cushman, M., Das, S. R., de Ferranti, S., Despres, J. P., Fullerton, H. J., Howard, V. J., Huffman, M. D., Isasi, C. R., Jimenez, M. C., Judd, S. E., Kissela, B. M., Lichtman, J. H., Lisabeth, L. D., Liu, S., Mackey, R. H., Magid, D. J., McGuire, D. K., Mohler, E. R., 3rd, Moy, C. S., Muntner, P., Mussolino, M. E., Nasir, K., Neumar, R. W., Nichol, G., Palaniappan, L., Pandey, D. K.,

Reeves, M. J., Rodriguez, C. J., Rosamond, W., Sorlie, P. D., Stein, J., Towfighi, A., Turan, T. N., Virani, S. S., Woo, D., Yeh, R. W., Turner, M. B., American Heart Association Statistics, C., & Stroke Statistics, S. (2016b). Heart Disease and Stroke Statistics-2016 Update: A Report From the American Heart Association. *Circulation, 133*(4), e38-360. doi:10.1161/CIR.0000000000000350

Wu, Z., Puigserver, P., Andersson, U., Zhang, C., Adelmant, G., Mootha, V., Troy, A., Cinti, S., Lowell, B., Scarpulla, R. C., & Spiegelman, B. M. (1999). Mechanisms controlling mitochondrial biogenesis and respiration through the thermogenic coactivator PGC-1. *Cell, 98*(1), 115-124. doi:10.1016/S0092-8674(00)80611-X

Xu, X., Duan, S., Yi, F., Ocampo, A., Liu, G. H., & Izpisua Belmonte, J. C. (2013). Mitochondrial regulation in pluripotent stem cells. *Cell Metab, 18*(3), 325-332. doi:10.1016/j.cmet.2013.06.005

Yamano, K., Matsuda, N., & Tanaka, K. (2016). The ubiquitin signal and autophagy: an orchestrated dance leading to mitochondrial degradation. *EMBO Rep, 17*(3), 300-316. doi:10.15252/embr.201541486

Yamano, K., & Youle, R. J. (2013). PINK1 is degraded through the N-end rule pathway. *Autophagy, 9*(11), 1758-1769. doi:10.4161/auto.24633

Yang, Z., & Klionsky, D. J. (2010). Eaten alive: a history of macroautophagy. *Nat Cell Biol, 12*(9), 814-822. doi:10.1038/ncb0910-814

Ye, X., Sun, X., Starovoytov, V., & Cai, Q. (2015). Parkin-mediated mitophagy in mutant hAPP neurons and Alzheimer's disease patient brains. *Hum Mol Genet, 24*(10), 2938-2951. doi:10.1093/hmg/ddv056

Yousef, M., Schannwell, C. M., Kostering, M., Zeus, T., Brehm, M., & Strauer, B. E. (2009). The BALANCE Study: clinical benefit and long-term outcome after intracoronary autologous bone marrow cell transplantation in patients with acute myocardial infarction. *J Am Coll Cardiol, 53*(24), 2262-2269. doi:10.1016/j.jacc.2009.02.051